Forward and reverse genetic approaches to identify genes involved in leg morphogenesis in *Drosophila*

BY

C2010
Xiaochen Wang

Submitted to the graduate degree program in Molecular Biosciences and the Graduate Faculty of the University of Kansas in partial fulfillment of the requirements for the degree of Doctor of Philosophy.

Committee members: _____

Chairperson: Robert Ward

_____

Robert Cohen

_____

Victoria Corbin

_____

Erik Lundquist

_____

Kristi Neufeld

_____

Joy Ward

Date defended: 04/21/2010

The Dissertation Committee for Xiaochen Wang certifies that this is approved version of the following dissertation:

Forward and reverse genetic approaches to identify genes involved in leg morphogenesis in *Drosophila*

Xiaochen Wang

Committee members: _____

Chairperson: Robert Ward

_____

Robert Cohen

_____

Victoria Corbin

_____

Erik Lundquist

_____

Kristi Neufeld

_____

Joy Ward

Date appoved: 04/26/2010

Abstract

The body plan of metazoan animals is ultimately defined by a series of coordinated morphogenetic events, some of which are controlled by hormone or endocrine signals. Development of *Drosophila* leg imaginal discs provides an ideal model to study hormone-regulated morphogenesis. During the onset of metamorphosis, a pulse of steroid hormone ecdysone triggers the rapid transformation of flat leg imaginal discs into rudimentary adult fly legs, largely through coordination of cell shape changes and cell rearrangements. The ecdysone-inducible early gene *broad* (*br*), is required for this morphogenesis. Leg development in amorphic br^5 mutant animals is arrested at a stage similar to that of a wild-type disc at puparium formation. Hypomorphic alleles of *br*, including br^1, demonstrate a low penetrance of malformed adult legs. To better understand how ecdysone regulates tissue morphogenesis, I used both forward and reverse genetic approaches to study leg morphogenesis in my graduate studies.

Previously, the Ward lab conducted two large-scale genetic screens and determined that the Rho1 signaling pathway interacts with *br* and plays a central role in imaginal discs morphogenesis. From these screens several unknown dominant *Enhancer of br* or *E(br)* alleles that showed interactions with both *br* and Rho1 pathway genes were isolated. My first project was to characterize *E(br)165*, which I determined was a mutation in *Sec61α* and renamed it $Sec61\alpha^1$. *Sec61α* encodes the main subunit of the translocon complex for co-translational import of proteins into the endoplasmic reticulum (ER). Since $Sec61\alpha^1$ (an EMS strong loss of function allele) is embryonic lethal, I concentrated on studying its role in embryogenesis. $Sec61\alpha^1$ specifically perturbs dorsal closure during embryogenesis. During dorsal closure in *Drosophila*, signaling events in the dorsalmost row of epidermal cells (DME cells) direct the migration of

lateral epidermal sheets towards the dorsal midline where they fuse to enclose the embryo. A Jun amino-terminal kinase (JNK) cascade in the DME cells induces the expression of Decapentaplegic (Dpp). Dpp signaling then regulates the cytoskeleton in the DME cells and amnioserosa to affect the cell shape changes necessary to complete dorsal closure. JNK signaling is normal in *Sec61α* mutant embryos, but Dpp signaling is attenuated, and the DME cells fail to establish an actinomyosin cable and epithelial migration fails. Consistent with this model, dorsal closure is rescued in *Sec61α* mutant embryos by an activated form of the Dpp receptor Thick veins. With regards to leg morphogenesis, these observations suggest that normal secretion levels have to be maintained during this process, and one or more dose-sensitive secreted proteins may be essential for hormone-regulated imaginal disc morphogenesis.

My second project was to identify and characterize genes that are regulated by ecdysone and the transcription factor *br* at the onset of metamorphosis in leg imaginal discs. To accomplish this, I conducted a series of microarray experiments to identify genes that are differently regulated by *br* in leg discs at the onset of metamorphosis. I also used microarrays to identify genes differentially expressed between mid third instar larva and 0 hr prepupa in wild type animals. Interestingly there is only a small subset of genes that are induced or repressed by both ecdysone and *br*. Northern blot analysis showed that, instead of *br* expression being induced by the late larval ecdysone pulse, *br* transcripts are already present in late third instar larvae. This suggests that *br* may function in concert with ecdysone to regulate leg morphogenesis. Consistent with this idea, early activation of *br* or early supply of ecdysone does not induce premature leg imaginal disc elongation, indicating that neither *br* nor ecdysone alone is sufficient to induce a leg development program. To examine the function of these *br*- and ecdysone-induced genes in more details, I conducted functional analyses by RNA interference knockdown

in distal leg segments. Ten of the 27 ecdysone- and *br*-induced genes thus far examined produce animals showing at least 20% malformed legs.

Some of the genes that were identified from the forward and reverse genetic screens overlap, or function in the similar pathways, indicating their important roles in ecdysone-regulated leg morphogenesis. These findings may thus help us to better understand hormone-regulated morphogenetic events in *Drosophila* and other organisms.

Acknowledgments

First of all, I would like to thank my mentor Dr. Robert Ward, who gave me incredible support and guidance during my graduate studies. He taught me almost every basic technique and experiment in person, and showed me how to do good research. I always benefit from having conversations with him, and he influenced me in many ways beyond his words. I just feel so fortunate that I had the opportunity to learn from him for the past almost 6 years.

I would like to thank my committee members, Dr. Yoshi Azuma, Dr. Xue-Wen Chen, Dr. Bob Cohen, Dr. Vicki Corbin, Dr. Erik Lundquist Dr. Kristi Neufeld and and Dr. Joy Ward. They always have given me great ideas and suggestions on my projects. I want to thank Dr. Stuart Macdonald for suggestions in analyzing the microarray data. Specially, I want to thank Dr. Vicki Corbin and Dr. Kristi Neufeld for improving my dissertation.

Many former and current graduate and undergraduate students and technicians contributed to my projects. I want to thank Kistie Brunsell for managing the lab so well and helping me in both my projects and my life in the US. I thank Elspeth Pearce for help with the design of the *Sec61α* rescue construct, and for conducting preliminary experiments in the functional analysis of the microarray genes. I thank David Gauthier, Aaron Welch and Maged Zein El-Din for help in the microarray project. I thank Greg Beitel, Matt Gibson, and Cindy Bayer for fly stocks. I thank Richard Fehon, Rebecca Hays and Liang Zhang for the antibodies used in the *Sec61α* study.

Last, I want to thank my parents for their understanding and support. Without them I cannot imagine how I could have finished my degree here.

Table of contents

List of Figures

List of Tables

Chapter 1

Introduction

Endocrine signals play important roles in morphogenesis

In metazoans the coordination of cell shape changes and cell rearrangement are essential for proper development. Among various regulation mechanisms, endocrine cues provide temporal control in several well-described morphogenetic events. For example, retinoic acid is required for embryonic heart morphogenesis in vertebrates (Niederreither, 2001), and estrogen is required for postnatal mammary epithelial growth and ductal morphogenesis (Bocchinfuso, 2000).

Drosophila is an ideal organism to study hormone-regulated morphogenesis. The insect steroid hormone ecdysone is synthesized from dietary cholesterol in the prothoracic gland (Grieneisen 1993; Henrich, 1999). Then peripheral tissues convert it into its active form, 20-hydroxyecdysone (hereafter referred to as ecdysone), which triggers the major transitions throughout the life cycle of *Drosophila* (Figure 1.1; Thummel, 2001). There is a pulse of ecdysone at the end of the 3rd instar larval stage that initiates prepuparium formation. At this time, the larva stops moving and everts its spiracles, signifying the onset of metamorphosis. The prothoracic gland, which is the source of ecdysone, is required for several days during metamorphosis, indicating that a sustained supply of ecdysone is necessary for metamophosis (Postlethwait, 1970). Tremendous morphogenetic events driven by this pulse of ecdysone take place, including cell death of the midgut, and elongation and evertion of the leg and wing imaginal discs (Thummel, 2001). After ~12 hrs, a smaller pulse of ecdysone triggers head eversion, continued elongation of leg and wings, and further destruction of larval tissues, including the salivary gland. This event marks the beginning of the pupal stage (Figure 1.1;

Thummel, 2001).

Ecdysone induces leg imaginal disc morphogenesis

Leg morphogenesis that begins in late 3rd instar larvae and continues through prepupal development is a great model to study cell shape changes and movement that are regulated by a hormone. The elongation and evagination of leg imaginal discs during metamorphosis has been well studied (Figure 1.2; Fristrom and Fristrom 1975). The adult fly's leg is made up of three parts, femur, tibia and tarsal segments. The leg imaginal disc is flat epithelium in 3rd instar larvae (Figure 1.2). The center of the disc develops into the most distal parts of the adult leg, the tarsal segments, whereas the outside of the disc develops into the femur and the intermediate areas develop into the tibia (Figure 1.2). The onset of metamorphosis is hereafter referred to as 0 hr. From -4 hr to 0 hr the discs experience a strong pulse of ecdysone that also triggers prepupal formation. In response to this ecdysone pluse, the leg discs undergo dramatic elongation (Figure 1.3), mainly due to cell shape changes and cell rearrangement (Condic, 1991, Fristrom, 1976, Taylor 2008). *In vitro*, leg discs that are cultured in medium with appropriate ecdysone treatment can elongate and evert (Milner, 1977), mimicking the development *in vivo*, which supports the model that ecdysone is the main trigger that drives leg morphogenesis.

Cell shape changes and cell rearrangement during imaginal disc morphogenesis are regulated through cytoskeleton and likely require intact cell-cell junctions. The actin-based cytoskeleton is likely the major force that mediates cell movement and cell shape changes. Defects in the cytoskeleton, i.e. through mutation of *zipper* (*zip*), which encodes nonmuscle myosin heavy chain, leads to malformed legs and wings (Fristrom and Fristrom, *The Development of Drosophila Melanogaster*). Imaginal disc cells are tightly associated along their

lateral surfaces by intercellular adhesions: zonulae adhesions, septate junctions, gap junctions and various cell adhesion molecules (Fristrom and Fristrom, *The Development of Drosophila Melanogaster*). Zonulae adhesions are junctions that form a continuous band near the apical ends of cells, which usually associate with the actin filaments (Fristrom and Fristrom, *The Development of Drosophila Melanogaster*). Septate junction is unique to invertebrate, whose function is corresponding to that of tight junction in vertebrates. They form ladder-like structures below zonulae adhesions, which was shown to essential in the dramatic cell rearrangement during imaginal disc morphogenesis (Fristrom, 1982). Gap junctions are composed of transmembrane channels that allow diffusion of small molecules (Fristrom and Fristrom, 1993).

Classic studies in *br*-regulated leg morphogenesis

Ecdysone works through a well-described transcriptional hierarchy. Ecdysone binds to its receptor, a heterodimer of the ecdysone receptor (EcR) and Ultraspiracle (USP). This then activates a few downstream transcriptional factors, including *Broad-Complex* (*BR-C*), *E74* and *E75* (all referred to as early-responding genes). The early-responding genes turn on more late-responding genes that function in tissue-specific responses (Thummel, 2001). *BR-C* encodes four zinc finger proteins, Z1, Z2, Z3 and Z4 (Kiss, 1988). Z2 encodes the genetic function of *broad* (*br*), which plays a specific role in imaginal disc morphogenesis (Bayer, 1997). For example, br^5 is an amorphic allele that has a premature stop codon in the Z2 domain. Leg imaginal discs from br^5 mutants fail to elongate and are arrested at 0 hr, even though the animal continues to develop and eventually dies during the prepupal stage (Figure 1.3; Bayer, 1997; Ward, 2003). Hypomorphic alleles, such as br^1, display a low penetrance malformed leg phenotype, characterized by short femur, tibia and tarsal segments (Figure 1. 4, Ward, 2003, Kiss, 1988).

This allele has been used effectively to identify new genes that play a role in leg morphogenesis (Beaton, 1988; Gotwals, 1991; Ward, 2003).

To find genes that interact with *br*, a genetic approach referred to as a dominant modifier screen, was first employed by Beaton (Beaton, 1988). br^1 itself displays a low penetrance of malformed legs. In adult hemizygous for br^1 that also carry a mutation in a gene that interacts with *br*, the malformed leg phenotype is amplified, producing a higher percentage of malformed legs. The interacting gene would be called a dominant enhancer of *br* or *E(br)*. Since many essential genes are early lethal when homozygous, the benefit of this screening method is to identify the later function of genes that might be involved in appendage morphogenesis.

Beaton et al. (1988) found that *Stubble/stubbloid* (*Sb/sbd*), which encodes a transmembrane serine protease (Appel, 1993), interacts with *br* in leg development. Dominant *Stubble* mutants are referred to as *Stubble* (*Sb*), whereas recessive mutants are *stubbloid* (*sbd*). In viable combinations of *Sb/sbd* mutants, the third pair of legs are always affected, showing short fat femur, tibia and tarsal segments. Sometimes the wings and the second pair of legs are affected as well. Although Sb functions as a protease, which may be required for rapid cell rearrangement during leg disc elongation, Sb may also function in signal transduction that affects the cytoskeleton, as Sb also interacts genetically with the Rho1 signaling pathway (Bayer, 2003). In 1991 Gotwal et al. conducted an open-ended dominant modifier of *br* screen, and identified *zip*, *Sb/sbd* and *blistered* (*bs*), which encodes a serum response factor transcription factor, as *E(br)* mutations. The phenotypes of these *E(br)* mutations are similar, showing short fat adult legs and malformed wings. In 1998, Halsell and Kiehart conducted a second-site noncomplementation screen (SSNC) with *zip*, and found that a deficiency that includes *br*, interacts with *zip* in leg

morphogenesis. The genes that were identified from all these screens suggest that both cytoskeletal and adhesion molecules interact with *br* in appendage morphogenesis.

In 2003, Ward et al. performed two large-scale screens with br^1, which led to the proposal that Rho1 signaling plays a central role in directing disc morphogenesis. In these screens they identified *Sb/sbd*, *bs*, the small GTPase *Rho1*, *Tropomyosin 1* or *Tm1* (a cytoplasmic actin binding protein) and several uncharacterized *E(br)* alleles (both EMS mutations and deficiencies). Rho1 is a small GTPase that is activated by guanine nucleotide exchange factors (GEFs) and inactivated by GTPase activation proteins (GAPs) (Van Aelst, 1997). Rho kinase is a key effector of activated Rho1, which activates the myosin regulatory light chain (encoded by *spaghetti squash* or *sqh*) either directly or by inactivating its inhibitor, myosin phosphatase (Van Aelst, 1997). In turn, the myosin regulatory light chain activates myosin heavy chain (encoded by *zip*) to allow it to move along actin filaments (Figure 1.5; Van Aelst, 1997). Genetic studies show that several Rho1 pathway molecules are required for imaginal disc morphogenesis: Rho1, RhoGEF2, myosin phosphatase, myosin regulatory light chain, and nonmuscle myosin heavy chain. SSNC between Rho1 pathway genes and several alleles of *sbd* and *E(br)* also generate malformed legs. Taken together, Rho1 signaling interacts with several genes that are known to have roles in leg imaginal disc development, and thus is likely essential in driving cell shape changes necessary for morphogenesis (Figure 1.5). There are many parts in this model, however, that are currently not clear. For example, *br* genetically interacts with the Rho1 pathway, but how do they interact? Does *br* regulate transcription of Rho1 or any of the Rho1 signaling genes? Are there other pathways controlled by *br* and ecdysone that regulate other aspects of the cell biology of the imaginal discs during metamorphosis?

My work in studying ecdysone-activated, *br*-regulated leg morphogenesis

The projects described in this thesis include both forward and reverse genetic approaches to identify and characterize genes involved in leg morphogenesis. The forward genetic approach involves the SSNC screen for *E(br)* mutations described before (Ward, 2003). My first project was to clone and provide a detailed characterization of one of the *E(br)* mutations, *E(br)165*. *E(br)165* shows strong genetic interactions with *br*, with 100% of the br^1/Y; *E(br)165*/+ flies showing malformed legs (Ward, 2003). *E(br)165* also shows moderate interaction with Rho1 pathway genes, including *Rho1*, *RhoGEF2* and *zip*. Animals homozygous for *E(br)165* are 100% embryonic lethal, with naked cuticle and severe dorsal closure defects. I mapped this mutation and found that it is allelic to *Sec61α*, the major subunit of the translocon complex for co-translational import of proteins into the ER. The *Sec61* tripartite translocon complex is composed of three subunits, α, β, and γ (Johnson, 1999). I renamed this mutant $Sec61\alpha^1$. $Sec61\alpha^1$ specifically perturbs dorsal closure during embryogenesis. After germ band retraction, epidermal tissue covers the ventral and lateral regions of the embryo leaving a large dorsal hole covered only by a squamous extraembryonic epithelium known as the amnioserosa. Coordinated cell shape changes in the absence of cell division in the epidermal cells, coupled with cell shape changes and cell death in the amnioserosa, drive the elongation of the lateral epidermal cell sheets dorsalward, where they meet at the dorsal midline and thereby enclose the embryo (Harden, 2002). Decapentaplegic (Dpp) signaling, which is required to complete dorsal closure by regulating the cytoskeleton in the DME cells and affecting the cell shape changes in amnioserosa, is attenuated in $Sec61\alpha^1$ (Wang, 2010). The characterization of $Sec61\alpha^1$ as an enhancer of *br* gene has important implication for leg morphogenesis. Several of the known *br*-interacting genes are transmembrane proteins, as well as a number of genes that I identified in

the reverse genetic approach described below, suggesting that normal protein secretion may be very important for leg morphogenesis. Importantly, this observation suggests that one or more dose-sensitive secreted protein may be necessary for hormone-regulated imaginal disc morphogenesis.

In addition to my characterization of *Sec61α*^{1} as an enhancer of *br* gene, the Ward lab cloned and characterized several other *E(br)* mutations. For example, a deficiency containing an *E(br)* mutation was found to be due to *ire-1*. Ire-1 is a protein kinase involved in the unfolded protein response (UPR), a process necessary to avoid damage when secretion is disrupted (Plongthongkum, 2007). The UPR is a mechanism by which cells use to cope with ER stresses that may be initiated by an accumulation of unfolded or misfolded proteins in the lumen of the ER. Thus Ire-1 may coordinate with *Sec61α* in regulating secretion during leg development. The second gene that was recently cloned was *Macroglobulin complement-related* (*Mcr*). Mcr is a secreted protein that functions in protein-binding and inhibition of extracellular proteases. *Drosophila Mcr* was shown to promote fungi phagocytosis, possibly by activation of signaling pathways within the phagocytic cell upon binding to the cell's surface (Stroschein-Stevenson, 2006). Preliminary studies show that septate junctions are disrupted during embryogenesis in *Mcr* mutants. Knockdown of *Mcr* in distal leg segments by RNAi generates the malformed leg phenotype, characterized by short fat tarsal segments (unpublished data). We interpret this result to suggest *Mcr* knockdown leads to a defect in cell rearrangements. Thus the ecdysone signaling pathway may regulate septate junctions (possibly through *Mcr*) as cells rearrange during morphogenesis.

Reverse genetics refers to a situation in which we know a gene that is expressed in a particular tissue of a stage of development, but do not know the phenotype associated with loss

of that gene in the developmental event. Therefore in reverse genetics a specific mutation is introduced to a particular gene in order to study it. My second project involved studying how ecdysone and *br* interact to regulate gene expression and morphogenesis in leg imaginal discs at the onset of metamorphosis by using microarray analysis followed by RNAi-induced gene knockdown. To identify genes that are regulated by ecdysone and *br*, I conducted a microarray screen by comparing the genes that are expressed in w^{1118} (wild type) leg discs at the onset of metamorphosis with those expressed in similarly staged br^5 mutant leg discs. br^5 is an amorphic allele, and br^5 leg imaginal discs are arrested at 0 hr as described previously (Figure 1.3). I also compared gene expression in w^{1118} leg discs dissected from -18 hr larvae with those dissected from 0 hr animals. Genes expressed at higher levels at 0 hr relative to at -18 hr in w^{1118} leg discs are considered genes that are induced by ecdysone, whereas genes that are expressed at lower levels at 0 hr relative to -18 hr are considered genes that are repressed by ecdysone. Genes induced or repressed by *br* were similarly identified from the comparison between w^{1118} and br^5 mutant leg discs at 0 hr. Interestingly, there is only a small overlap of genes that are induced or repressed by both ecdysone and *br*. Among the 363 genes induced by ecdysone and the 139 genes induce by *br*, only 31 genes are in common. Similarly, only 40 genes overlap between the 415 genes repressed by ecdysone and 221 genes repressed by *br*. This observation challenges the traditional model of ecdysone signaling. Consistent with the idea that ecdysone does not function strictly upstream of *br*, Northern blot analysis shows that *br* transcripts are present in late third instar larvae, prior to the late larval ecdysone pulse. This suggests that rather than a linear ecdysone->*br*->late genes signaling pathway, *br* may function in concert with EcR or another early gene to regulate leg morphogenesis.

To extend the microarray results, we conducted functional analyses by expressing snapback RNAs for the *br*-induced, ecdysone-induced genes. We have tested RNAi lines for 27 of the 31 genes, and 10 of the 27 genes produce animals that display malformed legs with a frequency of more than 20%. One of them, *CG12026,* which encodes a potential claudin (a transmembrane protein found in septate junctions in invertebrates and tight junction in vertebrates), displays a strong phenotype of malformed legs in all three RNAi lines tested. Another gene that also produces high penetrance of malformed legs is *CG7447*, which encodes a potential cell adhesion or signaling molecule. From the forward genetic screen, secretion pathways were found to be important during leg morphogenesis, and many of the genes I identified from the reverse genetic screen are predicted to encode secreted or transmembrane proteins, including *CG12026* and *CG7447*. Many of these genes identified from the microarray fall in similar pathways with genes identified in the forward genetic screens, suggesting that in addition to interacting with the Rho1 signaling pathway, *br* may also affect leg morphogenesis through cell rearrangements, regulating cell adhesion and modulation of cellular junctions.

My work in the past few years has identified several novel genes that participate in ecdysone-regulated leg morphogenesis. These genes include an essential gene in the secretary pathway, which implies that normal levels of one or more secreted proteins are necessary for leg morphogenesis. Genes that encode septate junction molecules, cell adhesion molecules and extracellular matrix protease were also found in both the forward and reverse genetic screens. These findings may help us to better understand hormone-regulated morphogenesis.

Figure 1.1

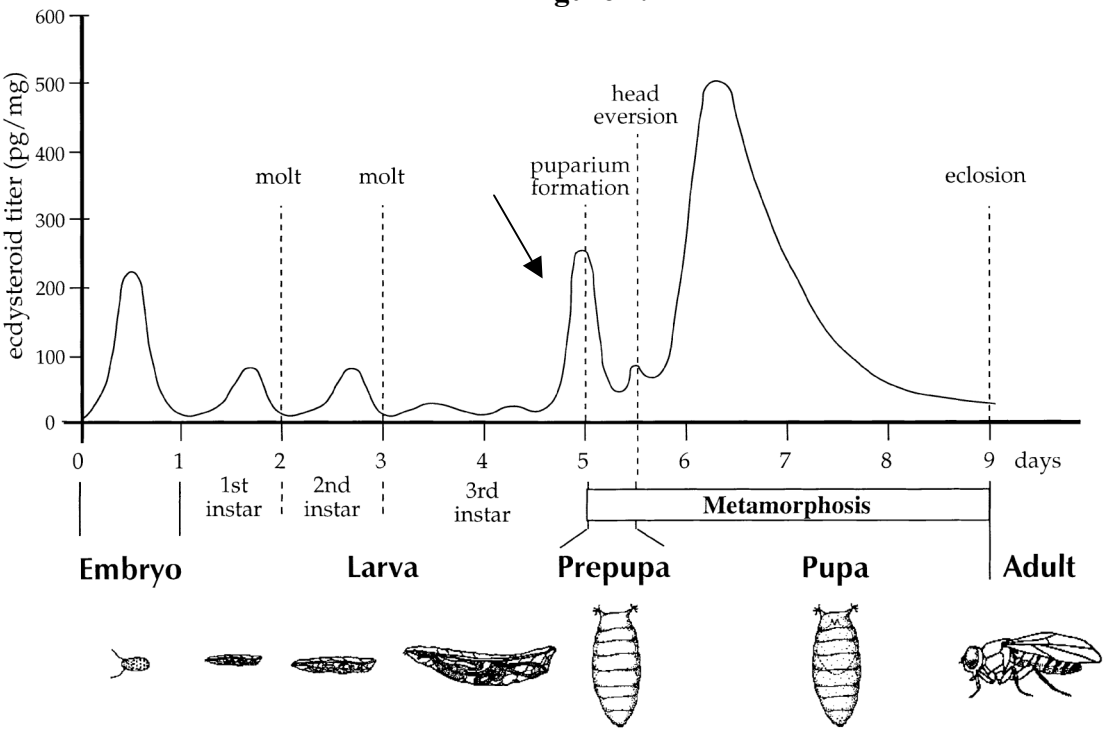

Fig. 1.1. Ecdysone pulses trigger each of the major developmental transitions in *Drosophila* (taken from Thummel, 2001)**.** The major developmental transitions are marked by dotted lines. The late 3rd instar ecdysone pulse (arrow) triggers puparium formation, as well as leg imaginal discs elongation and eversion, which is the focus of our studies.

Figure 1.2

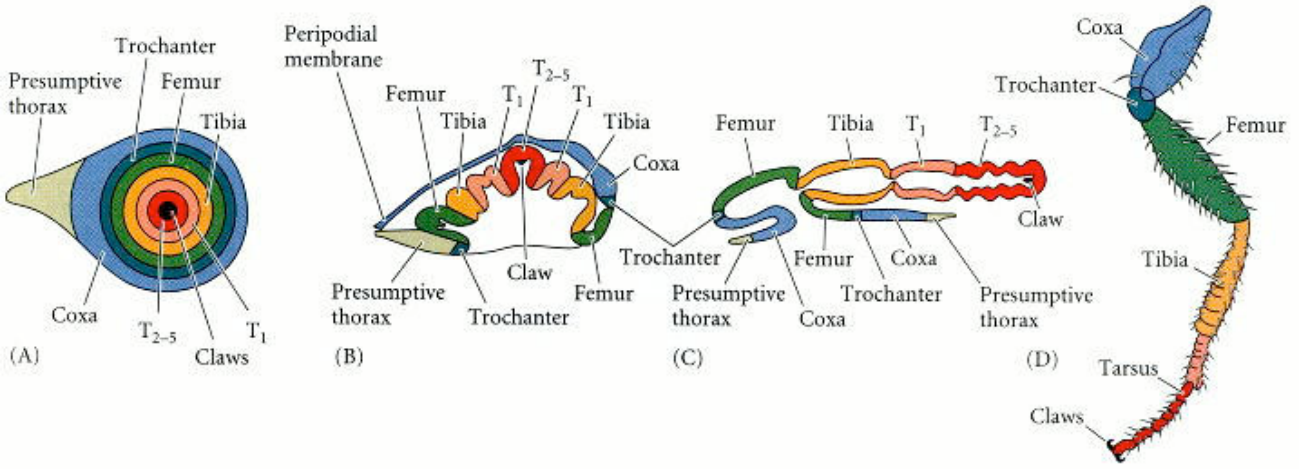

Fig. 1.2. Elongation sequence of *Drosophila* leg disc. (A) Surface view of uneverted disc. (B, C) Longitudinal section through (B) elongating and (C) fully everted leg disc. T1, basitarsus; T2–5, tarsal segments 2–5. (D) Adult leg. (taken from Fristrom and Fristrom 1975)

Figure 1.3

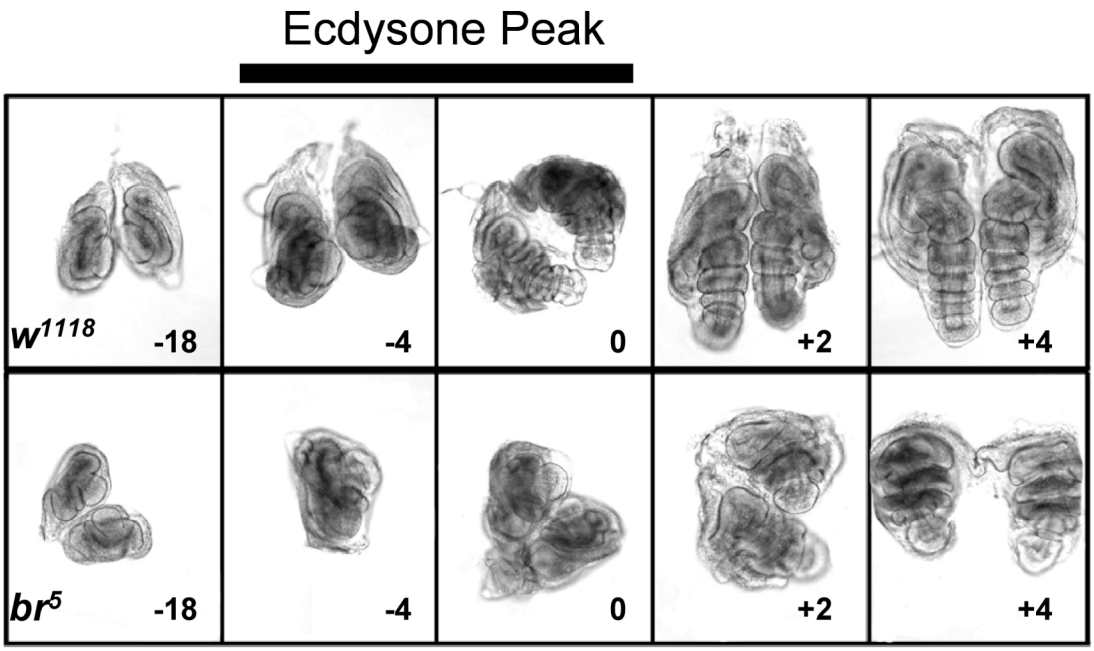

Fig. 1.3. Comparison of morphology of w^{1118} and br^5 leg imaginal discs from -18 hr to +4 hr. 0 hr is referred to as the onset of metamorphosis. Leg imaginal discs were dissected from -18 hr, -4 hr, 0 hr, +2 hr and +4 hr animals of w^{1118} (wild type, top panels) and br^5 mutants (bottom panels). The ecdysone pulse initiates from about 4 hrs before puparium formation. In response to this ecdysone signal, wild type leg discs elongate dramatically from flat epithelium to rudimental adult legs. However, leg discs of br^5 mutants fail to elongate and are arrested at a stage similar to that of wild type 0 hr.

Figure 1.4

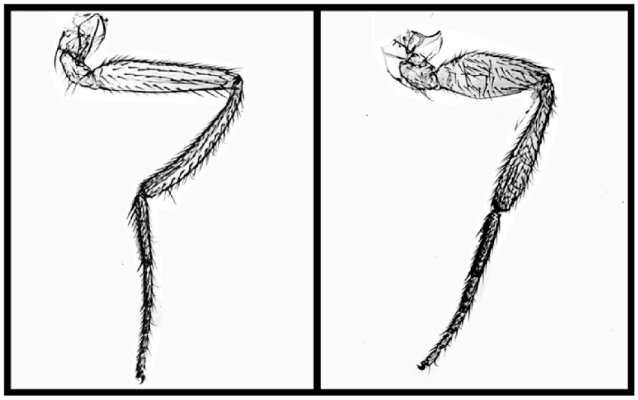

Fig. 1.4. A wild type adult fly leg (left, showing normal morphology) and a *br*^{1} leg (right, showing the malformed leg phenotype). Note the short, fat femur and tibia of the *br*^{1} malformed leg.

Figure 1.5

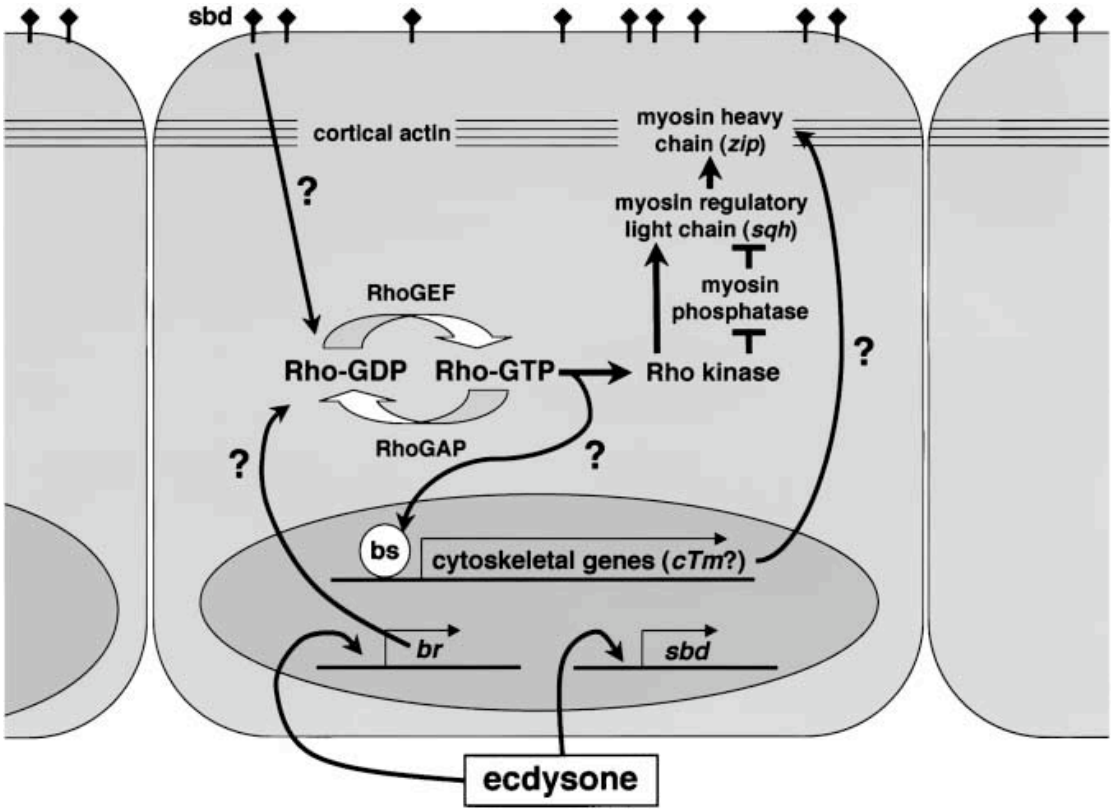

Fig. 1.5. Model of signaling that directs leg imaginal discs morphogenesis (taken from Ward, 2003). Details of the model are described in the text.

Reference

Appel, L. F., Prout, M., Abu-Shumays, R., Hammonds, A., Garbe, J. C., Fristrom, D., and Fristrom, J. (1993). The Drosophila Stubble-stubbloid gene encodes an apparent transmembrane serine protease required for epithelial morphogenesis. Proc Natl Acad Sci U S A 90, 4937-41.

Bayer, C. A., Halsell, S. R., Fristrom, J. W., Kiehart, D. P., and von Kalm, L. (2003). Genetic interactions between the RhoA and Stubble-stubbloid loci suggest a role for a type II transmembrane serine protease in intracellular signaling during Drosophila imaginal disc morphogenesis. Genetics 165, 1417-32.

Bayer, C. A., von Kalm, L., and Fristrom, J. W. (1997). Relationships between protein isoforms and genetic functions demonstrate functional redundancy at the Broad-Complex during Drosophila metamorphosis. Dev Biol 187, 267-82.

Beaton, A. H., Kiss, I., Fristrom, D., and Fristrom, J. W. (1988). Interaction of the Stubble-stubbloid locus and the Broad-complex of Drosophila melanogaster. Genetics 120, 453-64.

Bocchinfuso, W. P., Lindzey, J. K., Hewitt, S. C., Clark, J. A., Myers, P. H., Cooper, R., and Korach, K. S. (2000). Induction of mammary gland development in estrogen receptor-alpha knockout mice. Endocrinology 141, 2982-94.

Condic, M. L., Fristrom, D., and Fristrom, J. W. (1991). Apical cell shape changes during Drosophila imaginal leg disc elongation: a novel morphogenetic mechanism. Development 111, 23-33.

Fristrom, D. (1976). The mechanism of evagination of imaginal discs of Drosophila melanogaster. III. Evidence for cell rearrangement. Dev Biol 54, 163-71.

Fristrom, D. K. (1982). Septate junctions in imaginal disks of Drosophila: a model for the redistribution of septa during cell rearrangement. J Cell Biol 94, 77-87.

Fristrom, D and Fristrom, J. (1993) The Development of Drosophila Melanogaster. 1993 Cold Spring Harbor Laboratory Press.

Gotwals, P. J., and Fristrom, J. W. (1991). Three neighboring genes interact with the Broad-Complex and the Stubble-stubbloid locus to affect imaginal disc morphogenesis in Drosophila. Genetics 127, 747-59.

Grieneisen, M. L., Warren, J. T., and Gilbert, L. I. (1993). Early steps in ecdysteroid biosynthesis: evidence for the involvement of cytochrome P-450 enzymes. Insect Biochem Mol Biol 23, 13-23.

Halsell, S. R., and Kiehart, D. P. (1998). Second-site noncomplementation identifies genomic regions required for Drosophila nonmuscle myosin function during morphogenesis. Genetics 148, 1845-63.

Harden, N. (2002). Signaling pathways directing the movement and fusion of epithelial sheets: lessons from dorsal closure in Drosophila. Differentiation 70, 181-203.

Henrich, V. C., Rybczynski, R., and Gilbert, L. I. (1999). Peptide hormones, steroid hormones, and puffs: mechanisms and models in insect development. Vitam Horm 55, 73-125.

Johnson, A. E., and van Waes, M. A. (1999). The translocon: a dynamic gateway at the ER membrane. Annu Rev Cell Dev Biol 15, 799-842.

Kiss, I., Beaton, A. H., Tardiff, J., Fristrom, D., and Fristrom, J. W. (1988). Interactions and developmental effects of mutations in the Broad-Complex of Drosophila melanogaster. Genetics 118, 247-59.

Milner, M. J. (1977). The eversion and differentiation of Drosophila melanogaster leg and wing imaginal discs cultured in vitro with an optimal concentration of beta-ecdysone. J Embryol Exp Morphol 37, 105-17.

Niederreither, K., Vermot, J., Messaddeq, N., Schuhbaur, B., Chambon, P., and Dolle, P. (2001). Embryonic retinoic acid synthesis is essential for heart morphogenesis in the mouse. Development 128, 1019-31.

Plongthongkum, N., Kullawong, N., Panyim, S., and Tirasophon, W. (2007). Ire1 regulated XBP1 mRNA splicing is essential for the unfolded protein response (UPR) in Drosophila melanogaster. Biochem Biophys Res Commun 354, 789-94.

Postlethwait, J. H., and Schneiderman, H. A. (1970). Induction of metamorphosis by ecdysone analogues. Drosophila imaginal discs cultured in vivo. Biol Bull 138, 47-55.

Stroschein-Stevenson, S. L., Foley, E., O'Farrell, P. H., and Johnson, A. D. (2006). Identification of Drosophila gene products required for phagocytosis of Candida albicans. PLoS Biol 4, e4.

Taylor, J., and Adler, P. N. (2008). Cell rearrangement and cell division during the tissue level morphogenesis of evaginating Drosophila imaginal discs. Dev Biol 313, 739-51.

Thummel, C. S. (2001). Molecular mechanisms of developmental timing in C. elegans and Drosophila. Dev Cell 1, 453-65.

Van Aelst, L., and D'Souza-Schorey, C. (1997). Rho GTPases and signaling networks. Genes Dev 11, 2295-322.

Wang, X., and Ward, R. E. t. (2010). Sec61alpha is required for dorsal closure during Drosophila embryogenesis through its regulation of Dpp signaling. Dev Dyn 239, 784-97.

Ward, R. E., Evans, J., and Thummel, C. S. (2003). Genetic modifier screens in Drosophila demonstrate a role for Rho1 signaling in ecdysone-triggered imaginal disc morphogenesis. Genetics 165, 1397-415.

Chapter 2

Sec61α is required for dorsal closure during *Drosophila* embryogenesis through its regulation of Dpp signaling

Introduction

Dorsal closure is one of the final morphogenetic events necessary for elaborating the body plan of the *Drosophila* larva. Near the midpoint of embryogenesis, immediately after germ band retraction, epidermal tissue covers the ventral and lateral regions of the embryo leaving a large dorsal hole covered only by a squamous extraembryonic epithelium known as the amnioserosa. Coordinated cell shape changes in the absence of cell division in the epidermal cells, coupled with cell shape changes and cell death in the amnioserosa, drive the elongation of the epidermal cell sheets dorsalward, where they meet at the dorsal midline and thereby enclose the embryo.

Dorsal closure in wild type animals involves three distinct stages. Prior to the start of dorsal closure, the cells of the lateral epidermis are polygonal in shape. During the first phase of dorsal closure, known as initiation, the dorsalmost epithelial (DME) cells of the epidermis (also referred to as leading edge cells) elongate in the dorsal-ventral (D-V) axis, whereas the more ventral cells remain polygonal. These DME cells provide an organizing center for the events of dorsal closure. During the initiation phase, the DME cells accumulate actin and myosin in a contractile ring at the level of the adherens junction, which eventually link across these cells to create a continuous actin cable that coordinates the migration of the leading edge of the epithelium (Young et al., 1993). During the second phase of dorsal closure, known as epithelial migration,

the more ventral epidermal cells begin to elongate in the D-V axis as the epidermal sheets migrate towards the dorsal midline. This epidermal migration results from the contraction of the actinomyosin cable in the DME cells through a purse string mechanism (Young et al., 1993; Kiehart et al., 2000; Hutson et al., 2003). The actin cable is also necessary to maintain an organized leading front of the DME cells during the migration process (Bloor and Kiehart, 2002; Jacinto et al., 2002). Over the last several years it has become clear that additional forces are contributed by the amnioserosa, which undergoes coordinated cell shape changes, including contractions perpendicular to the anterior-posterior axis, as well as apical constrictions that eventually lead to those cells being extruded from the epithelium (Kiehart et al., 2000; Harden et al., 2002; Franke et al., 2005; Fernandez et al., 2007). The yolk sac also plays an essential role in these processes as it serves as an attachment substrate for the amnioserosal cells as they contract (Narasimha and Brown, 2004; Reed et al., 2004). Finally, during the completion or zippering phase of dorsal closure, the DME cells meet at the dorsal midline and fuse with DME cells from the contralateral side starting at the anterior and posterior ends and gradually suturing the epidermis towards the center. Again the DME cells show organizing activity by sprouting filopodia and lamellapodia that aid in the alignment and fusion of the two epidermal sheets (Jacinto et al., 2000).

Nearly a hundred genes have been identified whose mutant phenotype includes some defect in dorsal closure. Since it is only the epidermal cells that secrete cuticle late during embryogenesis, a failure to complete dorsal closure produces a characteristic dorsal open phenotype in the resulting dead embryos. Genes that produce this phenotype when perturbed have typically been grouped into two categories, those encoding signaling molecules that are likely required to regulate dorsal closure, and those that encode the cellular effectors of the

process. This later class includes cytoskeletal genes such as *zipper*, encoding non-muscle myosin (Young et al., 1993), *myosin phophatase* (Mizuno et al., 2002), *lethal(2)giant larvae*, (Manfruelli et al., 1996) and *chickadee* (Jasper et al., 2001), encoding profilin. Additionally, extracellular matrix genes including the integrin subunits *lethal(1)myospheroid* (Leptin et al., 1989) and *scab* (Stark et al., 1997), also play roles in dorsal closure, as do genes whose products are components of cellular junctions including *armadillo* (Peifer and Wieschaus, 1990), *canoe* (Miyamoto et al., 1995), *coracle* (Fehon et al., 1994), *discs large* (Perrimon, 1988), and *Neurexin* (Baumgartner et al., 1996).

Genetic and biochemical analyses of the genes predicted to encode signaling molecules reveal that although they fall into many classes, they generally impinge on two different conserved signaling pathways, a Jun amino-terminal kinase (JNK) pathway and a transforming growth factor β (TGF-β) pathway (reviewed in Harden, 2002). The JNK pathway is a conserved mitogen activated protein kinase (MAPK) cascade consisting of sequentially acting serine/threonine kinases that lead to the phosphorylation of the transcription factor DJun. DJun then complexes with DFos (encoded by *kayak*), which together make up the adapter protein 1 (AP-1) transcriptional complex (Riesgo-Escovar and Hafen, 1997a). Although JNK signaling is active in both the amnioserosa and the dorsal epidermis during germ band retraction, it is restricted to the DME cells during the initiation of dorsal closure (Reed et al., 2001).

A critical transcriptional target of the JNK pathway in the DME cell is the TGF-β ligand *decapentaplegic* (*dpp*; Glise and Noselli, 1997; Hou et al., 1997; Riesgo-Escovar and Hafen, 1997b). Dpp binds to its receptor, which is a heterotetramer of two type I receptors encoded by *thick veins* (*tkv*) and two type II receptors encoded by *punt* (reviewed in O'Connor et al., 2006). Upon binding of Dpp to its receptor complex, the receptor phosphorylates the SMAD protein

Mothers Against Dpp (Mad) that then binds to a co-SMAD named Medea and translocates to the nucleus where it regulates the transcriptional response to the Dpp signal. Mutations in *tkv* and *punt* display dorsal open phenotypes (Affolter et al., 1994; Nellen et al., 1994; Arora et al., 1995). Detailed analysis of the cellular events occurring in *tkv* mutant embryos indicates that Dpp signaling is required for the DME cells to maintain an actinomyosin contractile cable and drive the dorsalward movement of the lateral epidermis, as well as for the cell shape changes in the amnioserosa (Fernandez et al., 2007).

Here we report on the isolation and characterization of a strong loss of function mutation in *Sec61α*, the major subunit of the protein translocon complex for co-translational insertion into the endoplasmic reticulum. Surprisingly, zygotic loss of *Sec61α* results in specific defects in dorsal closure during mid-embryogenesis. *Sec61α* mutant embryos initiate dorsal closure correctly, as indicated by normal JNK signaling in the DME cells, but cannot generate or maintain a robust contractile actin/myosin cable, and thus fail during the epithelial migration stage of dorsal closure. Strong reductions in the levels of phosphorylated Mad in the lateral epidermis indicate that Dpp signaling is strongly reduced in *Sec61α* mutant embryos. In support of this idea, an activated Tkv receptor provides a highly penetrant, partial rescue of the dorsal closure defects in *Sec61α* mutant animals.

Materials and Methods

Drosophila Strains

Sec61α^{1} is an EMS induced mutation on the *E(br)165* chromosome reported in Ward et al. (2003). *P{lacW}Sec61α*^{k04917}, *Df(2L)BSC6*, *332.3-Gal4*, *e22c-Gal4*, *T80-Gal4*, *UAS-Dpp, puc*^{E69}, and *w*^{1118} were obtained from the Bloomington *Drosophila* Stock Center (Bloomington, IN). *UAS-Tkv*^{Q253D} (Nellen et al., 1996) was obtained from Matt Gibson (Stowers Institute). *w*^{1118} was used as the wild type strain for all the experiments reported here. All *Drosophila* stocks were maintained on media consisting of corn meal, sugar, yeast, and agar in incubators maintained at a constant temperature of 21°C or in a room that typically fluctuated between 21°C and 22.5°C. Genetic experiments were conducted in incubators controlled at a constant temperature of 25ºC.

Molecular Analysis of *Sec61α*^{1}

Complementation analyses confirmed a lethal mutation in the region uncovered by *Df(2L)BSC6* (breakpoints 26D3;26F7) that also failed to complement the P-element allele *P{lacW}Sec61α*^{k04917}. Sequencing of genomic DNA isolated from homozygous mutant late embryos (by the DNA Facility of the Iowa State University Office of Biotechnology in Ames, IA) confirmed that the chromosome had a mutation in *Sec61α.* Both DNA strands were sequenced to confirm this result.

To generate a *Sec61α* genomic rescue construct, we PCR amplified genomic DNA isolated from *w*^{1118} embryos using the following primers: 5'-TCGGCACTAGCACTGAATACT-3' and 5'-ATAGCAGGTAGCCGAACGTG-3'. This generated a 4.4 kb genomic fragment containing all of *Sec61α* and extending ~100 bp into the upstream gene *DLP* and ~350 bp into the

downstream gene *CG9536* (Note that these genes are oriented in opposite directions, and thus the genomic rescue construct only extends into the 5' UTR of each gene). We blunt-end ligated this fragment into a StuI-cut pCasper 4 vector (Thummel et al., 1988). We checked orientation by restriction digest and sequenced the *Sec61α* portion of the plasmid (Iowa State University DNA Facility). The plasmid was injected into w^{1118} embryos at the Duke University Model System Genomics facility (Duke University, Durham, NC). We crossed four independent third chromosome inserts into our $Sec61\alpha^{1}$ stock, and all four rescued the embryonic lethality of $Sec61\alpha^{1}$.

Lethal Phase and Phenotypic Analyses

$Sec61\alpha^{1}$, $P\{lacW\}Sec61\alpha^{k04917}$ and *Df(2L)BSC6* were balanced with *CyO, P{w⁺, Dfd-EYFP}* (Le et al., 2006) in order that mutant embryos and larvae could be unambiguously identified by the absence of YFP. In order to identify mutant animals at earlier stages of development, we also balanced $Sec61\alpha^{1}$ with *CyO, P{ftz/lacB}*. Embryos were collected for four hours at 25ºC, aged for twelve hours and then selected based upon the absence of YFP. Embryonic lethality was determined as the percentage of unhatched embryos 48 hours after selecting non-YFP-expressing mutant embryos produced through a four-hour egg collection. Larval lethality was determined as the percentage of non-pupariating mutant larvae seven days after selecting newly hatched mutant larvae. Pupal lethality was determined as the percentage of non-eclosing mutant pupae ~seven days after pupariating. All experiments were performed in triplicate and means with standard deviations were determined. Non-hatched embryos were dechorionated in 6% sodium hypochloride, mounted on microscope slides in Hoyer's medium and subsequently examined for cuticular phenotypes on a Nikon Eclipse 80*i* compound microscope. All cuticular phenotypes

were documented on a Nikon Eclipse 80*i* compound microscope equipped with a Photometrics CoolSNAP *ES* high performance digital CCD camera. Photomicrographs were cropped and adjusted for brightness and contrast with Adobe Photoshop (version CS3, San Jose, CA), and figures were compiled in Adobe Illustrator (version CS3, San Jose, CA).

Time-lapse movies were generated by mounting stage 17 *Sec61α*^{l}*/CyO, P{w*$^{+}$*, Dfd-EYFP}* and *Sec61α*^{l} mutant embryos on apple juice plates. We first collected a fluorescence image to distinguish the mutant and heterozygous embryos by YFP expression, and then automatically collected brightfield images every minute for 140 minutes using MetaMorph (Molecular Devices, Sunnyvale, CA) software on a Nikon Eclipse 80*i* compound microscope equipped with a Photometrics CoolSNAP *ES* high performance digital CCD camera using a 4X Nikon Plan Apo lens.

Antibody Production and Immunostaining

A Spaghetti squash (Sqh)-GST fusion protein was generated by blunt-end ligating nucleotides 217 to 811 of GenBank nucleotide sequence AY122159 (generated by PCR and verified by sequence analysis) into a PGEX2TK vector (GE Healthcare Bio-Sciences AB, Uppsala, Sweden) digested with SmaI. This fragment represents the entire coding sequence of Sqh. The protein was overexpressed in *E. Coli* BL21 (DE3) cells, and purified on glutathione sepharose 4 fast flow (GE Healthcare) according to standard procedures (Rebay and Fehon, 2000). Purified protein was used for antibody generation in mice at the Pocono Rabbit Farm and Laboratory Inc. (PRF&L, Canadensis, PA).

Embryos were fixed and processed for antibody staining as described (Fehon et al., 1991). Embryonic staging was determined by gut morphology. The following primary antibodies were

used at the given dilutions: mouse anti-Neuroglian 1:100 (clone BP104 from the Developmental Studies Hybridoma Bank at the University of Iowa, Iowa City, IA), mouse anti-β-galactosidase 1:100 (clone 40-1a, DSHB), mouse anti-Fasciclin III 1:100 (clone 7G10, DSHB), mouse anti-phosphoMAD 1:250 (from P. ten Dijke), mouse anti-Sqh 1:1000, guinea pig anti-Uninflatable 1:20 (Zhang and Ward, 2009), rabbit anti-GFP 1:250 (Clontech, Mountain View, CA), mouse anti-Coracle 1:400 and guinea pig anti-Coracle 1:10,000 (gifts from Richard Fehon, University of Chicago; Fehon et al., 1994), and FITC conjugated monoclonal anti-phosphotyrosine (Sigma, St. Louis, MO) 1:50. Secondary antibodies were obtained from Jackson ImmunoResearch Laboratories (West Grove, PA) and used at 1:800. Alexa Fluor 555 conjugated wheat germ agglutinin (WGA) was used at a concentration of 5μg/ml (Invitrogen, Carlsbad, CA). Rhodamine conjugated Chitin Binding Probe (CBP) was used at 1:500 according to the manufacturers recommendation (New England Biolabs Inc., Beverly, MA). Confocal images were acquired on a Zeiss LSM510 Meta Laser Scanning Confocal Microscope (Carl Zeiss Inc, Thornwood, NY). Photomicrographs were cropped and adjusted for brightness and contrast with Adobe Photoshop, and figures were compiled in Adobe Illustrator. The photomicrographs used to compile Fig. 4 were additionally modified with an unsharp mask filter (50%, 3 pixel radius, 5 level threshold) in Adobe Photoshop.

Dpp and tkv^{Q253D} Rescue Experiments

We first individually recombined *T80-Gal4*, *e22c-Gal4*, and *332.2-Gal4* onto *Sec61α^{l}* chromosomes, and balanced then over *CyO, P{w^{+}, Dfd-EYFP}*, creating *-Gal4, *Sec61α^{l}/CyO, P{w^{+}, Dfd-EYFP}*. We then crossed *UAS-tkv^{Q253D}* and *UAS-Dpp* into *Sec61α^{l}/CyO, P{w^{+}, Dfd-EYFP}*, creating *Sec61α^{l}/+; UAS-tkv^{Q253D}/+* and *Sec61α^{l}/+; UAS-Dpp/+*. Finally we crossed

these *Gal4* and *UAS-tkv*^{Q253D} lines together and collected embryos from a 4 hour collection. We aged the embryos for 16 hours such that all the embryos would be 16-20 hours after egg laying. At this point all *Sec61α*^{1}/+ embryos would have completed dorsal closure and secreted cuticle that would prevent the embryos from being stained with antibodies. We fixed and stained the embryos as described above, and examined all stained embryos for dorsal open phenotypes. We considered an embryo to have been rescued if the dorsal hole was small and the brain and guts were completely confined to the interior of the animal. Since only half of the *Sec61α*^{1} mutant embryos would contain either *UAS-tkv*^{Q253D}/+ or *UAS-Dpp*/+, the % rescue reported in Table 2.2 would have a theoretical maximum value of 50%. The experiment was done in triplicate and mean with standard deviations were calculated.

Results

Identification of *Sec61α* alleles

While mapping an EMS-induced mutation recovered from a screen for dominant modifiers of the transcription factor *broad* (Ward et al., 2003), we identified a mutation that failed to complement *Df(2L)BSC6* (cytology 26D3;26F7). We tested loss of function mutations for genes that map to this interval and found that the mutation failed to complement *P{lacW}Sec61α*^{k04917} (Table 2.1). *P{lacW}Sec61α*^{k04917} (hereafter referred to as *Sec61α*^{k04917}) has a *P*-element inserted into the second intron of the *Sec61α* gene (Fig. 2.1A). *Sec61α* encodes the major subunit of the tripartite translocon complex required for co-translational insertion of proteins into the endoplasmic reticulum (Johnson and van Waes, 1999). Sequence analysis of genomic DNA isolated from mutant embryos revealed a nonsense mutation in *Sec61α* (G/C to A/T transition at nucleotide 683 of GenBank sequence **AY069569** generating a Trp^{193} to stop mutation; Fig. 2.1A). We have therefore named this mutation *Sec61α*^{1}. *Sec61α*^{1} is predicted to encode a protein that is prematurely truncated at the end of the fifth of ten transmembrane domains, almost certainly creating a nonfunctional protein (Fig. 2.1A).

Lethal phase analyses of *Sec61α*^{1} support the molecular analysis and indicate that it is an amorphic allele. Specifically, *Sec61α*^{1}, *Df(2L)BSC6* and *Sec61α*^{1}*/Df(2L)BSC6* mutant animals are completely embryonic lethal, and cuticle preparations of the dead embryos for all of these genotypes showed no ventral denticle belts, differentiated head skeleton or any recognizable cuticle (Table 2.1 and Figs. 2.1C, D and data not shown). In contrast, *Sec61α*^{k04917} and *Sec61α*^{1}*/Sec61α*^{k04917} mutant animals showed only ~50% embryonic lethality (Table 2.1), with

the majority of the animals dying in early first instar, suggesting that *Sec61α*^{k04917} is a hypomorphic allele.

Sec61α mutant animals show specific defects in dorsal closure during embryogenesis

Since *Sec61α*^{1} mutant animals have little to no epidermal cuticle, we were able to examine the terminal phenotype of these animals by indirect immunofluorescence using antibodies against Coracle (Cor). Cor is expressed in all ectodermally derived epithelial cells and localizes to septate junctions (Fehon et al., 1994). All late stage 17 *Sec61α*^{1} mutant embryos have no epidermis over the dorsal third of the embryo with the brain and gut extruded through the dorsal hole (Fig. 2.2B), indicating a completely penetrant defect in dorsal closure. There is little variability in this terminal phenotype as we never observed dorsally closed or partially closed mutant embryos. *Sec61α*^{1}*/Df(2L)BSC6* mutant embryos showed identical phenotypes in both penetrance and expressivity (Fig. 2.2C). Interestingly, *Df(2L)BSC6* mutant embryos also survived to late embryogenesis and showed identical defects in dorsal closure (Fig. 2.2D).

To demonstrate that the dorsal closure defects of *Sec61α*^{1} were due to the loss of *Sec61α*, we generated a genomic rescue construct consisting of the entire *Sec61α* gene and extending ~100 bp into the 5' UTR of the upstream gene *DLP* and ~350 bp into the 5' UTR of the downstream gene *CG9536* (Fig. 2.1A; note the genes are oriented in opposite directions). Four independent insertions of this construct rescued the embryonic lethality, and thus the dorsal closure defect of *Sec61α*^{1} mutant animals (Fig. 2.1E and Table 2.1). The rescue, however, was not complete with *Sec61α*^{1}. For example, although 95 ($\pm$ 1)% of *Sec61α*^{1}*;P{Sec61α line CM15-1}* animals hatched as larvae, none of them eclosed and most died as pharate adults (Table 2.1). Rescue of *Sec61α*^{1}*/Sec61α*^{k04917} mutant animals with this *Sec61α* genomic construct was more

complete, resulting in >70% viable adults (Table 2.1). Together these results suggest that either there is a very strong requirement for *Sec61α* in late pupae that the rescue constructs cannot produce (but is enough in conjunction with $Sec61\alpha^{k04917}$), or that the $Sec61\alpha^{1}$ chromosome possesses a second-site pupal lethal mutation.

Although $Sec61\alpha^{1}$ mutants showed a completely penetrant defect in dorsal closure, most other morphogenetic events occurring during mid embryogenesis continued to completion. Most notably, 100% of $Sec61\alpha^{1}$ mutant animals have normally involuted heads, even though dorsal closure has completely failed ($n > 500$ mutant embryos observed; Fig. 2.2B). We therefore assessed other embryonic morphogenetic events in $Sec61\alpha^{1}$ mutant embryos. To assess the morphogenesis of the peripheral nervous system we stained wild type and $Sec61\alpha^{1}$ mutant stage 14 embryos with an antibody that recognizes Neuroglian, and found that peripheral nervous system development was unaffected by lack of zygotic *Sec61α* expression (Supplemental Figs. 2.1A, B). Similarly we assessed the morphogenesis of the salivary glands by staining stage 14 wild type and $Sec61\alpha^{1}$ mutants with antibodies against Cor, and again found no differences (Supplemental Figs. 2.1C, D). We next used chitin binding probe, wheat germ agglutinin and antibodies against Uninflatable (a protein that localizes to the apical plasma membrane in tracheal cells; Zhang and Ward, 2009) to assess tracheal morphogenesis. Although the patterning of the tracheal system was unaffected in $Sec61\alpha^{1}$ mutant embryos, the diameter of the tracheal tubes was smaller (Supplemental Figs. 2.1E, F and data not shown). Tracheal morphogenesis requires the secretion of chitin into the lumen of the tracheae starting at stage 14. This chitin forms a cylinder in the center of the lumen that is required for proper radial expansion of the tracheae (Araujo et al., 2005; Devine et al., 2005; Tonning et al., 2005). Later in development, the expression and secretion putative chitin modifying enzymes encoded by *serpentine* and

vermiform are required for tracheal length control (Luschnig et al., 2006; Wang et al., 2006). It appears that chitin secretion into the tracheal lumen is reduced in *Sec61α*^{1} mutant embryos resulting in the diametric defects, however since the tracheae are not convoluted nor show other tracheal length defects, it is likely that the secretion of the putative chitin modifying enzymes occurred normally. One additional tracheal defect that was observed was a failure in the fusion of some tracheal metameres. ~ 50% of *Sec61α*^{1} mutant embryos had at least one discontinuity (n = 98, data not shown). Finally, just to exclude the possibility that *Sec61α* mutant embryos were dying about the time of dorsal closure, thus rendering these defects nonspecific, we generated time-lapse movies of late stage 17 *Sec61α*^{1} and *Sec61α*^{1}*/CyO, Dfd-EYFP* embryos and observed that the *Sec61α*^{1} mutant embryos were alive and moving through the end of embryogenesis (data not shown). Taken together these observations suggest that zygotic loss of *Sec61α*^{1} has very specific effects on the morphogenetic process of dorsal closure during mid embryogenesis.

Dorsal closure initiates but fails during the epithelial migration phase in *Sec61α* mutant embryos

In order to determine how zygotic loss of *Sec61α* might result in such specific defects in dorsal closure we first carefully examined the dorsal closure defects in *Sec61α*^{1} mutant embryos through a time course analysis. We collected wild type and mutant embryos at one hour intervals, aged them to 12-16 hours after egg laying, and stained them with antibodies against Cor to visualize the epidermis. Overall, *Sec61α* mutant embryos showed a one to two hour developmental delay and were going through dorsal closure when their heterozygous siblings had already completed the process. We therefore used gut and head morphology to accurately stage the animals. At the end of germ band retraction in mutant and wild type animals the cells of

the lateral epidermis are polygonal in shape. During the initiation phase of dorsal closure in stage 13 wild type embryos the DME cells elongate in the dorsal-ventral axis (Fig. 2.3A), whereas the more ventral cells remain polygonal. DME cells in stage 14 *Sec61α*^{1} mutant embryos also elongate in the dorsal-ventral axis, suggesting that initiation of dorsal closure had begun normally (Fig. 2.3C). Subsequently, during the epithelial migration phase of dorsal closure in wild type embryos, the more ventral lateral epidermal cells elongate dorsally as the epidermal sheets are coordinately pulled towards the dorsal midline (Figs. 2.3B, D). During this process the leading edge of the epidermis maintains an organized appearance showing a continuous curve along the anterior-posterior axis (Fig. 2.3B). In contrast, the leading edge of the epidermis appears disorganized and the lateral epidermal cells fail to fully elongate in stage 15 *Sec61α*^{1} mutant embryos (Fig. 2.3E). The DME cells eventually revert to a non elongated state (Figs. 2.3E, G). Finally, during the zippering phase of dorsal closure in wild type embryos (stage 15), the DME cells meet at the dorsal midline and fuse with the contralateral leading edge cells starting at the anterior and posterior ends and gradually suturing the epidermis towards the center (Figs. 2.3D, F). In *Sec61α*^{1} mutant embryos, although there is some zippering observed at the anterior and posterior ends of the epidermis, the majority of the DME cells never come in close apposition and therefore cannot fuse. Subsequently, either the amnioserosa tears away or is degraded (presumably through apoptosis), allowing the underlying brain and guts to protrude through the epidermal hole (Fig. 2.3G). Although we noted some variability in the extent to which *Sec61α*^{1} mutant embryos completed the epithelial migration phase, we never observed mutant embryos that were completely closed ($n > 500$ mutant embryos observed). Taken together, these observations suggest that initiation occurs normally in *Sec61α*^{1} mutant embryos, but that epithelial migration is severely affected.

Since the guts protrude from the dorsal surface in late stage 16 *Sec61α*^{1} mutant embryos (Fig. 2.3G), we wanted to address when the amnioserosa was breaking down in these animals. We therefore stained wild type and *Sec61α*^{1} mutant embryos with antibodies against phospho-tyrosine to visualize amnioserosal cells in addition to the epidermis. We found that the amnioserosa was completely intact through stage 14 in the mutant embryos, just as in wild type (Figs. 2.3 H, I), but started to tear apart from the epidermis in stage 15 mutant embryos (Fig. 2.3 K).

One of the hallmarks of the specification of the DME cells is the execution of a Jun amino terminal kinase (JNK) signaling pathway. At the end of this signaling pathway, Jun and Fos induce the expression of *puckered* (*puc*), which encodes a phosphatase that negatively regulates the JNK pathway (Ring and Martinez Arias, 1993; Hou et al., 1997; Riesgo-Escovar and Hafen, 1997b). We therefore examined embryos produced by *Sec61α*^{1}*/Cyo, Dfd-EYFP ; puc*^{E69}/+ parents for the expression of *puc* (as determined by β-gal expression of the *puc* enhancer trap). In two independent experiments we examined 285 stage 14-16 embryos that we could unambiguously identify as either *Sec61α*^{1} or one of the two *EYFP* genotypes (*Sec61α*^{1}*/Cyo, Dfd-EYFP* or *Cyo, Dfd-EYFP/Cyo, Dfd-EYFP*). We could also distinguish each embryo as *puc*^{E69}*/ puc*^{E69}, *puc*^{E69}/+, or +/+. The same percentage of *Sec61α*^{1} embryos expressed *puc*, as did their non-mutant siblings (67% in both cases, with a Mendelian expectation of 75%). When we examined individual *Sec61α*^{1}*;Puc*^{E69}/+ embryos we found that *puc* was clearly expressed in the DME cells. In fact, to the extent that we could tell by confocal microscopy, each DME cell expressed *puc* (Figs. 2.4A, B). Thus, loss of *Sec61α* did not appear to affect the JNK signaling pathway in the DME cells associated with the initiation of dorsal closure.

Zygotic loss of *Sec61α* attenuates Dpp signaling during dorsal closure

Another major consequence of JNK signaling in the DME cells is the expression and secretion of Dpp (Ring and Martinez Arias, 1993; Hou et al., 1997; Riesgo-Escovar and Hafen, 1997b). Dpp is a TGF-β/BMP ligand that binds to a receptor complex consisting of a Type-I receptor (encoded by *thick veins*, *tkv*) and a type-II receptor (encoded by *punt*, *put*) in the epidermal cells and in the amnioserosa (Affolter et al., 1994; Nellen et al., 1994; Simin et al., 1998). All three of these proteins go through the secretory pathway and thus must enter the endoplasmic reticulum through Sec61α. Mutations in *tkv* and *put* show similar dorsal closure phenotypes including initial elongation of the DME cells and subsequent failure to maintain a uniform migration front at the leading edge with non elongated ventral epidermal cells (Riesgo-Escovar and Hafen, 1997a; Simin et al., 1998; Ricos et al., 1999). These defects in the organization of the DME cells and inability to drive the epidermal migration in *tkv* mutant embryos result in part from a loss of an actinomyosin cable in the DME cells (Zahedi et al., 2008). We therefore examined the expression of the myosin regulatory light chain (encoded by *spaghetti squash*; Karess et al., 1991) in the DME cells in $Sec61\alpha^{1}$ mutant embryos. Notably, Sqh was absent or very strongly reduced at the leading edge of the DME cells of stage 14 mutant embryos compared to wild type embryos (Figs. 2.5A, B). Sqh expression in the lateral epidermis was similar, however, between wild type and $Sec61\alpha^{1}$ mutant embryos, indicating that this is a specific loss of the myosin cable in the DME cells of $Sec61\alpha^{1}$ mutant embryos.

In order to more directly determine whether lack of zygotic *Sec61α* expression affected Dpp signaling, we examined the levels of phosphorylated Mothers Against Dpp (Mad) in wild type and $Sec61\alpha^{1}$ mutant embryos. The expression of phosphorylated Mad (pMad) has been extensively used as a readout of Dpp signaling at various stages of *Drosophila* development

including during dorsal closure (e.g. Dorfman and Shilo, 2001; Fernandez et al., 2007). In early stage 14 wild type embryos, pMad is found at high levels in 4-5 rows of lateral epidermal cells ventral to the DME cells (Fig. 2.5C). In contrast, in four independent collections of *Sec61α^{l}* mutant embryos, we consistently observed strongly reduced or absent pMad staining in early stage 14 mutant embryos (Fig. 2.5D; *n*=51 early stage 14 *Sec61α^{l}* mutant embryos).

If a mutation in *Sec61α* affects dorsal closure through the expression of Dpp or one of its receptors, we reasoned that it should be possible to rescue that defect by specifically activating the Dpp signaling pathway during mid embryogenesis. We therefore used the UAS-GAL4 system (Brand and Perrimon, 1994) to express a constitutively activated form of the Tkv receptor (Nellen et al., 1996), *tkv^{Q253D}*, in the epidermis (using *e22c-* and *T80-Gal4;* Jacinto et al., 2000) or in the amnioserosa (*332.3-Gal4*; Harden et al., 2002) of *Sec61α^{l}* mutant embryos. Since the expression of *tkv^{Q253D}* did not rescue the cuticle defect of *Sec61α^{l}* mutant embryos (data not shown), we assessed the terminal phenotype of the mutant embryos by indirect immunofluorescence of 16-20 hour old mutant embryos stained with Cor. In control experiments we first determined that 100% (*n*=206) of 16-20 hour AEL *Sec61α^{l}* mutant embryos robustly stain with Cor antibodies, whereas only 1% (*n*=150) of *Sec61α^{l}*/+ embryos stain well with Cor. We could thus identify the *Sec61α^{l}* mutant embryos in these experiments with near certainty. In addition we performed control experiments to examine the phenotypes of *Sec61α^{l},*-Gal4/Sec61α^{l}* (where * indicates *e22c* or *332.3*), and found that 100% of the embryos that stained with Cor at 16-20 hours AEL were completely dorsally open with the brains and guts extruded (Fig. 2.6A and data not shown). Experimentally we crossed *,*-Gal4, Sec61α^{l}/CyO* flies to *Sec61α^{l}/+;UAS- tkv^{Q253D}*/+ flies. Complete rescue of dorsal closure would result in 50% of the Cor staining embryos displaying a completely open dorsal surface and 50% showing a closed

dorsal surface. Animals expressing *UAS- tkv^{Q253D}* using all three *Gal4* lines showed nearly completely penetrant rescue (Table 2.2). The degree of rescue was slightly variable, ranging from animals possessing a small dorsal hole, but with the brain and guts completely contained within the embryo (Fig. 2.6B), to animals with the lateral epidermal sheets completely apposed at the dorsal midline, but not necessarily fused (Fig. 2.6C). In general *e22c-Gal4* produced a stronger degree of rescue than *T80-Gal4* or *332.3-Gal4*. We conducted an identical set of experiments using *UAS-Dpp* instead of *UAS- tkv^{Q253D}*. We observed ~20% of the expected rescue using *e22c-Gal4* to drive the expression of *Dpp*, with less penetrant rescue resulting from expression driven by *T80-Gal4* and *332.3-Gal4* (Table 2.2). The degree of rescue was similarly variable with the *UAS- tkv^{Q253D}*experiments (data not shown). Taken together, these results strongly indicate that zygotic loss of *Sec61α* results in specific defects in dorsal closure through a reduction in Dpp signaling during mid embryogenesis.

As a further test of the model that zygotic loss of *Sec61α* results in reduced Dpp signaling during mid embryogenesis, we analyzed midgut morphogenesis in *Sec61α^{1}* mutant embryos since Dpp is known to be required for this process (Immergluck et al., 1990; Panganiban et al., 1990). During midgut morphogenesis Dpp is secreted from the visceral mesoderm starting at stage 14 and is required in the underlying endoderm for the second midgut constriction. By stage 16 a four-chambered midgut is clearly apparent in wild type animals (Fig. 2.7A). Consistent with a reduction in Dpp signaling, we never observed a four-chambered midgut in stage 16 *Sec61α^{1}* mutant embryos ($n > 100$ mutant embryos). Although the guts were sometimes more extremely affected, the most obvious defect observed was a lack of the second midgut constriction (Fig. 2.7B). Since *Sec61α^{1}* mutant embryos eventually display extruded guts due to defective dorsal closure, and we observed a developmental delay in these animals, we wanted to be sure that we

were not simply observing mutant animals prior to the formation of this constriction. We therefore examined the midgets in early stage 17 *Sec61α*^{1} mutant embryos that were expressing *tkv*^{Q253D} in the epidermis (using *e22c-Gal4*). Epidermal expression of Tkv^{Q253D} was sufficient to rescue dorsal closure to the point of preventing gut extrusion, but is not predicted to rescue any Dpp signaling defects in the mesoderm and underlying endoderm. We never observed a four-chambered midgut in these animals (Fig. 2.7C), consistent with the notion that Dpp signaling is particularly sensitive to the zygotic loss of *Sec61α* during mid embryogenesis.

Discussion

Zygotic loss of *Sec61α* has a specific effect on dorsal closure

Sec61α encodes the major subunit of the translocon complex in the endoplasmic reticulum (reviewed in Johnson and van Waes, 1999). The translocon complex consists of three subunits: Sec61α, β, and γ, with the 10 transmembrane domain α subunit forming the major pore through the membrane. The truncated product of the *Sec61α^{1}* mutation, if expressed at all, would almost certainly produce a nonfunctional protein, and therefore prevent proteins from entering the ER and secretory pathway. The identical phenotypes observed in *Sec61α^{1}*, *Sec61α^{1}/Df(2L)BSC6* and even *Df(2L)BSC6* homozygous mutant embryos demonstrate that *Sec61α^{1}* is a nonfunctional, amorphic allele.

Sec61α is produced maternally and the maternal complement is likely partially functional at least through mid embryogenesis. The Berkeley *Drosophila* Genome Project gene expression pattern database shows that *Sec61α* is strongly expressed in stage 1-3 embryos (Tomancak et al., 2002). In addition, a *Sec61α:GFP* protein trap transgenic line is expressed in germline cysts (Snapp et al., 2004). Evidence that the maternal contribution still has function in mid embryogenesis includes direct and indirect measures of protein expression in *Sec61α^{1}* mutant embryos (that have a complete zygotic loss of *Sec61α*). For example, the transmembrane protein Neuroglian is expressed in *Sec61α^{1}* mutant embryos at levels indistinguishable to those of wild type embryos that were fixed and stained in parallel and imaged using the same parameters (Supplemental Figs. 2.1). We similarly observed only a slight reduction in the expression of the transmembrane proteins E-cadherin and α-integrin in mutant embryos as compared to wild type (data not shown). Since these proteins could have been secreted hours previous, however, we

wanted to assess a secreted protein that is not expressed until later in development. We can observe this indirectly through the function of Serpentine and Vermiform, two putative chitin deacetylases that are first synthesized in stage 12 embryos and subsequently secreted into the tracheal lumen at stage 14. These enzymes are required for tube length control in tracheae (Luschnig et al., 2006; Wang et al., 2006), and although there is reduced chitin secreted into the tracheae of *Sec61α*^{1} mutant embryos, tracheal length is not affected, suggesting that these enzymes were secreted and functioned properly (Supplemental Figs. 2.1). Taken together, these observations suggest that the maternal contribution of *Sec61α* still has some function (and perhaps fairly good function) at mid embryogenesis. By the end of embryogenesis, however, secretion appears to be more strongly affected as the mutant embryos fail to secrete chitin and thus display a naked cuticle phenotype.

At mid embryogenesis, the zygotic loss of *Sec61α* produces a highly specific and fully penetrant defect in dorsal closure. This phenotype is observed in *Sec61α*^{1}, *Sec61α*^{1}*/Df(2L)BSC6*, and even *Df(2L)BSC6* mutant animals. We were intrigued by the fact that although dorsal closure was completely disrupted in these embryos, head involution occurred normally, and therefore examined other developmental processes occurring roughly concurrently with dorsal closure that required secreted or transmembrane proteins for proper execution. For example, tracheal patterning and morphogenesis are dependent on several signaling pathways, most notably FGF signaling, which requires the transmembrane receptor Breathless in the tracheal cells to receive a secreted FGF signal encoded by *branchless* (reviewed in Affolter and Caussinus, 2008). Although the early events of patterning occur prior to dorsal closure, the formation and extension of the dorsal branch occurs during stages 12-15 of embryogenesis and require both the aforementioned FGF signaling pathway as well as Notch-Delta signaling to inhibit the cells

ventral to the dorsal tip from becoming migratory. In addition, connecting the adjacent metamers to form a complete tracheal network requires cell adhesion and specialized vesicle trafficking in the fusion cells that occurs during stages 14-16 (Jiang et al., 2007). Although one or two of metameres in about half of the embryos are not completely fused, the vast majority of these fusion events occurs normally, and thus it appears that tracheal morphogenesis is largely occurring normally in *Sec61α*^{1} mutant embryos (Supplemental Fig. 2.1 and data not shown). Similarly, the migration of the neurons and glia of the peripheral nervous system require guidance from secreted ligands and transmembrane receptors (reviewed in Cooper, 2002). We found that the peripheral neurons are correctly positioned in the *Sec61α*^{1} mutant embryos, again suggesting that the secretion of all these factors had occurred normally. Finally, the salivary gland is specified during stage 11 of embryogenesis, invaginates and executes a posterior migration over the visceral mesoderm during stage 14 (reviewed in Myat, 2005). This process requires the apposition of the salivary gland epithelium with the visceral mesoderm in a process requiring integrins. As shown in Fig. Supplemental Figs. 2.1, posterior migration of the salivary gland occurred normally in *Sec61α*^{1} mutant embryos. Thus, of all the morphogenetic events occurring simultaneously during mid embryogenesis, zygotic loss of *Sec61α* specifically perturbs dorsal closure.

It should be noted that zygotic loss of *Sec61β* does not show a similar defect in dorsal closure, but rather only shows defects in cuticle secretion late in embryogenesis (Valcarcel et al., 1999). Maternal loss of *Sec61β*, however, results in earlier embryonic lethality with defects in D-V patterning resulting from improper Gurken signaling (Valcarcel et al., 1999; Kelkar and Dobberstein, 2009). *Sec61β* encodes a peripheral component of the translocon complex that is not essential for protein translocation across the ER or for cell viability in yeast (Toikkanen et

al., 1996; Leroux and Rokeach, 2008). Recent work in yeast has rather demonstrated a unique role for *Sec61β* in post-ER trafficking to the plasma membrane via the exocyst (Toikkanen et al., 2003). In support of this, Kelkar and Dobberstein (2009) showed that Gurken is normally inserted into the ER in *Sec61β* germ line clones in *Drosophila*, but fails to traffic to the plasma membrane. Together these observations suggest that *Sec61β* does not have a strong effect on protein translocation into the ER, and thus it is not surprising that *Sec61β* does not show identical phenotypes to *Sec61α*.

Sec61α dorsal closure defects result from attenuated Dpp signaling

Dorsal closure is regulated by the complex interplay of several well-characterized signaling pathways including wingless, Notch, JNK and Dpp (Harden, 2002), most of which have components that are transmembrane or secreted (all of the JNK signaling proteins are cytoplasmic, although it has often been assumed that there is a membrane receptor necessary to initiate the cascade). The terminal phenotype of $Sec61\alpha^{1}$ and $Sec61\alpha^{1}$/*Df(2L)BSC6* mutant embryos is informative as the dorsal surface is completely exposed with extruded brain and guts, whereas the head involutes correctly. Mutations in JNK signaling component genes show similarly strong defects in dorsal closure, but additionally fail in head involution producing terminal phenotypes that are fully exposed from near the posterior pole through the head (for example Riesgo-Escovar and Hafen, 1997b). Thus any potential secreted upstream signals in the JNK signaling pathway appear to be unaffected by zygotic loss of *Sec61α*. Closer examination of the events of dorsal closure support this notion. The DME cells in $Sec61\alpha^{1}$ mutant embryos elongate in the D-V axis indicating that these cells had been correctly specified, a process requiring JNK signaling. Most telling, *puc* is expressed normally in the DME cells of mutant

embryos (Fig. 2.4). Although observing the β-gal signal from the *puc*^{E69} enhancer trap line does not allow for a quantitative measure of the strength of JNK signaling, it appeared that JNK signaling is active in every DME cell in *Sec61α*^{1} mutant embryos (Fig. 2.4B).

Our results strongly suggest that zygotic loss of *Sec61α* attenuates either the secretion of Dpp from the DME cells, or its reception in the epidermis and/or amnioserosa. Four pieces of evidence support this conclusion. First, the phenotypes associated with loss of *Sec61α* overlap those of mutations in the Dpp receptors *tkv* and *punt*. In all three mutations, the DME cells elongate in the D-V axis normally, whereas the lateral epidermal cells only partially elongate (Fig. 2.3; Riesgo-Escovar and Hafen, 1997a; Simin et al., 1998; Ricos et al., 1999). In addition, during the epithelial migration phase of dorsal closure the leading edge is irregular in both *tkv* and *Sec61α* mutant embryos (Fig. 3; Fernandez et al., 2007). Furthermore, the amnioserosa tears away from the epidermis in stage 15 *Sec61α*^{1} mutant embryos, just as it does in *tkv* mutant embryos (Fig. 2.3; Fernandez et al., 2007). Finally, the terminal phenotype observed in strong loss of function mutations in *Sec61α*, *tkv*, and *punt* is a large square dorsal hole accompanied by normal head involution (Fig. 2.2; Affolter et al., 1994; Nellen et al., 1994; Arora et al., 1995). The second piece of evidence in support of a loss of Dpp signaling in *Sec61α* mutant embryos is a strong reduction in the actinomyosin cable in the DME cells. Dpp regulates the expression of *zipper* (encoding nonmuscle myosin) in the DME cells (Arquier et al., 2001). We observed a strong and specific reduction in the levels of the myosin regulatory light chain (Sqh) in the DME cells, although we could clearly observe wild type levels of Sqh in other epidermal cells in the *Sec61α*^{1} mutant (Fig. 2.5). The third piece of evidence in support of reduced Dpp signaling is the elimination or strong reduction of pMad staining in the lateral epidermis in early stage 14 *Sec61α* mutant embryos (Fig. 2.5). The final and strongest piece of evidence implicating loss of

Dpp signaling in *Sec61α*^{1} mutant embryos was the highly penetrant and very strong rescue of dorsal closure by *tkv*^{Q253D} (Table 2.2 and Fig. 2.6), and the less penetrant, yet equally strong, rescue of *Sec61α*^{1} mutant embryos by epidermal expression of *Dpp* (Table 2.2).

It is noteworthy that although the penetrance of the rescue was similar if *tkv*^{Q253D} was expressed in the epidermis (*e22c-Gal4* or *T80-Gal4*) or the amnioserosa (*332.3-Gal4*), the overall strength of the rescue (degree of closure) was more pronounced with the epidermal expression. These results are consistent with the observations of Fernandez et al. (2007) that the expression of *tkv*^{Q253D} in the epidermis gave stronger rescue of the dorsal closure defects in strong loss of function *tkv* mutants (in terms of penetrance in this case) than expression in the amnioserosa. Our results further support their conclusion that Dpp signaling is required in both the epidermis and amnioserosa for normal dorsal closure. Finally, it is not surprising that the rescue of *Sec61α*^{1} by *tkv*^{Q253D} was not complete since the Tkv^{Q253D} protein would have had to go through the secretory pathway, and thus may not have been expressed at comparable levels to the experiments aimed at rescuing a *tkv* mutation (Fernandez et al., 2007).

Our results also suggest that Dpp signaling is attenuated, but likely not eliminated by zygotic loss of *Sec61α*. This notion is supported by the observation that although the phenotypes are similar between *Sec61α*^{1} and *tkv* mutants, there are minor differences. Specifically, in *tkv* mutant embryos, the DME cells bunch together at segmental boundaries (Ricos et al., 1999), and although we observed this phenotype in *Sec61α*^{1} embryos, the penetrance was substantially reduced (data not shown). In addition, although we found strong reductions in the actinomyosin cable in the leading edge of *Sec61α*^{1} mutant embryos, we still could observe a faint, often discontinuous, cable linking DME cells (Fig. 2.5). We also occasionally observed pMad staining

in the lateral epidermis of *Sec61α*^{1} mutant embryos, although it was always clearly attenuated compared to wild type embryos (Fig. 2.5).

Taken together these results suggest a model in which zygotic loss of *Sec61α* gradually reduces traffic through the secretory pathway as the maternal stores are turned over, eventually resulting in a situation in which the expression of a dose-sensitive secreted protein falls below a critical threshold necessary to support dorsal closure. Our results indicate that the protein in question functions in the Dpp signaling pathway, and thus is most likely Dpp or one of its receptors. The observation of defective midgut constrictions in *Sec61α* mutant animals (Fig. 2.7) further supports the notion that Dpp signaling is specifically sensitive to loss of *Sec61α* at this stage of development, since Dpp signaling during mid embryogenesis is necessary for the formation of the second midgut constriction (Immergluck et al., 1990; Panganiban et al., 1990). Our experiments, however, could not definitively distinguish whether the dose-sensitive factor was Dpp itself or one of its receptors, but the *tkv*^{Q253D} rescue experiments argue that it has to be at the level of one of the receptors or upstream in the pathway. In addition, the rescue of dorsal closure in *Sec61α* embryos by epidermal expression of Dpp indicates that there is not a complete absence of Tkv or Put at the plasma membrane. We suggest that Dpp is the most likely candidate, as *dpp* is one of the few haploinsufficient genes encoded by the *Drosophila* genome (Spencer et al., 1982). *dpp* expression must be finely controlled in early embryogenesis due to its role as a morphogen for initial D-V patterning of the embryo (reviewed in O'Connor et al., 2006). Perhaps the dose-sensitivity of Dpp or its receptors during dorsal closure is a consequence of this earlier requirement to maintain precise levels of Dpp, although it is also possible that Dpp signaling during dorsal closure requires similar levels of tight control to precisely coordinate the cellular behaviors of at least two distinct tissues, the lateral epidermis and the amnioserosa.

Figure 2.1

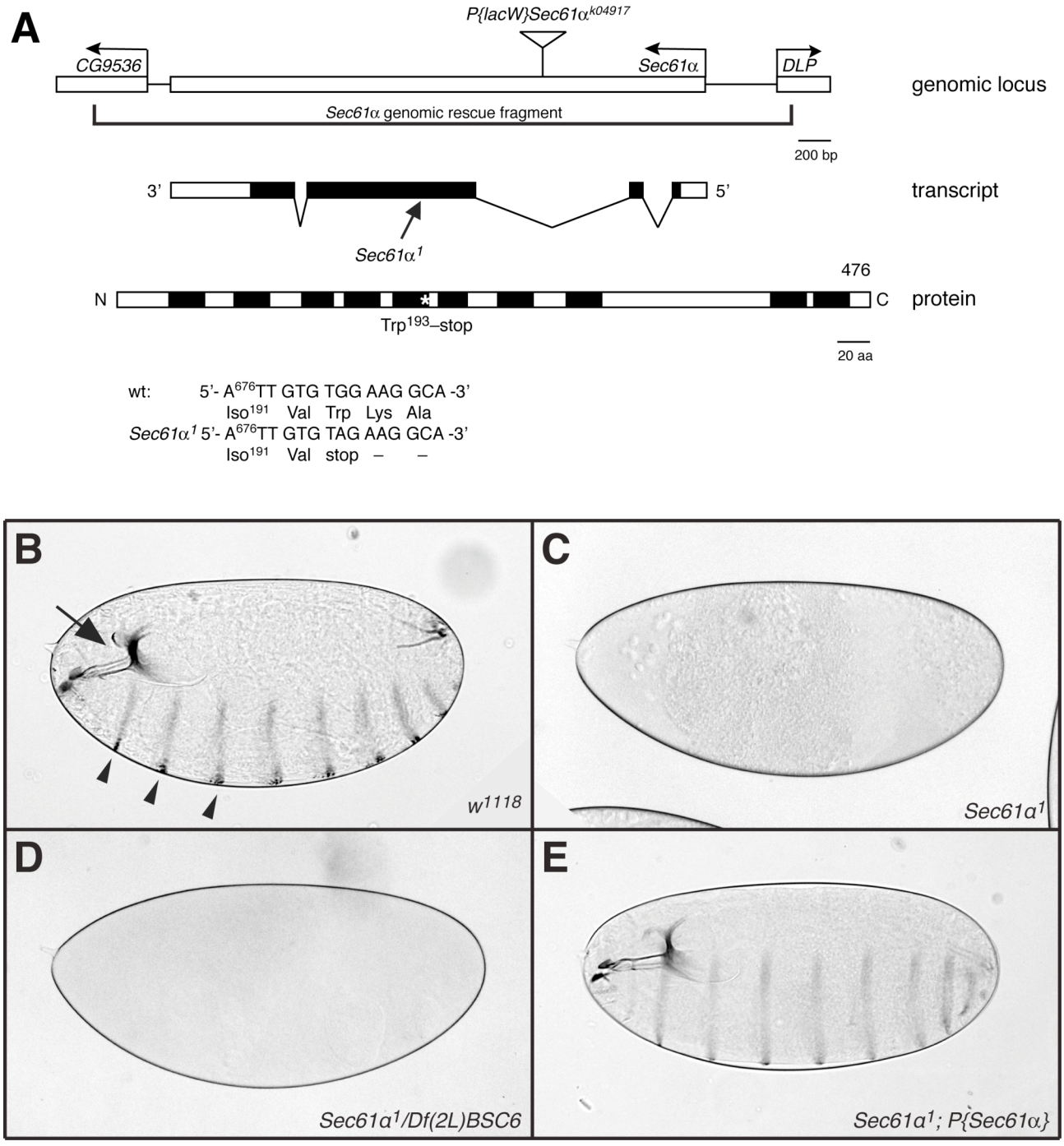

Fig. 2.1. Molecular organization of the *Sec61α* locus, and embryonic cuticle defects associated with zygotic loss of function alleles of *Sec61α*. (A) Schematic diagrams of the genomic locus (top), transcript (middle), and protein of *Sec61α*. The centromere is to the right of this genomic fragment. The transcript is drawn to scale with the genomic diagram, with exons

depicted as rectangles and coding regions filled with black. Introns are depicted as bent lines below the exons. Black bars in the protein schematic represent the location of the ten transmembrane domains. The genomic region used as a rescue construct is indicated by the bracketed line. *P{lacW} Sec61α*^{k04917} in inserted into the second intron as shown. The location of the *Sec61α*^{1} mutation is indicated by an arrow in the transcript and an asterisk in the protein. The nucleotide and protein sequences of the *Sec61α*^{1} mutation are shown below the protein. Nucleotide sequence number is based on GenBank sequence **AY069569**. (B-E) Brightfield photomicrographs of cuticle preparations from wild type and *Sec61α* mutant animals. (B) A w^{1118} late stage 17 embryo showing normal cuticular features including ventral denticle belts (arrowheads) and head skeleton (arrow). (C) A *Sec61α*^{1} mutant embryo showing no cuticular features. (D) A *Sec61α*^{1}*/Df(2L)BSC6* mutant embryo also showing no cuticle. (E) A *Sec61α*^{1} late stage 17 mutant embryo containing two copies of the *Sec61α* genomic rescue fragment inserted on the third chromosome shows normal cuticular features. All embryos are depicted with anterior to the left and the dorsal surface facing up. The embryos in (B) and (E) were taken prior to hatching, but would have hatched given the chance.

Figure 2.2

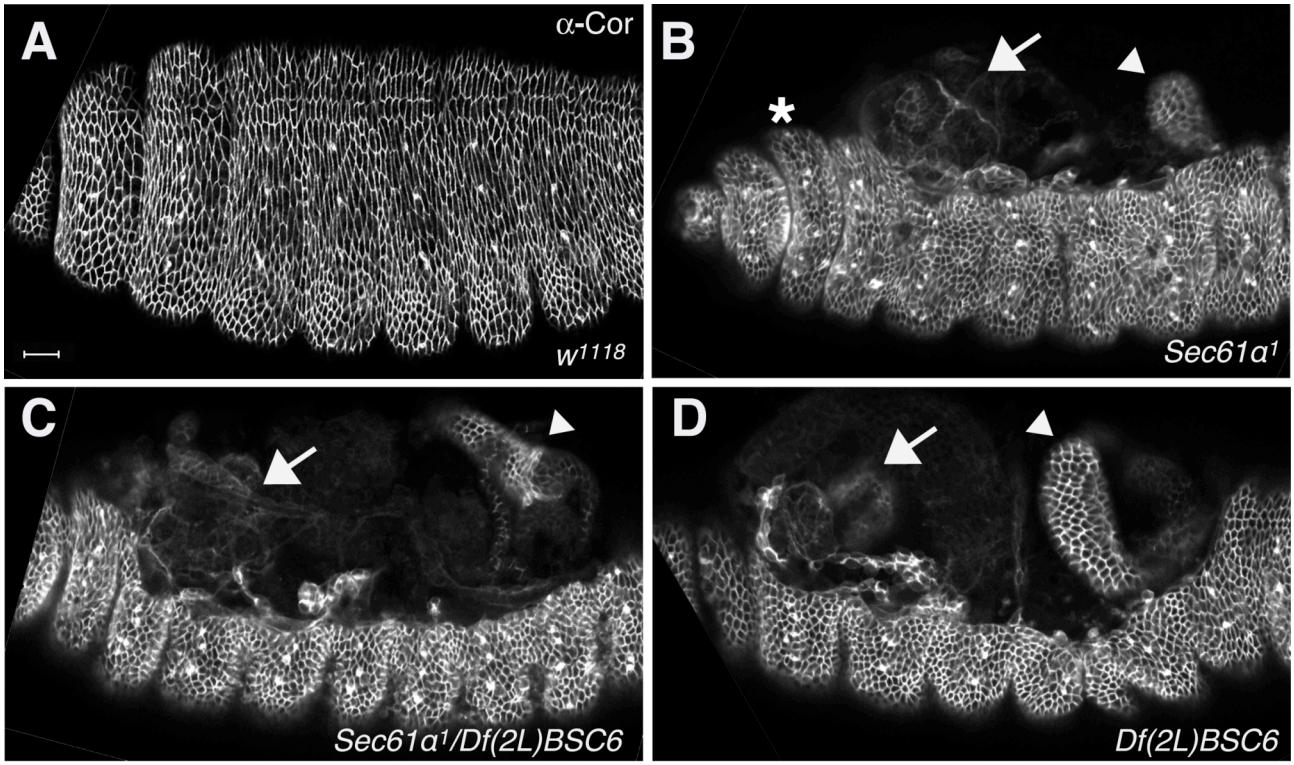

Fig. 2.2. *Sec61α* mutant animals show defects in dorsal closure. (A-D) Confocal optical sections of (A) w^{1118} stage 16 embryo, (B) *Sec61α*^{1} late stage 17 embryo, (C) *Sec61α*^{1}*/Df(2L)BSC6* late stage 17 embryo, and (D) *Df(2L)BSC6* late stage 17 embryo all stained with antibodies against Coracle to visualize cell outlines in the epidermis. Anterior is to the left and dorsal is up in all cases. Note that in all the mutant animals there is no epidermal cells covering the dorsal surface, and the brain (arrows) and guts (arrowheads) are extruded from the dorsal hole. Note that although dorsal closure has failed, head involution has occurred (asterisk in B indicates the dorsal anterior region of the epidermis after head involution had occurred). (Scale bar: 20μm).

Figure 2.3

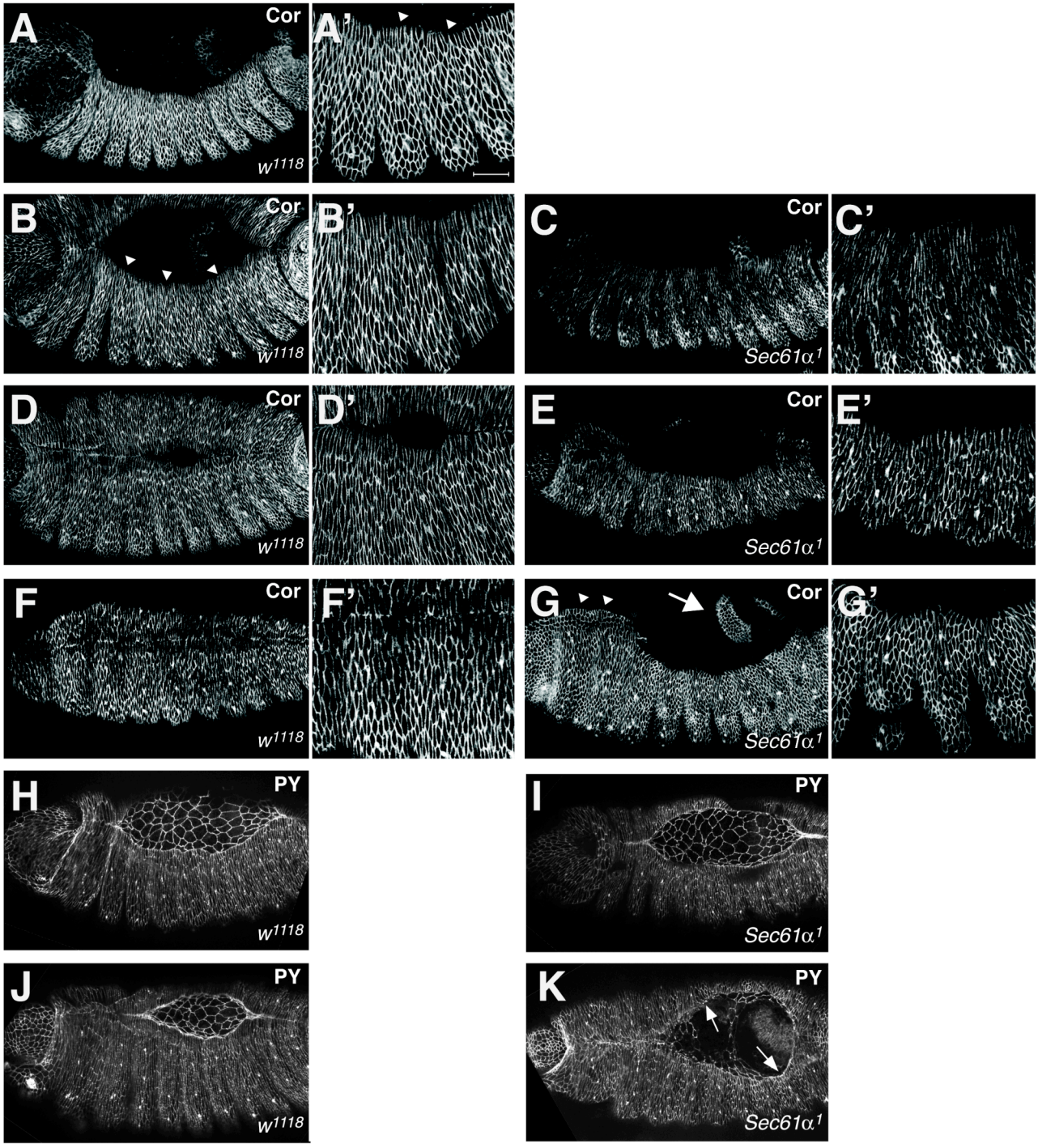

Fig. 2.3. *Sec61α* mutant animals initiate dorsal closure but fail during the epithelial migration phase. (A-G) Confocal optical sections of w^{1118} (A, B, D, F) and $Sec61\alpha^{1}$ (C, E, G) embryos stained with antibodies against Coracle (Cor) to visualize epidermal cells during dorsal closure. Anterior is to the left in all cases and lateral or dorsal views are shown. A', B' etc show

higher magnification views of the DME cells and lateral epidermis of the embryos shown in A, B etc. (A, A') Stage 13 wild type embryo showing the initiation of dorsal closure. Note that the DME cells are elongated in the dorsal-ventral (D-V) axis (arrowheads in A'), whereas the lateral epidermal cells remain polygonal. (B, B') Stage 14 wild type embryo showing D-V elongation of both the DME cells and the lateral epidermis. Note also the uniform curvature of the leading edge of the epithelium (arrowheads in B). (C, C') Stage 14 *Sec61α*^{1} mutant embryo showing elongated DME cells and mostly elongated lateral epidermal cells. (D, D') Stage 15 wild type embryo near the completion of dorsal closure. The DME cells are still elongated and the contraleteral DME cells are zippering together starting at the anterior and posterior ends. (E, E') Stage 15 *Sec61α*^{1} mutant embryo. The DME cells and lateral epidermis are not strongly elongated in the D-V axis, and the leading edge does not present a uniformly curved appearance. The amnioserosa is still intact in this embryo as the brain and guts have not broken through the dorsal surface. (F, F') Stage 16 wild type embryo after the completion of dorsal closure. (G, G') Stage 16 *Sec61α*^{1} mutant embryo after dorsal closure has failed. In this case the all of the epidermal cells are polygonal, the leading edge of the epidermis is irregular and the amnioserosa has clearly degraded or been torn away as the hindgut is protruding through the dorsal surface (arrow). Note also that head involution has occurred normally (arrowheads). (H-K) confocal optical sections of w^{1118} (H, J) and *Sec61α*^{1} (I, K) embryos stained with antibodies against Phospho-tyrosine (PY) to visualize the amnioserosa and epidermis during dorsal closure. The amnioserosa is intact in w^{1118} stage 14 (H) and stage 15 (J) embryos, as well as in the stage 14 *Sec61α*^{1} mutant embryo (I), but has torn away from the epidermis of the stage 15 *Sec61α*^{1} mutant embryo (arrows in K). (scale bars: 20μm).

Figure 2.4

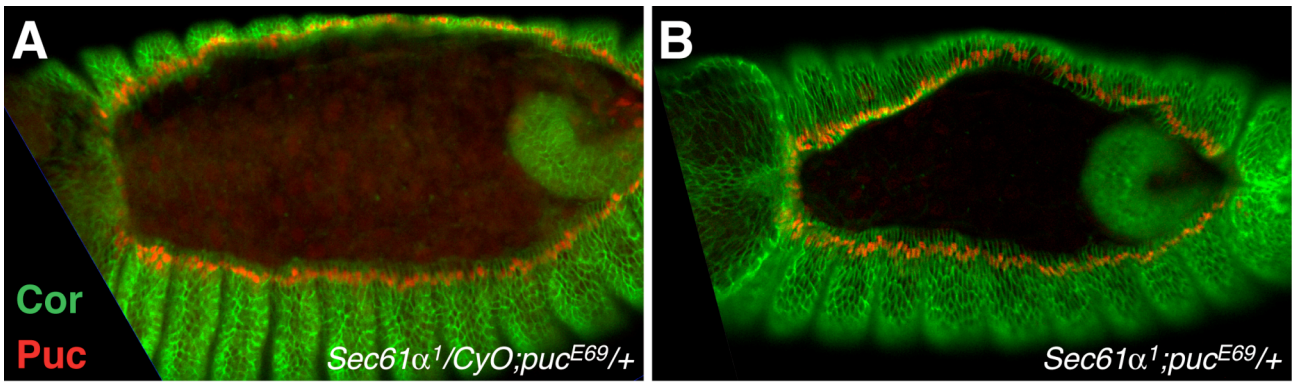

Fig. 2.4. JNK signaling occurs normally in the DME cells of Sec61α mutant embryos. Confocal optical sections of a *Sec61α^{1}/CyO, P{Dfd-YFP};puc^{E69}/+* stage 14 embryo (A) and a *Sec61α^{1};puc^{E69}/+* stage 14 embryo stained with antibodies against Cor (in green) to outline epidermal cells and against β-Gal to recognize *puc^{E69}* expression (red) in the DME cells. Note that each DME cell expresses *puc* in both mutant and heterozygous embryos. Anterior is to the left and dorsal is up in all these images.

Figure 2.5

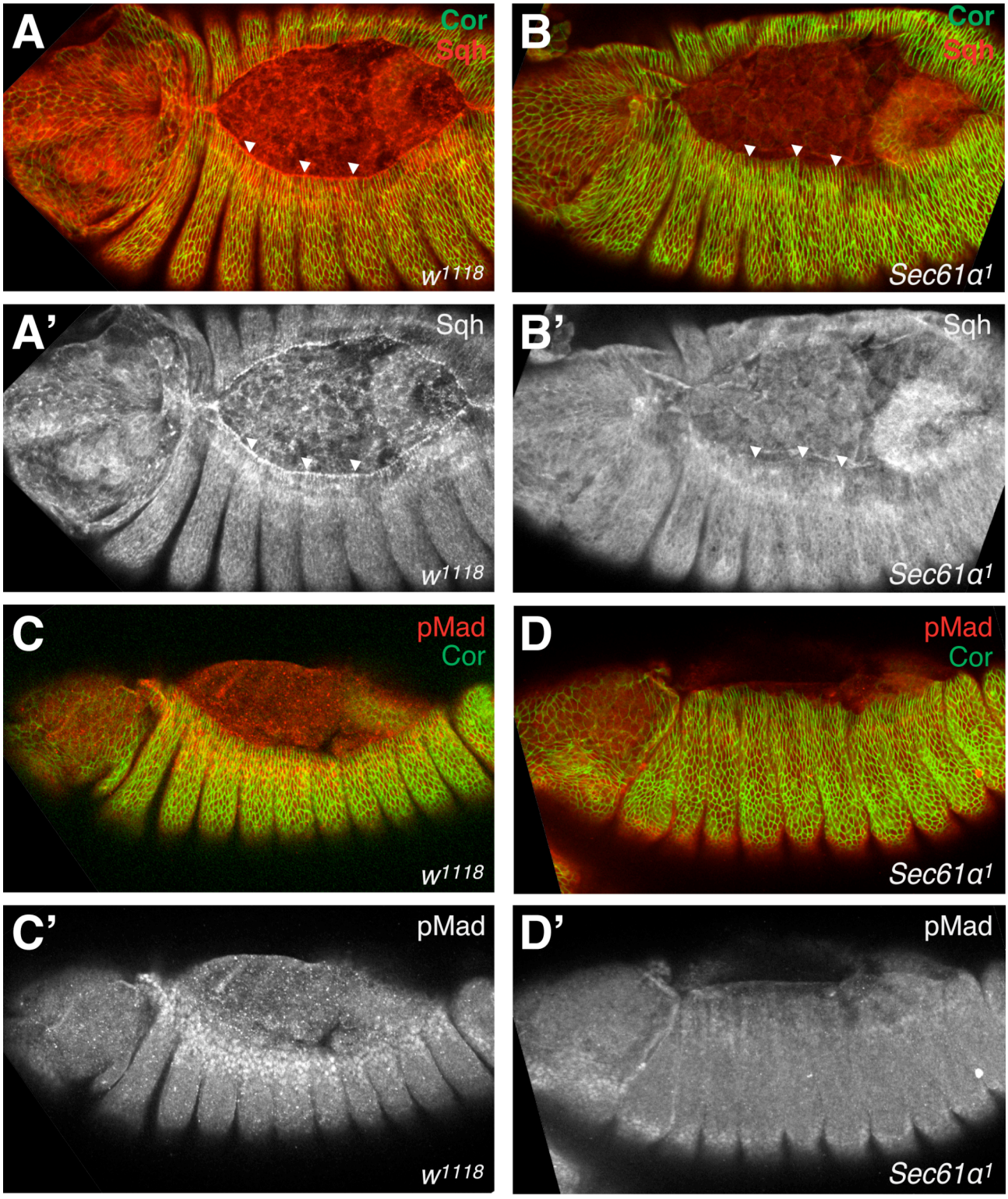

Fig. 2.5. The actinomyosin cable is strongly reduced or eliminated in the DME cells of Sec61α mutant embryos, and Dpp signaling is attenuated. (A, B) Confocal optical sections of

stage 14 w^{1118} (A) and $Sec61\alpha^{1}$ (B) mutant embryos stained for antibodies against Spaghetti squash (Sqh, red) and Coracle (Cor, green). A' and B' show the Sqh channel alone. Cor staining outlines the epidermal cells and clearly shows the interface between the DME cells and the amnioserosa. Note the thick cable of Sqh running through the leading edge of the wild type DME cells that is nearly absent in the $Sec61\alpha^{1}$ mutant embryo (arrowheads). (C, D) Confocal optical sections of stage 14 w^{1118} (C) and $Sec61\alpha^{1}$ (D) mutant embryos stained for antibodies against phosphorylated Mad (pMad, red) and Coracle (Cor, green). C' and D' show the pMad channel alone. In the w^{1118} embryo, pMad is strongly expressed in the nuclei of lateral epidermal cells in a band that extends 4-5 cells ventral to the DME cells. In the $Sec61\alpha^{1}$ mutant embryo, pMad staining is strongly reduced.

Figure 2.6

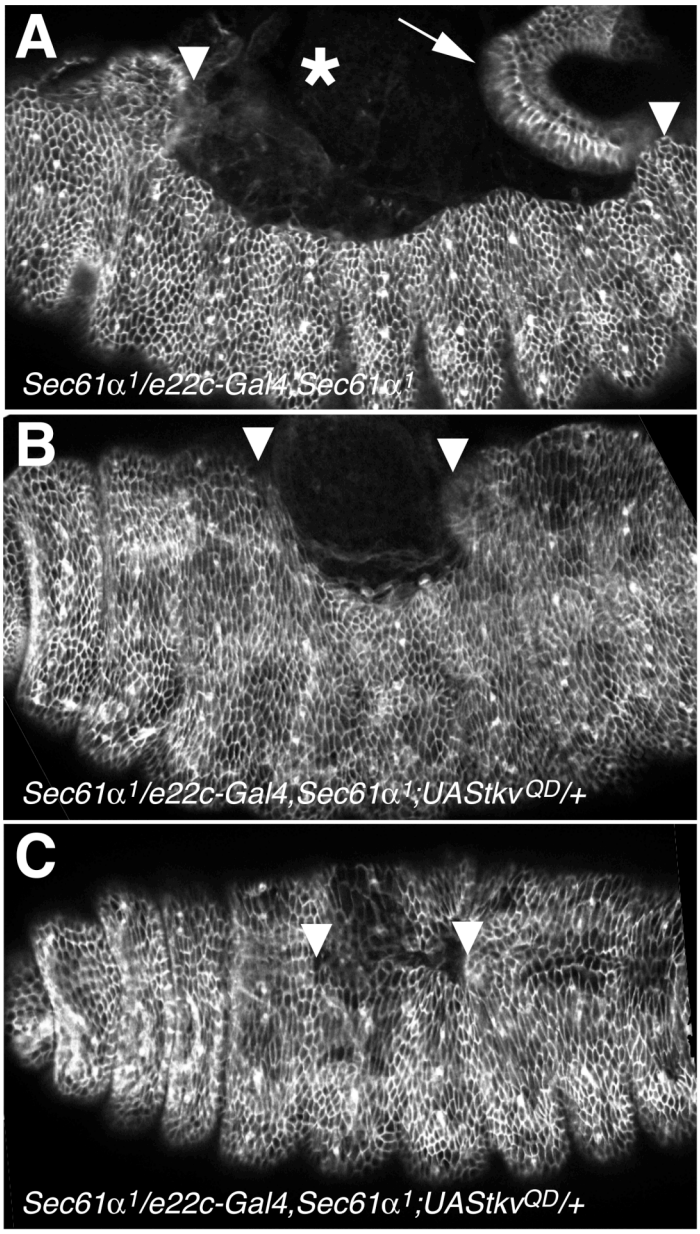

Fig. 2.6. An activated Thick veins receptor can partially rescue the dorsal closure defects of *Sec61α*^{1}. (A) Confocal optical section of a non-rescued, *Sec61α*^{1}*/e22c-Gal4, Sec61α*^{1} stage 17 embryo. Note that the dorsal surface is completely open and the brain (asterisk) and guts (arrow) are extruded. Arrowheads (in A-C) mark the anterior and posterior extent of the open dorsal surface. (B, C) Confocal optical sections of partially rescued, presumably *Sec61α*^{1}*/e22c-Gal4, Sec61α*^{1}*;tkv*^{QD}/+ embryos, showing the range of phenotypes observed. The weakest rescued embryos (B) showed a small dorsal hole with the brain and guts confined to the interior. Stronger rescue (C) resulted in a nearly completely enclosed embryo, with only a small gap where the lateral epidermal sheets were apposed but had not fused.

Figure 2.7

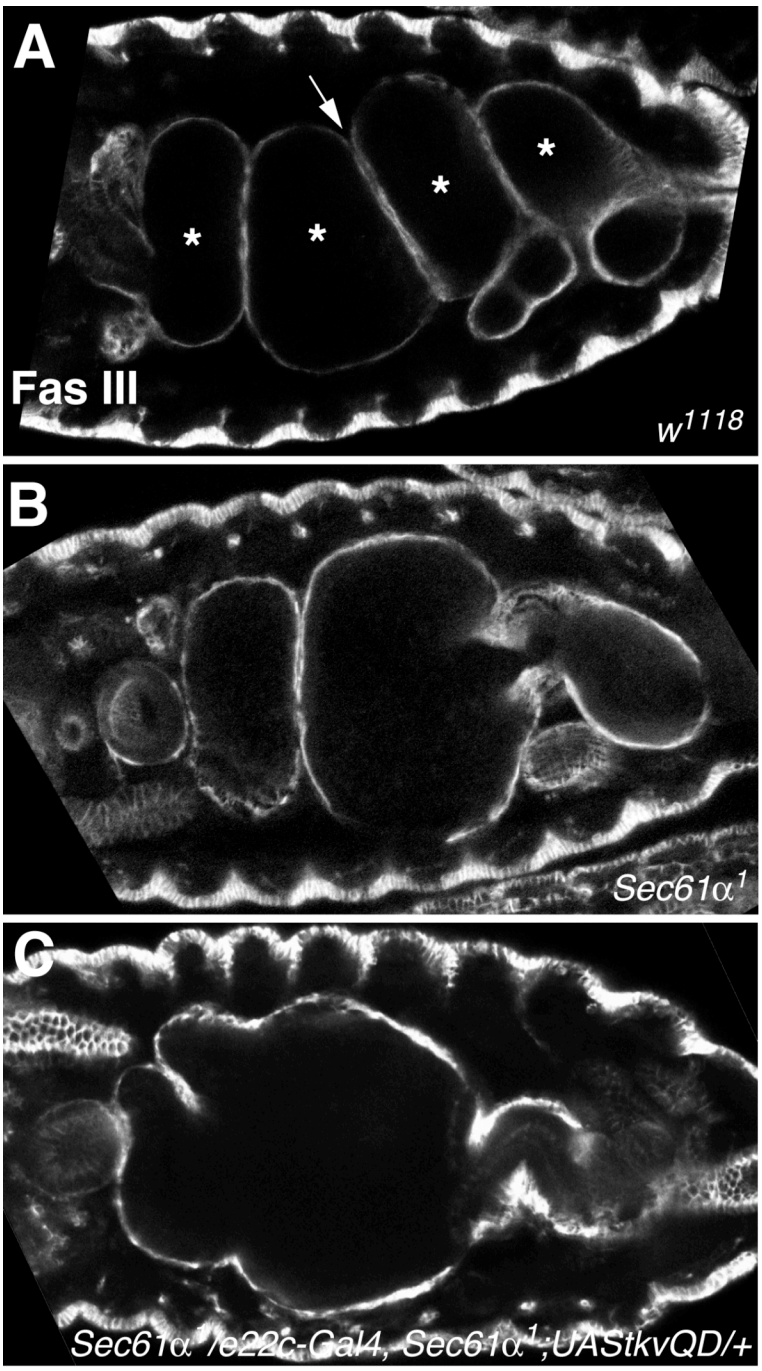

Fig. 2.7. Midgut morphogenesis is defective in *Sec61α* mutant embryos. Confocal optical sections of a stage 16 w^{1118} embryo (A), a stage 16 $Sec61\alpha^{1}$ mutant embryo (B) and a stage 17 $Sec61\alpha^{1}$/e22c-Gal4, $Sec61\alpha^{1}$;tkv^{QD}/+ embryo (C) stained with antibodies against Fasciclin III (Fas III). Note the four chambers of the midgut in w^{1118} embryo (asterisks) and the disorganized midguts in the $Sec61\alpha^{1}$ mutant embryos. The second midgut constriction is indicated by an arrow in panel A and is missing is $Sec61\alpha^{1}$ mutant embryos.

Supplemental Figure 2.1

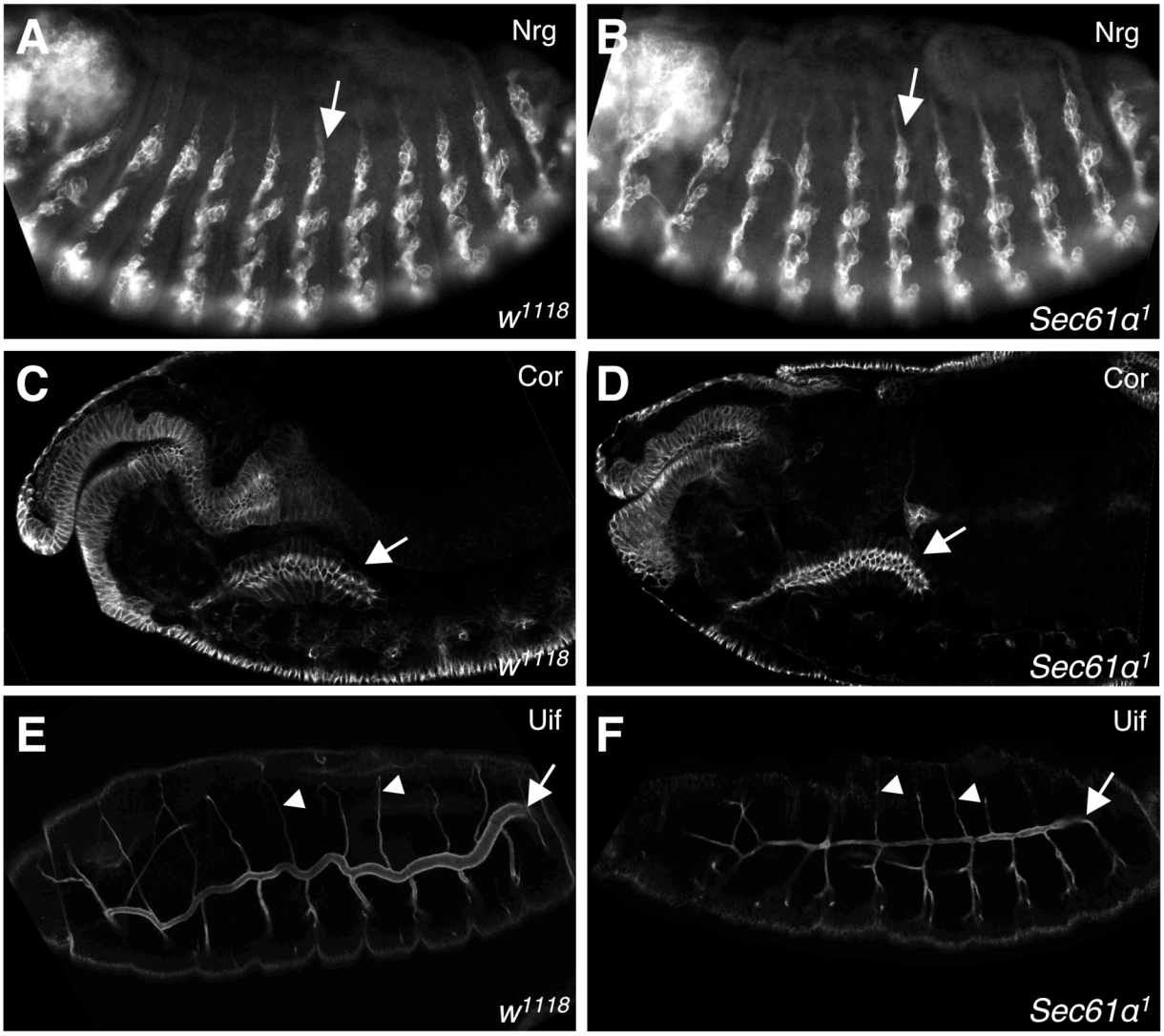

Supplemental Fig. 2.1. Most mid-embryonic morphogenetic events occur normally in *Sec61α* mutant embryos. Confocal optical sections of w^{1118} (A, C, and E) and $Sec61\alpha^{1}$ mutant (B, D, and F) embryos stained with antibodies against Neuroglian (A, B), Coracle (C, D), or Uninflatable (E, F). In all cases anterior is to the left. Wild type and mutant animals for each experiment were fixed and stained in parallel and imaged using identical settings. (A, B) The peripheral nervous system (a segmentally repeated unit is indicated by the arrow) is normally patterned in stage 14 $Sec61\alpha^{1}$ mutant embryos. (C, D) Salivary gland morphogenesis (dorsal and posterior migration of the gland) has occurred normally in stage 14 $Sec61\alpha^{1}$ mutant embryos as judged by Cor staining to visualize the gland. The salivary gland (arrow) occupies its normal position and has fully elongated towards the posterior. Note also that Cor is correctly localized to the apical lateral membrane (the region of the septate junction) in the mutant embryos. (E, F) Tracheal patterning is normal in stage 15 $Sec61\alpha^{1}$ mutant embryos, but the diameter of the tracheal tubes is smaller. The dorsal trunk is indicated by an arrow. The dorsal branches are notably present in $Sec61\alpha^{1}$ mutant embryos (indicated by arrowheads).

Table 2.1
Lethal-phase of *Sec61α* mutant and rescued animals

Genotype	% Embryonic lethality[a] (*n*)[b]	% Larval lethality[a] (*n*)[b]	% Pupal lethality[a] (*n*)[b]
Sec61α^{1}	100 (400)	N/A	
Sec61α^{1}/*Df(2L)BSC6*	100 (299)	N/A	
Sec61α^{1}/*Sec61α*^{k04917}	46 ± 6 (448)	100 (250)	
Sec61α^{k04917}	58 ± 8 (582)	100 (250)	
Sec61α^{1};*P{Sec61α}*^{c}	5 ± 1 (397)	37 ± 4 (376)	100 (237)
Sec61α^{1}/*Sec61α*^{k04917}; *P{Sec61α}*^{c}/+	2 ± 3 (298)	22 ± 8 (292)	4 ± 3 (230)

[a] mean ± sd from three independent experiments
[b] total number of animals of indicated genotype that were scored
[c] genomic rescue construct line CM15-1

Table 2.2
tkv^{Q253D} rescue of $Sec61\alpha^{1}$ mutant animals

Cross	% $Sec61\alpha^{1}$ embryos showing DC rescue[a] (*n*)[b]
e22c-Gal4, Sec61α[1]/CyO **X** *Sec61α[1]/+; UAS-tkv[Q253D]/+*	67 ± 6 (55)
T80-Gal4, Sec61α[1]/CyO **X** *Sec61α[1]/+; UAS-tkv[Q253D]/+*	49 ± 5 (63)
332.3-Gal4, Sec61α[1]/CyO **X** *Sec61α[1]/+; UAS-tkv[Q253D]/+*	45 ± 2 (329)
e22c-Gal4, Sec61α[1]/CyO **X** *Sec61α[1]/+; UAS-Dpp/+*	10 ± 3 (106)
T80-Gal4, Sec61α[1]/CyO **X** *Sec61α[1]/+; UAS-Dpp/+*	3 ± 3 (255)
332.3-Gal4, Sec61α[1]/CyO **X** *Sec61α[1]/+; UAS-Dpp/+*	5 ± 3 (105)

[a] 16-20 hr AEL progeny of the indicated crosses were fixed and stained with antibodies against Coracle. Only $Sec61\alpha^{1}$ mutant animals stain at this stage. % DC rescue reflects the mean ± sd from three independent experiments. Note that maximal expected rescue is 50%.
[b] Total number of embryos that stained with Cor.

References

Affolter M, Caussinus E. 2008. Tracheal branching morphogenesis in Drosophila: new insights into cell behaviour and organ architecture. Development 135:2055-2064.

Affolter M, Nellen D, Nussbaumer U, Basler K. 1994. Multiple requirements for the receptor serine/threonine kinase thick veins reveal novel functions of TGF beta homologs during Drosophila embryogenesis. Development 120:3105-3117.

Araujo SJ, Aslam H, Tear G, Casanova J. 2005. mummy/cystic encodes an enzyme required for chitin and glycan synthesis, involved in trachea, embryonic cuticle and CNS development--analysis of its role in Drosophila tracheal morphogenesis. Dev. Biol. 288:179-193.

Arora K, Dai H, Kazuko SG, Jamal J, O'Connor MB, Letsou A, Warrior R. 1995. The Drosophila schnurri gene acts in the Dpp/TGF beta signaling pathway and encodes a transcription factor homologous to the human MBP family. Cell 81:781-790.

Arquier N, Perrin L, Manfruelli P, Semeriva M. 2001. The Drosophila tumor suppressor gene lethal(2)giant larvae is required for the emission of the Decapentaplegic signal. Development 128:2209-2220.

Baumgartner S, Littleton JT, Broadie K, Bhat MA, Harbecke R, Lengyel JA, Chiquet-Ehrismann R, Prokop A, Bellen HJ. 1996. A Drosophila neurexin is required for septate junction and blood-nerve barrier formation and function. Cell 87:1059-1068.

Bloor JW, Kiehart DP. 2002. Drosophila RhoA regulates the cytoskeleton and cell-cell adhesion in the developing epidermis. Development 129:3173-3183.

Cooper HM. 2002. Axon guidance receptors direct growth cone pathfinding: rivalry at the leading edge. Int. J. Dev. Biol. 46:621-631.

Devine WP, Lubarsky B, Shaw K, Luschnig S, Messina L, Krasnow MA. 2005. Requirement for chitin biosynthesis in epithelial tube morphogenesis. Proc. Natl. Acad. Sci. U S A 102:17014-17019.

Dorfman R, Shilo BZ. 2001. Biphasic activation of the BMP pathway patterns the Drosophila embryonic dorsal region. Development 128:965-972.

Fehon RG, Dawson IA, Artavanis-Tsakonas S. 1994. A Drosophila homologue of membrane-skeleton protein 4.1 is associated with septate junctions and is encoded by the coracle gene. Development 120:545-557.

Fehon RG, Johansen K, Rebay I, Artavanis-Tsakonas S. 1991. Complex cellular and subcellular regulation of notch expression during embryonic and imaginal development of Drosophila: implications for notch function. J. Cell Biol. 113:657-669.

Fernandez BG, Arias AM, Jacinto A. 2007. Dpp signalling orchestrates dorsal closure by regulating cell shape changes both in the amnioserosa and in the epidermis. Mech. Dev. 124:884-897.

Franke JD, Montague RA, Kiehart DP. 2005. Nonmuscle myosin II generates forces that transmit tension and drive contraction in multiple tissues during dorsal closure. Curr. Biol. 15:2208-2221.

Glise B, Noselli S. 1997. Coupling of Jun amino-terminal kinase and Decapentaplegic signaling pathways in Drosophila morphogenesis. Genes Dev. 11:1738-1747.

Harden N. 2002. Signaling pathways directing the movement and fusion of epithelial sheets: lessons from dorsal closure in Drosophila. Differentiation 70:181-203.

Harden N, Ricos M, Yee K, Sanny J, Langmann C, Yu H, Chia W, Lim L. 2002. Drac1 and Crumbs participate in amnioserosa morphogenesis during dorsal closure in Drosophila. J. Cell Sci. 115:2119-2129.

Hou XS, Goldstein ES, Perrimon N. 1997. Drosophila Jun relays the Jun amino-terminal kinase signal transduction pathway to the Decapentaplegic signal transduction pathway in regulating epithelial cell sheet movement. Genes Dev. 11:1728-1737.

Hutson MS, Tokutake Y, Chang MS, Bloor JW, Venakides S, Kiehart DP, Edwards GS. 2003. Forces for morphogenesis investigated with laser microsurgery and quantitative modeling. Science 300:145-149.

Immergluck K, Lawrence PA, Bienz M. 1990. Induction across germ layers in Drosophila mediated by a genetic cascade. Cell 62:261-268.

Jacinto A, Wood W, Balayo T, Turmaine M, Martinez-Arias A, Martin P. 2000. Dynamic actin-based epithelial adhesion and cell matching during Drosophila dorsal closure. Curr. Biol. 10:1420-1426.

Jacinto A, Woolner S, Martin P. 2002. Dynamic analysis of dorsal closure in Drosophila: from genetics to cell biology. Dev. Cell 3:9-19.

Jasper H, Benes V, Schwager C, Sauer S, Clauder-Munster S, Ansorge W, Bohmann D. 2001. The genomic response of the Drosophila embryo to JNK signaling. Dev. Cell 1:579-586.

Jiang L, Rogers SL, Crews ST. 2007. The Drosophila Dead end Arf-like3 GTPase controls vesicle trafficking during tracheal fusion cell morphogenesis. Dev. Biol. 311:487-499.

Johnson AE, van Waes MA. 1999. The translocon: a dynamic gateway at the ER membrane. Annu. Rev. Cell Dev. Biol. 15:799-842.

Karess RE, Chang XJ, Edwards KA, Kulkarni S, Aguilera I, Kiehart DP. 1991. The regulatory light chain of nonmuscle myosin is encoded by spaghetti-squash, a gene required for cytokinesis in Drosophila. Cell 65:1177-1189.

Kelkar A, Dobberstein B. 2009. Sec61beta, a subunit of the Sec61 protein translocation channel at the endoplasmic reticulum, is involved in the transport of Gurken to the plasma membrane. BMC Cell Biol. 10:11.

Kiehart DP, Galbraith CG, Edwards KA, Rickoll WL, Montague RA. 2000. Multiple forces contribute to cell sheet morphogenesis for dorsal closure in Drosophila. J. Cell Biol. 149:471-490.

Le T, Liang Z, Patel H, Yu MH, Sivasubramaniam G, Slovitt M, Tanentzapf G, Mohanty N, Paul SM, Wu VM, Beitel GJ. 2006. A new family of Drosophila balancer chromosomes with a w- dfd-GMR yellow fluorescent protein marker. Genetics 174:2255-2257.

Leptin M, Bogaert T, Lehmann R, Wilcox M. 1989. The function of PS integrins during Drosophila embryogenesis. Cell 56:401-408.

Leroux A, Rokeach LA. 2008. Inter-species complementation of the translocon beta subunit requires only its transmembrane domain. PLoS One 3:e3880.

Luschnig S, Batz T, Armbruster K, Krasnow MA. 2006. serpentine and vermiform encode matrix proteins with chitin binding and deacetylation domains that limit tracheal tube length in Drosophila. Curr. Biol. 16:186-194.

Manfruelli P, Arquier N, Hanratty WP, Semeriva M. 1996. The tumor suppressor gene, lethal(2)giant larvae (1(2)g1), is required for cell shape change of epithelial cells during Drosophila development. Development 122:2283-2294.

Miyamoto H, Nihonmatsu I, Kondo S, Ueda R, Togashi S, Hirata K, Ikegami Y, Yamamoto D. 1995. canoe encodes a novel protein containing a GLGF/DHR motif and functions with Notch and scabrous in common developmental pathways in Drosophila. Genes Dev. 9:612-625.

Mizuno T, Tsutsui K, Nishida Y. 2002. Drosophila myosin phosphatase and its role in dorsal closure. Development 129:1215-1223.

Myat MM. 2005. Making tubes in the Drosophila embryo. Dev. Dyn. 232:617-632.

Narasimha M, Brown NH. 2004. Novel functions for integrins in epithelial morphogenesis. Curr. Biol. 14:381-385.

Nellen D, Affolter M, Basler K. 1994. Receptor serine/threonine kinases implicated in the control of Drosophila body pattern by decapentaplegic. Cell 78:225-237.

Nellen D, Burke R, Struhl G, Basler K. 1996. Direct and long-range action of a DPP morphogen gradient. Cell 85:357-368.

O'Connor MB, Umulis D, Othmer HG, Blair SS. 2006. Shaping BMP morphogen gradients in the Drosophila embryo and pupal wing. Development 133:183-193.

Panganiban GE, Reuter R, Scott MP, Hoffmann FM. 1990. A Drosophila growth factor homolog, decapentaplegic, regulates homeotic gene expression within and across germ layers during midgut morphogenesis. Development 110:1041-1050.

Peifer M, Wieschaus E. 1990. The segment polarity gene armadillo encodes a functionally modular protein that is the Drosophila homolog of human plakoglobin. Cell 63:1167-1176.

Perrimon N. 1988. The maternal effect of lethal(1)discs-large-1: a recessive oncogene of Drosophila melanogaster. Dev. Biol. 127:392-407.

Rebay I, Fehon RG. 2000. Generating antibodies against Drosophila proteins. In: Sullivan W, Ashburner M, Hawley RS, editors. Drosophila Protocols. Cold Spring Harbor, New York: Cold Spring Harbor Laboratory Press. pp 389-411.

Reed BH, Wilk R, Lipshitz HD. 2001. Downregulation of Jun kinase signaling in the amnioserosa is essential for dorsal closure of the Drosophila embryo. Curr. Biol. 11:1098-1108.

Reed BH, Wilk R, Schock F, Lipshitz HD. 2004. Integrin-dependent apposition of Drosophila extraembryonic membranes promotes morphogenesis and prevents anoikis. Curr. Biol. 14:372-380.

Ricos MG, Harden N, Sem KP, Lim L, Chia W. 1999. Dcdc42 acts in TGF-beta signaling during Drosophila morphogenesis: distinct roles for the Drac1/JNK and Dcdc42/TGF-beta cascades in cytoskeletal regulation. J. Cell Sci. 112 (Pt 8):1225-1235.

Riesgo-Escovar JR, Hafen E. 1997a. Common and distinct roles of DFos and DJun during Drosophila development. Science 278:669-672.

Riesgo-Escovar JR, Hafen E. 1997b. Drosophila Jun kinase regulates expression of decapentaplegic via the ETS-domain protein Aop and the AP-1 transcription factor DJun during dorsal closure. Genes Dev. 11:1717-1727.

Ring JM, Martinez Arias A. 1993. puckered, a gene involved in position-specific cell differentiation in the dorsal epidermis of the Drosophila larva. Development Suppl.:251-259.

Simin K, Bates EA, Horner MA, Letsou A. 1998. Genetic analysis of punt, a type II Dpp receptor that functions throughout the Drosophila melanogaster life cycle. Genetics 148:801-813.

Snapp EL, Iida T, Frescas D, Lippincott-Schwartz J, Lilly MA. 2004. The fusome mediates intercellular endoplasmic reticulum connectivity in Drosophila ovarian cysts. Mol. Biol. Cell 15:4512-4521.

Spencer FA, Hoffmann FM, Gelbart WM. 1982. Decapentaplegic: a gene complex affecting morphogenesis in Drosophila melanogaster. Cell 28:451-461.

Stark KA, Yee GH, Roote CE, Williams EL, Zusman S, Hynes RO. 1997. A novel alpha integrin subunit associates with betaPS and functions in tissue morphogenesis and movement during Drosophila development. Development 124:4583-4594.

Thummel CS, Boulet AM, Lipshitz HD. 1988. Vectors for Drosophila P-element-mediated transformation and tissue culture transfection. Gene 74:445-456.

Toikkanen J, Gatti E, Takei K, Saloheimo M, Olkkonen VM, Soderlund H, De Camilli P, Keranen S. 1996. Yeast protein translocation complex: isolation of two genes SEB1 and SEB2 encoding proteins homologous to the Sec61 beta subunit. Yeast 12:425-438.

Toikkanen JH, Miller KJ, Soderlund H, Jantti J, Keranen S. 2003. The beta subunit of the Sec61p endoplasmic reticulum translocon interacts with the exocyst complex in Saccharomyces cerevisiae. J. Biol. Chem. 278:20946-20953.

Tomancak P, Beaton A, Weiszmann R, Kwan E, Shu S, Lewis SE, Richards S, Ashburner M, Hartenstein V, Celniker SE, Rubin GM. 2002. Systematic determination of patterns of gene expression during Drosophila embryogenesis. Genome Biol. 3:RESEARCH0088.

Tonning A, Hemphala J, Tang E, Nannmark U, Samakovlis C, Uv A. 2005. A transient luminal chitinous matrix is required to model epithelial tube diameter in the Drosophila trachea. Dev. Cell 9:423-430.

Valcarcel R, Weber U, Jackson DB, Benes V, Ansorge W, Bohmann D, Mlodzik M. 1999. Sec61beta, a subunit of the protein translocation channel, is required during Drosophila development. J. Cell Sci. 112:4389-4396.

Wang S, Jayaram SA, Hemphala J, Senti KA, Tsarouhas V, Jin H, Samakovlis C. 2006. Septate-junction-dependent luminal deposition of chitin deacetylases restricts tube elongation in the Drosophila trachea. Curr. Biol. 16:180-185.

Ward RE, Evans J, Thummel CS. 2003. Genetic modifier screens in Drosophila demonstrate a role for Rho1 signaling in ecdysone-triggered imaginal disc morphogenesis. Genetics 165:1397-1415.

Young PE, Richman AM, Ketchum AS, Kiehart DP. 1993. Morphogenesis in Drosophila requires nonmuscle myosin heavy chain function. Genes Dev. 7:29-41.

Zahedi B, Shen W, Xu X, Chen X, Mahey M, Harden N. 2008. Leading edge-secreted Dpp cooperates with ACK-dependent signaling from the amnioserosa to regulate myosin levels during dorsal closure. Dev. Dyn. 237:2936-2946.

Zhang L, Ward RE. 2009. uninflatable encodes a novel ectodermal apical surface protein required for tracheal inflation in Drosophila. Dev. Biol. 336:201-212.

Chapter 3

Ecdysone and *broad* interact to regulate gene expression and morphogenesis in leg imaginal disc at the onset of metamorphosis

Introduction

Endocrine signals provide temporal cues and direct proper coordination in many developmental morphogenetic events. For example, retinoic acid signals in the vertebrate embryo direct anterior posterior body elongation, axial rotation and heart morphogenesis (Niederreither, 2001). These events are mainly accomplished through forces generated at the actin cytoskeleton. Unfortunately we have very little knowledge of how hormonal signals can direct cellular events at the cytoskeleton. One excellent way to address these questions is to examine simple hormone-dependent morphogenetic events in genetically tractable model organisms.

A striking example of hormone-directed morphogenesis occurs at the onset of metamorphosis in *Drosophila*, at which time a sharp rise in the titer of the hormone 20-hydroxyecdysone (hereafter referred as ecdysone) directs the elongation and eversion of imaginal discs, ultimately resulting in the fusion of these structures into rudimentary adult structures in a little over 12 hours (von Kalm, 1995). The development of leg imaginal discs from late third instar larva to early prepupa is thus an ideal model system for studying hormone-directed morphogenesis. At the end of third larval instar, the leg imaginal discs are comprised of a single-layered columnar epithelium. Beginning approximately four hours before puparium

formation, coincident with a sharp rise in ecdysone, the leg discs rapidly elongate in the proximal-distal axis. This dramatic morphogenesis is largely driven by changes in cell shape and cell rearrangements (Fristrom, 1976; Taylor, 2008). Most of the events of leg elongation can be recapitulated in cultured discs treated with physiological levels of ecdysone, demonstrating the key role for ecdysone in directing leg morphogenesis (Milner, 1977).

Ecdysone functions through a nuclear hormone signaling cascade. Extensive genetic and biochemical evidence has shown that ecdysone binds to its receptor, which is a heterodimer of Ecdysone receptor (EcR) and Ultraspiracle, and then induces a few so-called "early-response genes" (Thummel, 2001). These early-response genes mostly encode transcription factors that then regulate a much larger set of so-called "late-response genes". It is thought that the function of these late response genes is to participate in tissue- and stage-specific biological responses to the hormone.

The *Broad-Complex* (*BR-C*) is a key early-response gene that appears to play specific roles in regulating imagainal disc morphogenesis. Early studies of *BR-C* revealed that the gene encodes a family of four zinc-finger transcription factors that have three separable genetic functions (DiBello, 1991, Bayer, 1997). The *broad* (*br*) genetic function is encoded by the *Z2* isoform (Bayer, 1997). Amorphic alleles of *br*, such as br^5, result in prepupal lethality with arrested imaginal discs that fail to elongate or evert, indicating an essential requirement for *br* in the early stages of leg imaginal disc morphogenesis (Kiss, 1988). In contrast, hypomorphic alleles of *br*, such as br^1, are viable as adults with weakly penetrant of broad wings and malformed legs (Beaton, 1988).

The weakly penetrant malformed leg phenotype associated with br^1 has been used successfully in forward genetic approaches to identify new genes that function in concert with *br*

in regulating leg morphogenesis. Results from three independent dominant enhancer screens revealed that the type II transmembrane serine protease *Stubble/stubbloid* (*Sb/sbd*), the serum response factor transcription factor encoded by *blistered* (*bs*), nonmuscle myosin encoded by *zipper (zip*), and *Rho1* are all br^1-interacting genes (Beaton, 1988; Gotwals, 1991; Ward, 2003). Ward et al. (2003) went on to show that several Rho1 signaling pathway genes interact with *br*, suggesting that ecdysone and *br* may function to regulate the actin cytoskeleton through a Rho-dependent signaling pathway. However, none of the genes thus far characterized from these genetic screens has revealed how the *br* transcription factor regulates the activity of the Rho signaling pathway. In particular, extensive Northern blot analyses of genes encoding core Rho signaling components revealed that all of these genes are expressed in leg imaginal discs at uniform levels all throughout the period of leg morphogenesis, indicating that ecdysone and *br* are not required for the expression of these core signaling genes (data not shown).

As a complementary approach to understand how ecdysone and *br* may regulate genes that function in hormone-dependent leg morphogenesis, we have cataloged gene expression in leg imaginal discs from -18 hr and 0 hr w^{1118} (wild type) larvae and prepupae and from 0 hr br^5 prepupae by whole genome microarray analysis. We have compared RNAs expressed at 0 hr between w^{1118} and br^5 as a means to identify *br*-regulated genes. We have also compared RNAs that are expressed between -18 hr and 0 hr in w^{1118} leg discs to identify genes that are regulated by ecdysone. Surprisingly, there are only 31 genes in common between the 363 genes induced by ecdysone and the 139 genes induce by *br*. Similarly, only 40 genes overlap between the 415 genes repressed by ecdysone and the 221 genes repressed by *br*. Consistent with these microarray results, and challenging the traditional notion of a linear ecdysone signaling pathway, Northern blot analysis showed that *br* (*Z2*) transcripts are present in third instar leg imaginal

discs prior to the late larval ecdysone pulse. Furthermore, neither activation of *br*, nor early ecdysone feeding alone was sufficient to trigger a precocious leg morphogenesis program, suggesting that *br* may function in concert with ecdysone signaling at the late larval ecdysone pulse to regulate leg imaginal disc morphogenesis. To study these genes functionally in the context of leg morphogenesis, we obtained transgenic lines capable of expressing double stranded RNA under the control of an upstream activating sequence (UAS) for 27 of the 31 ecdysone-induced, *br*-induced genes. Expression of these snapback RNAs was driven by *Distal-less-Gal4 (Dll-Gal4*), resulting in strong expression in the distal half of the leg (and a few other tissues including the wing margin, antennae, and mouth parts; Ward, 2003b). Ten of these 27 genes produced animals showing at least 20% malformed legs when treated in this way, suggesting that these genes normally function in leg morphogenesis. Thus this study has greatly increased our knowledge of the secondary response genes regulated by ecdyone and *br* that are necessary to induce a hormonal morphogenesis program during development.

Materials and methods

Drosophila stocks

All Drosophila stocks were maintained on media consisting of corn meal, sugar, yeast, and agar in incubators maintained at a constant temperature of 21°C or in a room that typically fluctuated between 21°C and 22.5°C. *ybr*^{5}, *Distal-less* (*Dll*)-*Gal4*, heat shock (*hs*)-*Gal4*, *P{UAS-Dcr-2.D}1 w*^{1118}, and *w*^{1118} were obtained from the Bloomington Drosophila Stock Center (Bloomington, IN). *escargot* (*esg*)-*Gal4* was obtained from Carl Thummel (University of Utah). *w; hs-Z2 (CD5-4C); hs-Z2 (CD5-1)* was obtained from Cindy Bayer (University of Central Florida). All the RNA interference stocks described here were obtained from the Vienna *Drosophila* RNAi Center (VDRC, Vienna, Austria; Dietzl, 2007). *Dll-Gal4*, *hs-Gal4*, and *esg-Gal4* were balanced with *CyO, P{w*$^{+}$*, Dfd-EYFP}* (Le., 2006). *w*^{1118} was used as the wild type control, unless otherwise noted. Genetic experiments were conducted in incubators controlled at a constant temperature of either 21ºC or 25ºC, as indicated.

Fly staging, dissection and photography of live leg imaginal discs

w^{1118} and *ybr*^{5}*/binsn* flies were staged on food supplemented with 0.05% bromophenol blue as described (Andres, 1994). *w*^{1118} and *ybr*^{5}*/Y* mutant animals were selected (mutant males were selected using the yellow marker) at -18 hr (blue gut larvae), -4 hr (white gut larvae), 0 hr (white prepupae), +2 hr and +4 hr relative to puparium formation (0 hr). Leg imaginal discs were dissected in Phosphate Buffered Saline (PBS), and then transferred to fresh PBS. Brightfield photomicrographs were captured within 5 minutes on a Nikon Eclipse 80i microscope equipped with a Photometrics CoolSNAP ES high performance digital CCD camera using a Plan APO

10X (0.45NA) objective. All digital images were cropped and adjusted for brightness and contrast in Adobe Photoshop (version CS3, San Jose, CA), and figures were compiled using Adobe Illustrator (version CS3).

RNA isolation, microarray hybridizations and analyses

In order to control for potential genetic effects from the autosomes and Y chromosome, we crossed $ybr^5/Binsn$ females to w^{1118} males and then crossed the resulting ybr^5/w^{1118} females with w^{1118} males. This cross produced ybr^5/Y and w^{1118}/Y males that at a population level had identical autosomes and Y chromosomes. Since we selected the br^5 animals based upon the *yellow* cuticular phentopyes, we tested to make sure that *y* and *br* did not recombine apart to any significant degree. *y* and *br* are reported to map 0.2 cM apart on the X chromosome (Gatti ,1989), and in two separate experiments we did not detect any recombination between these genes ($n > 200$).

Third instar ybr^5/Y and w^{1118}/Y larvae were staged on food supplemented with 0.05% bromophenol blue. Blue gut larvae (-18 hr) and white prepupae (0 hr) were selected and leg imagainal discs were hand-dissected in PBS. Total RNA was isolated using TriPure (Roche, Indianapolis, IN) and then purified over RNAeasy columns (Qiagen, Valencia, CA). No amplification steps were performed and a total of > 12 μg of total purified RNA was obtained for each sample. Quadruplicate independent samples were obtained for ybr^5/Y and w^{1118}/Y white prepupae and triplicate independent samples were obtained for w^{1118}/Y -18 hour larvae. cRNA synthesis, labeling, fractionation, hybridization to Affymetrix GeneChip Drosophila Genome Arrays (first generation from Affymetrix, Santa Clara, CA), and confocal scanning were performed at the University of Maryland Biotechnology Institute Microarray Core Facility

(College Park, MD). We compared w^{1118} between -18 hr and 0 hr (ecdysone regulated gene set) and ybr^{5} and w^{1118} at 0 hr (*br* regulated gene set). Statistical analyses were performed using the Cyber-T statistical package (http://cybert.microarray.ics.uci.edu/). We made three arbitrary cuts to the data. First, we only considered genes that were expressed based upon an Affymetrix call of present and a signal value of > 300 in one of the conditions (e.g. w^{1118} at 0 hr). Second, we only considered genes that showed differential expression with a P value < 0.05 (from Cyber-T). Finally, we only considered genes that showed a 1.5 or greater fold difference. Microarray data from this study can be accessed at the National Center for Biotechnology Information Gene Expression Omnibus website, with accession numbers: (To be deposited).

Validation of the microarray results was conducted using Northern blot analyses. w^{1118} and ybr^{5} were staged on food supplemented with 0.05% bromophenol blue. Total RNA from leg imaginal discs hand-dissected from -18 hr and -4 hr larvae and white prepupae was isolated using TriPure. ~10 μg of total RNA per sample was separated by formaldehyde gel electrophoresis, transferred to nylon membranes (GeneScreen Plus, PerkinElmer, Waltham, MA), and hybridized to specific probes labeled by random priming of gel-purified fragments (Prime-It II, Stratagene, La Jolla, CA). Probes for *Ecr*, *E74*, *E75*, *BR-C* common exon, *br Z2* and *rp49* (used as a control for loading and transfer) are described in Andres and Thummel (1994), Other gene-specific probes were generated by PCR from w^{1118} genomic DNA using the following primers. Forward and reverse primers to make the *Ama* probe are: 5'TGCAACTGACCGCTTATCTTGG3' and 5'AAGACCGATTAGAAGCCGCAG3'; forward and reverse primers to make the *bnb* probe are: 5'TCTCAGTGAGGGTCATTGTGC3' and 5'ATGGTGACTGGGCAATGGG3';

forward and reverse primers to make the *CG7447* probe are: 5'TCACTTGCAGTGCCATCGAG3' and 5'TCCTTGGGATCTGTGGGATAGC3'.

Statistical methods to identify significant enrichment of molecular functions, biological processes or InterPro motifs in the microarray data relative to the Drosophila genome were performed using the FatiGO web server (Al-Shahrour, 2006), using the parameter "over-represented terms in list 1" of the Fisher exact test.

Functional analyses

To amplify potential RNA interference we crossed a *UAS-Dicer* transgene into the *Gal4* lines used to drive the expression of the gene-specific double stranded RNA (Dietzl, 2007). Specifically, *P{UAS-Dcr-2.D}1, w^{1118}; Pin^{1}/CyO* flies were crossed with *Dll-GAL4* or *esg-GAL4* flies to produce *P{UAS-Dcr-2.D}1, w^{1118}; Dll-GAL4 /CyO, dfd-YFP* and *P{UAS-Dcr-2.D}1, w^{1118}; esg-GAL4 /CyO, dfd-YFP*. Virgin females of these genotypes were then mated to *UAS-RNAi* males. The vials were maintained in incubators maintained at a constant temperature of either 21°C or 25°C. The adults were transferred twice to new vials and newly eclosing F_1 flies were separated by genotype and examined for malformed legs each day for a total of 10 days per vial.

Prior to conducting the screen we crossed males from eight different RNAi lines (VDRC stock #1613 (*UAS-sbd RNAi*), 30934 (*UAS-CG7447 RNAi*), 106464 (*UAS-CG7447 RNAi*), 3299 (*UAS-dy RNAi*), 102255 (*UAS-dy RNAi*), 42480 (*UAS-CG12026 RNAi*), 43385 (*UAS-CG12026 RNAi*), 102005 (*UAS-CG12026 RNAi*)) to w^{1118} virgin females at 25°C. We examined all the progeny for malformed legs to determine the dominant background penetrance of malformed

legs in these stocks. We also crossed *P{UAS-Dcr-2.D}1, w^{1118}; Dll-GAL4 /CyO, dfd-YFP* female with w^{1118} male at 25°C to determine the penetrance of malformed legs in this background.

We considered an animal to be malformed if it displayed malformation in at least one leg, and defined a leg as malformed if any femur, tibia or tarsal segment was bent or twisted or was excessively short and fat.

Ecdysone feeding and *br-Z2* overexpression studies

We maintained w^{1118} and *w^{1118}; hs-br-Z2; hs-br-Z2* flies (in which the *br-Z2* isoform can be induced by exposing flies to 37°C for 30 minutes) in incubators controlled at 21°C on food containing 0.05% bromophenol blue. Mid third instar larvae (blue gut stage) from either w^{1118} or the *br-Z2* transgenic lines were collected and treated in the following four ways. In the first experiment we fed flies with regular yeast paste and maintained them at 21°C. In the second experiment we fed flies with yeast paste supplemented with 0.33mg/ml ecdysone (a level sufficient to induce ecdysone signals in McBrayer, 2007) and maintained them at 21°C. In the third experiment we heat shocked the vials in a water bath at 37°C for 30 minutes and then returned them to 21°C and fed the animals with regular yeast paste. In the forth experiment we heat shocked the vials in a water bath at 37°C for 30 minutes and then returned them to 21°C, but then fed the animals with yeast paste supplemented with 0.33mg/ml ecdysone. In all experiments we collected animals that pupariated between 18 and 24 hours of the treatment and then dissected leg imaginal discs from the 0 hr prepupae and examined their morphology.

Adult specimen preparations

Adult legs were dissected from the third thoracic segment in PBS, cleared in 10% KOH overnight, and mounted in Euporal (Bioquip, Gardena, CA) on microscope slides. Images of adult leg cuticles were captured on a Photometrics CoolSNAP ES high performance digital CCD camera with a Nikon Eclipse 80i microscope. All digital images were cropped and adjusted for brightness and contrast in Adobe Photoshop (version CS3, San Jose, CA), and figures were compiled using Adobe Illustrator (version CS3).

Results

br function is required early during leg morphogenesis

br^{5} is an amorphic allele, and *br*^{5} mutant animals are reported to display an early prepupal developmental arrest in which the imaginal discs fail to fully elongate and do not evert (Kiss 1988). In order to more fully characterize the developmental defects associated with *br*^{5} during imaginal disc morphogenesis, we collected leg imaginal discs from staged *br*^{5} larvae and prepupae and compared them to leg imaginal discs from identically staged *w*^{1118} animals (Figure 3.1). Leg imaginal discs from a *w*^{1118} (wild type) mid third instar larva (~18 hr prior to puparium formation) consist of roughly circular tissue composed of tall columnar cells that is covered and apposed by the squamous peripodial epithelium. The columnar epithelium has approximately two concentric folds due to apical constriction of the cells in the folds. By late third instar (~ 4 hr prior to pupariation) the disc appears larger and has initiated a slight elongation from the center as well as an additional concentric fold or two. By the onset of metamorphosis (0 hr or pupariation), the disc is more dramatically elongated from the center, while the columnar epithelium has increased the number of concentric folds to as many as five. The disc continues to elongate from the center (corresponding to the distal end of the elongated disc) in early prepupae, and continues to divide the disc into noticeable proximal-distal segments as more concentric folds are introduced and deepen. Specifically, by 4 hr after pupariation the future 5 tarsal segments and the distal half of the tibia are clearly distinguishable due to the folding of the epithelium. *br*^{5} mutant leg imaginal discs are indistinguishable from wild type through the larval stages, but are clearly aberrant at the onset of metamorphosis (Figure 3.1). This developmental defect is obvious both in the degree of elongation (*br*^{5} mutant discs are much less elongated) and

in the folding, in which the br^5 discs have fewer folds, but those folds appear to be deeper. Over the next several hours the br^5 discs do not appreciably elongate, but they do continue to form additional deep folds (although typically not enough to unambiguously distinguish the presumptive leg segments). Thus, based strictly on the morphology of br^5 mutant leg discs, it appears that *br* function is necessary for the elongation of leg discs and that this function is clearly required by the onset of metamorphosis in wild type animals.

Identification of genes regulated by *br* at the onset of metamorphosis in leg imaginal discs

In order to begin to determine how *br* may control the early events of leg morphogenesis, we wanted to identify the genes that are regulated by *br* during this process. At the time we began these studies only two genes were known to be regulated by *br* in larval or prepupal imaginal discs: *IMP-E3* and *Brg-P9* (Ward, 2003). To identify additional *br*-regulated genes we probed Affymetrix whole Drosophila genome gene chips with RNA isolated from staged w^{1118} and br^5 mutant leg imaginal discs. We chose to collect RNA from these animals at the onset of metamorphosis for the following reasons. First, our phenotypic analysis indicated that br^5 mutant discs are obviously arrested by 2 hr after puparium formation, and thus the genes required for normal development must be affected by this time point. Second, ecdysone, which is required for imaginal disc morphogenesis, peaks between -4 and 0 hr (Thummel, 2001). Since ecdysone is thought to induce *br* expression, we speculated that the window for *br*'s regulation of genes necessary for imaginal disc morphogenesis must fall between -4 and +2 hr relative to pupariation, with the critical period most likely centered on 0 hr given the need for these genes to be both transcribed and translated. Collecting RNA from 0 hr leg discs should therefore capture many of the genes regulated by *br* that function during morphogenesis.

A statistical analysis of the Affymetrix gene chips revealed that 360 genes are differentially expressed between br^5 and w^{1118} in leg imaginal discs at the onset of metamorphosis (Figure 3.2). Of these genes, 139 are normally induced by *br* in these cells, whereas 221 are repressed by *br*. We validated a subset of these genes by Northern blot analyses (Supplemental Figure 3.1). We used the FatiGO functional enrichment program (Al-Shahrour, 2007) to identify any annotated biological processes, molecular functions, or InterPro motifs that were over-represented in these genes relative to the Drosophila genome. There were no InterPro motifs over-represented and only one molecular function was over-represented: Gene Ontology (GO):0042302 structural constituent of cuticle (at level 3 in the GO database). There were several GO biological processes that were over-represented and all of them relate to carbohydrate or alcohol metabolic or catabolic processes (data not shown). When we parsed the list to only *br*-induced or -repressed genes, the structural constituent of cuticle was significantly over-represented in the *br*-repressed genes, whereas all the remaining GO categories were found in the *br*-induced genes. Thus it appears that *br* function is required to inhibit chitin synthesis, perhaps to allow the imaginal discs to undergo morphogenesis unimpeded from the overlying cuticle, whereas *br* function is important in the metabolic processes necessary to generate the energy required for morphogenesis.

We conducted a complementary experiment in which we compared total RNA from w^{1118} leg imaginal discs between -18 hr and 0 hr. We expected that this comparison would identify most of the genes regulated by the ecdysone signaling pathway in leg discs at the onset of metamorphosis. This analysis revealed 778 genes that are differentially expressed in leg imaginal discs between these two time points, of which 363 are induced at the onset of metamorphosis, and 415 are repressed (Figure 3.2). A subset of these genes was verified using Northern blot

analyses (Supplemental Figure 3.1). In addition, examination of the list reveals a number of known ecdysone regulated genes including *ImpL1*, *ImpL3*, *ImpE2*, *Eip78C*, *Eig71Ee*, *Sb*, *DHR64*, *viking*, and *Sgs* genes *3*, *4*, *5*, and *8* (Andres 1993; Gates, 2004), adding further validation to the experiment.

_br_ is expressed in third instar imaginal discs prior to the late larval ecdysone pulse

The most surprising observation from these microarray analyses is that the list of *br*-regulated genes does not more substantially overlap with the ecdysone-regulated genes. Given the well-accepted ecdysone-signaling hierarchy model, one would expect that the *br*-regulated genes would more or less represent a subset of all ecdysone-regulated genes. In fact, we found that only 31 of the 139 (22%) *br*-induced genes are represented in the ecdysone-induced genes (Table 3.1). Similarly only 40 of the 221 (18%) *br*-repressed genes are ecdysone-repressed (Table 3.2). This observation prompted us to examine whether *br* expression was really regulated by the late larval pulse of ecdysone. *br* genetic function is encoded by the Z2 isoform of the *BR-C* (Bayer, 1997). We therefore used northern blot analysis to probe RNA isolated from staged wing and leg imaginal discs for the expression of *BR-C* isoforms. Using a probe against the *BR-C* common exon we found that *Z2* and/or *Z3* were already expressed in -18 hr imaginal discs and persisted in imaginal discs until the onset of metamorphosis, at which time the *BR-C Z1* isoform began to become expressed (Figure 3.3). By +4 hr after puparium formation, *Z2* and/or *Z3* could not be detected, whereas *Z1* was strongly expressed. Examining this blot with a *Z2* specific probe confirmed that all the larval samples contained *Z2* RNA (data not shown). Thus, *br* function could be available through at least the later half of the third instar, and the late larval pulse of

ecdysone served to produce an isoform switch in these discs (*Z2* to *Z1*) rather than an upregulation of *br* (*Z2*).

This observation challenged the simple model that the late larval pulse of ecdysone was responsible for inducing *br* function that would then be responsible for triggering a morphogenesis program in the discs. To test this idea, we took advantage of a transgenic line containing two copies of a heat-inducible *Z2* transgene created by Bayer et al. (Bayer, 1997). We heat shocked third instar larvae 24-18 hr before puparium formation and examined the morphology of the leg imaginal discs at purpariation. If the expression of *Z2* is sufficient to induce a leg morphogenesis program we reasoned that these leg discs should exhibit precocious elongation. We never observed precocious elongation in the heat-induced *Z2* transgenic animals ($n > 30$ animals) as compared to control w^{1118} and non heat-induced *hs-Z2* transgenic animals (Figure 3.4A, B). We next reasoned that if ecdysone signaling itself was sufficient to activate a leg morphogenesis program, then feeding wild type mid third instar larvae might result in precocious elongation. We therefore fed mid third instar w^{1118} larvae with yeast paste containing either 20-hydroxyecdysone at 0.33mg/ml in ethanol or ethanol alone. Animals that pupariated between 18 and 24 hours after the initiation of feeding were examined for leg disc morphology at the onset of metamorphosis. We again never observed precocious elongation in any of these animals compared to control animals (Figure 3.4C).

Taken together, we postulated that *Z2* encoded Br protein was present in late third instar imaginal discs, and that this pool of Br may then function in concert with ecdysone signaling activated by the late larval ecdysone pulse. To test this idea we combined these treatments and fed ecdysone-containing yeast paste to *hs-Z2* animals that had been induced by a 30 min heat

induction 18-24 hr prior to pupariation. Under these conditions we never observed precocious elongation in any of these animals compared to control animals (Figure 3.4D).

Functional analysis of *br*-induced, ecdysone-induced genes reveals requirements during leg morphogenesis

If the *br*-induced, ecdysone-induced genes include the key secondary response genes necessary for the leg morphogenesis program, then we should be able to identify these genes by functionally removing them in leg imaginal discs and examining the adult legs for morphological defects. To accomplish this we used stocks from the Vienna Drosophila RNAi Center that contain transgenes capable of expressing double stranded RNAs driven by an upstream activating sequence (UAS) promoter. Stocks targeting 27 of the 31 *br*-induced, ecdysone-induced genes were obtained, with an average of two independent insertion lines for each gene. To knock down the expression of these genes in leg imaginal discs undergoing morphogenesis, we used two different Gal4-expressing lines: *escargot (esg)-Gal4* and *Distal-less (Dll)-Gal4*. Whereas *esg-Gal4* is pan imaginal disc, *Dll-Gal4* is restricted to the distal half of the tibia and the tarsal segments (Ward et al., 2003b). To titrate the RNAi phenotype we conducted these experiments at two temperatures, 21°C and 25°C, and in either the presence or absence of *UAS-Dicer* (Dietzl, 2007). Thus we were able to generate an allelic series of RNAi knockdown from 21°C, no Dicer (weakest) to 25°C, no Dicer that was similar to 21°C with Dicer, to 25°C with Dicer (strongest).

We first conducted a series of control experiments to determine whether the *UAS-Dicer; Dll-Gal4* line or several of the *UAS-RNAi* lines would show dominant effects in leg morphogenesis. We therefore took individual VDRC RNAi stocks or the *Gal4* driver lines and crossed them to

w^{1118} at 25°C and examined the progeny for malformed legs. We detected a small 2% level of malformation in the *UAS-Dicer; Dll-Gal4*, but did not detect any malformations in the RNAi lines (Table 3.3).

We next induced RNAi for the 27 genes in legs using the *Dll-Gal4* and *esg-Gal4* drivers. We found that the *esg-Gal4* is a fairly weak driver, and thus only completed the analysis for all the genes using *UAS-Dicer; esg-Gal4* at 25°C. Similarly, since *Dll-Gal4* alone at 21°C was generally very weak we did not completely test all of the *br*-induced, ecdysone-induced genes using this condition. The results of these experiments are listed in Table 3.4. Notably, 10 of the 27 genes produced animals showing at least 20% malformed legs in at least one of the conditions tested (with an $n > 25$ animals). Examples of the malformed legs produced in these crosses are shown in Figure 3.5. In general the malformations produced by *Dll-Gal4*-driven RNAi are limited to the distal tibia and tarsal segments suggesting that they may be functioning in a cell autonomous manner. In addition, all of the mutant phenotypes could be classified as malformed rather than incorrectly patterned, with the most obvious malformation consisting of short and fat segments rather than bent or twisted segments. One gene that showed substantial malformations under all conditions tested was *sbd*. *sbd* mutations have been shown previously to affect leg morphogenesis, both when homozygous and as dominant enhancers of *br*, *Rho1* and *zip* (Beaton, 1988; Gotwals, 1991; Ward, 2003; Bayer 2003), which suggests that these functional analyses are working as expected. Six of these genes (*sbd*, *CG7447*, *CG7778*, *dusky(dy)*, *CG15756*, and *CG33993*) are particularly interesting, as they show highly penetrant leg malformations under nearly all conditions tested (Table 3.4). Three additional lines produced no adults under any condition tested. We examined the vials in these crosses and determined that RNAi against *E(spl)mα* and *knk* were embryonic or larval lethal and thus could not assess the effect of gene-

specific RNAi on leg development in these animals. In contrast, RNAi against *CG1969* produced some pupae and pharate adults, and these animals displayed malformed legs, although we have not quantified the penetrance of this phenotype.

Discussion

A microarray screen for new *br*-regulated genes

Here we have presented the results of a pair of microarray analyses intended to identify genes that are regulated by ecdysone and by the ecdysone primary response gene *broad* during the process of leg imaginal disc morphogenesis during metamorphosis. Previous work had demonstrated that *br* function is essential for imaginal disc morphogenesis (Kiss 1988, and Ward 2003b). Here we show that morphogenesis arrests by 2 hr after puparium formation in animals hemizygous for an amorphic allele of *br*. Since *br* encodes a transcription factor (DiBello, 1991), we postulated that *br* function must be required for the regulation of genes expressed near the onset of metamorphosis in order for their products to regulate a morphogenesis program in the imaginal discs. Few genes were previously known to be regulated by *br* in imaginal discs at this time point (Bayer, 1996; Ward, 2003), and thus a microarray approach offered the potential to dramatically increase our understanding of the regulation of imaginal disc morphogenesis. From this analysis we identified 360 genes that are regulated by *br* in leg imaginal discs at the onset of metamorphosis, of which 139 are normally induced by *br* and 221 repressed. One of the two previously known *br*-regulated genes, *ImpE3*, was identified by the analysis, whereas the other gene, *Brg-P9*, was not included on the chip, and thus could not be assessed. To further confirm the validity of the microarray, we probed a series of northern blots and showed that we could identify specific examples of gene induced and repressed by *br*. Thus we believe that the genes identified from this analysis reflect a true representation of the *br*-regulated genes in leg imaginal discs at the onset of metamorphosis.

Many of the genes normally induced by *br* at the onset of metamorphosis encode proteins involved in metabolism, and in particular catabolic processes involving carbohydrates and alcohols. This finding is significant in terms of the events occurring at this stage of Drosophila development. During the early stages of metamorphosis the obsolete larval tissues are degraded through apoptosis and autophagy, whereas the imaginal discs initiate morphogenetic programs resulting in the formation of a rudimentary adult in about 12 hrs (von Kalm, 1995). Within the first few hrs of pupariation, the main tracheal spiracles are broken, severing an important connection between the oxygen rich ambient environment and the encased prepupa (Robertson, 1936). Although the early stages of imaginal disc morphogenesis occur in the absence of cell proliferation, there are extensive cell shape changes and cell rearrangements occurring that are likely very expensive from an energy balance perspective. Thus in a potentially hypoxic environment, the input of energy from catabolic sources is likely crucial for successful completion of the morphogenetic program.

As a means to further parse the list of *br*-regulated genes in order to identify the genes that are most likely to be playing important roles in the leg morphogenesis program, we conducted a second set of microarray comparisons between RNAs isolated from wild type leg imaginal discs prior to the late larval ecdysone pulse and at the onset of metamorphosis. From this analysis we identified 778 genes that are differentially expressed between -18 hr and 0 hr leg discs, of which 363 are upregulated and 415 are downregulated. We propose that these genes would capture a large subset of the ecdysone-regulated genes required for leg morphogenesis, and thus have labeled them as "ecdysone-regulated" genes. Consistent with this idea, we identified a number of well-described ecdysone-regulated genes in this set including several *Imp*, *Eip* and *Sgs* genes (Andres, 1993).

As ecdysone signaling is known to be required for imaginal disc morphogenesis, showing an arrest very similar to what is observed in *br* mutants when the Ecdysone receptor is reduced by genetic mutation or RNA interference (Lam, 2000; Davis, 2005), and *br* is thought to function downstream of the ecdysone signaling pathway, we expected that the *br*-regulated genes would thus be a subset of these "ecdysone-regulated" genes. To our surprise we found only ~20% of the *br*-regulated genes are also ecdysone-regulated. Included in this set, however, are genes that are known to be both ecdysone- and *br*-regulated (*ImpE3*; Ward 2003) and genes that have been strongly implicated in imaginal disc morphogenesis (*sbd*; Beaton 1988; Gotwals 1991; Ward 2003; Bayer 2003).

The ecdysone signaling pathway in imaginal discs

The strong lack of overlap between the *br*-regulated and ecdysone-regulated genes in leg imaginal discs raised the question of whether a canonical ecdysone signaling pathway was operating in late larval imaginal discs. To address this question we used Northern blot analysis to monitor the expression of the *Ecdysone receptor* (*EcR*) and other primary response genes in whole animals and in imaginal discs. The pattern of *EcR* was identical in imaginal discs and whole animals, as was the expression of the *E74* early genes. Furthermore, the overall pattern of expression at times surrounding the late larval ecdysone pulse (which peak from -4 hr to 0 hr) was normal for all the genes examined, strongly indicates a normal response to the hormone in late larval imaginal discs. *E75* and *BR-C*, however, showed substantial expression in -18 hr imaginal discs that was not represented (or was greatly reduced) in whole animals. This precocious expression of *E75* and *BR-C* hints at a more complex regulation of these genes in imaginal discs. There is some evidence for at least one small ecdysone pulse ~24 hr prior to

pupariation that may be responsible for initiating wandering behavior (D'Avino, 1995). It is possible that these genes are more sensitive to ecdysone and can be induced by this pulse, however, there must also be as yet unknown tissue-specific co-factors that allow for expression of *E75* and *BR-C* in imaginal discs in response to this systemic pulse of ecdysone. Alternatively, these genes could be induced in mid third instar larvae independently of the hormone.

The predominant isoform of *BR-C* expressed in mid third instar imaginal discs is *Z2* (and possibly *Z3*). Expression of the *BR-C* locus is complex, with two distinct promoters driving the expression of the four *BR-C* isoforms. Although there is a temporal differences in promoter usage in which the proximal promoter is used earlier than the distal promoter, both promoters are capable of generating all 4 isoforms (Bayer, 1996). It should be noted that the three higher molecular weight bands (10, 9, and 7 kb) detected using a probe to the common exon are also detected by both *Z2* and a *Z3* specific exon probes, indicating that the final isoform is processed post-transcriptionally from a larger transcript. A *Z2* specific probe indicated that *Z2* is indeed expressed at -18 hr in larval imaginal discs (data not shown). At the onset of metamorphosis an isoform switch occurs in which *Z2* (and *Z3*) expression is repressed and *Z1* (4.4 kb band) is induced. Although this isoform switch is coincident with the ecdysone pulse, it is not likely due to differential promoter usage, but rather reflects alternative splicing of the primary transcript that may be regulated by the ecdysone signaling pathway.

There are several possible non-exclusive hypotheses for how *br* may regulate transcription to control a morphogenesis program in leg imaginal discs at the onset of metamorphosis. First, given the fact that *br Z2* expression is normally turned off at the onset of metamorphosis, it is possible that some of the genes that are repressed by *br* (and likely ecdysone) must be turned off to allow morphogenesis to occur. One potential example of this is *MYP-75D*. *MYP-75D* encodes

a subunit of the myosin phosphatase complex that is required to negatively regulate nonmuscle myosin activity (Vereshchagina, 2004). We and other labs have previously shown that leg morphogenesis requires Rho signaling and myosin activity (Bayer, 2003; Gotwals, 1991; Halsell, 1998; Ward, 2003). Thus failure to inactivate myosin phosphatase at the end of larval development may inhibit the ability of those cells to undergo coordinated changes in cell shape and rearrangement. Additional studies will be necessary to assess the phosphorylation of the myosin regulatory light chain in *br* mutant prepupae as a readout of myosin activity. An argument against *br*-dependent repression as the primary driving force behind leg morphogenesis can be made based upon the observation that a heat-inducible *Z2* transgene expressed in both larvae and prepupae can undergo normal leg morphogenesis (Bayer, 1996). In fact, the expression of *Z2* at both larval stages and in 0 hr prepupae was necessary to provide rescue of the amorphic br^5 mutation.

Alternative hypotheses regarding the role of *br* in leg morphogenesis postulate an inductive role for *br*-dependent transcription, and either require an additional input from the ecdysone signaling pathway or operate independent of this signal. To address these issues we conducted a series of experiments using a heat-inducible *Z2* transgene in wild type animals. If *br* is sufficient to induce a morphogenesis program, then we surmised that early induction of *br* would result in precocious leg development in 0 hr prepupae. We never observed this result, suggesting additional controls on leg morphogenesis. An attractive cofactor would be the Ecdysone receptor or another of the primary response genes that would be induced at the onset of metamorphosis by ecdysone signaling. To address this we combined early expression of the *Z2* transgene coincident with ecdysone feeding (at a level that has physiological effects in the animal; McBrayer, 2007). Again, we observed no precocious elongation of the leg imaginal discs in these animals,

suggesting that either the ecdysone feeding was not sufficient to produce a high titer ecdysone response in imaginal discs, or that we are missing yet one or more competence factors that allow the imaginal discs to respond appropriately to ecdysone signaling and *br* function. One piece of evidence that a combination of *br*-induced transcription and ecdysone signaling is important for the leg morphogenesis program is the finding that RNAi-induced knockdown of several of the *br*-induced, ecdysone-induced genes result in leg malformations. At this point we have not ruled out the possibility that additional genes induced by *br* at earlier stages of development (thus ecdysone independent) may also function in the leg morphogenesis program. It is even possible that one of the *br*-induced, non ecdysone-induced genes serves as the aforementioned competence factor postulated for the morphogenesis program.

New insights into imaginal disc morphogenesis

Our previous forward genetic screens indicated that the Rho signaling pathway plays a critical role in directing leg morphogenesis in conjunction with *br*, likely through its well described roles in modulating the actin cytoskeleton (Ward, 2003). The identification of a component of the myosin phosphatase as an ecdysone-repressed, *br*-repressed gene supports this notion and provides the first direct link between the ecdysone and Rho signaling pathway. These microarray results, however, did not suggest any potential positive input from the ecdysone signaling pathway to the Rho pathway. In fact these results supported our earlier Northern blot analyses that showed that the core components of the Rho signaling pathway (for example *Rho1*, *Rho kinase*, *RhoGEF2*, *zip*, and *sqh*) are expressed in leg imaginal discs throughout late larval and early prepupal development, and their expression is not dependent upon ecdysone signaling or *br* function (Ward, 2003 and data not shown). It is possible that ecdysone and *br* may regulate the

expression of a tissue- or temporal-specific regulator of the Rho signaling pathway, for example a scaffolding protein that may serve to assemble an active Rho complex at the right time or region of the cell to affect localized cell shape changes, apical constrictions or cell rearrangements.

RNAi knockdown of several *br*-induced, ecdysone-induced genes suggest novel potential mechanisms contributing to leg morphogenesis including modulations of the extracellular matrix and cell signaling. Six of the 27 *br*-induced , ecdysone-induced genes that we could test through leg specific RNA interference showed strong effects on leg morphogenesis under several different conditions. Two of these genes, *dusky* and *CG15756* encode proteins that may bind chitin. For example, *dusky* encodes a transmembrane protein with a zona pellucida domain and a domain homologous to several vertebrate and invertebrate apical matrix components (Roch, 2003). It is only expressed in cuticle-secreting tissues and is thought to be involved in interactions between the apical membrane, the cytoskeleton and the cuticle. In addition, *sbd* encodes a transmembrane serine protease that was previously shown to be induced by ecdysone in imaginal discs at the onset of metamorphosis (Appel 1993). Recent work has indicated that *sbd* interacts genetically with the Rho signaling pathway (Bayer, 2003), suggesting a role in cell signaling that may connect the ecdysone and Rho signaling pathways. Additional potential signaling molecules identified from this microarray screen include *CG7447*, which encodes a 512 amino acid secreted protein with an N-terminal EMI (cysteine rich) domain and an EGF domain, and *CG33993*, which possesses an SH2 domain. Our future work will include more detailed examination of the function of these genes during normal leg imaginal disc morphogenesis. Through these analyses we can better understand the mechanisms by which ecdysone regulates events at the cytoskeleton to drive specific morphogenetic events during leg

development. We anticipate that these findings will be generally applicable and will serve as an excellent paradigm to address the mechanisms of hormone-dependent morphogenesis in a wide range of species.

Figure 3.1

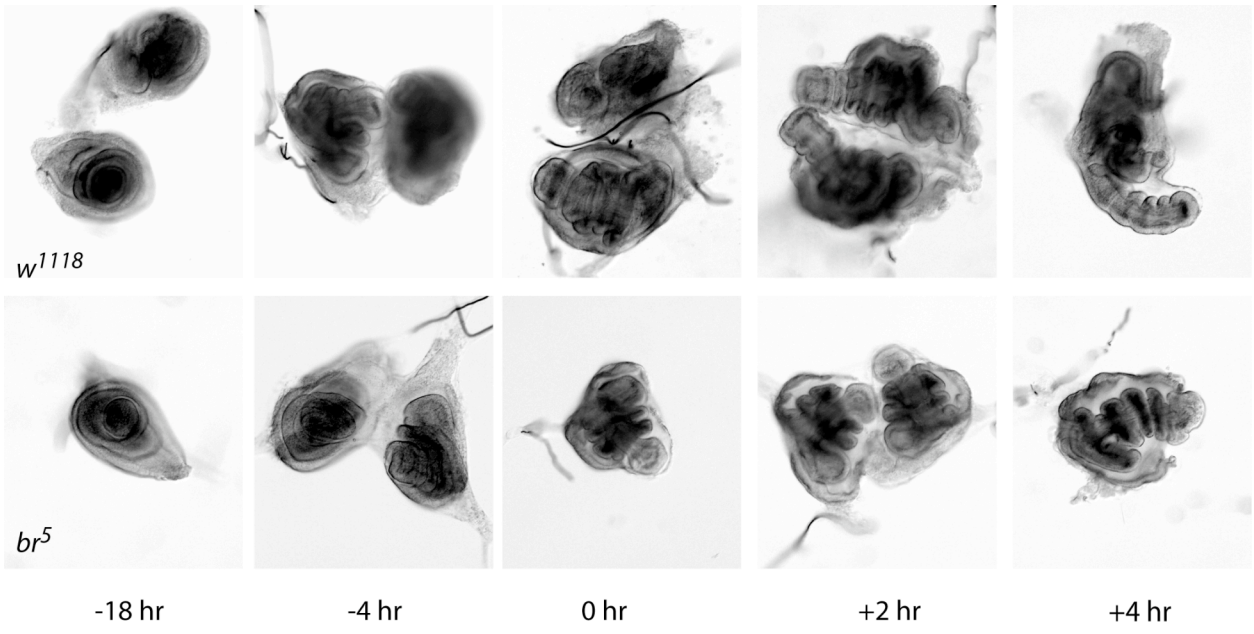

Fig. 3.1 Morphology of leg imaginal discs undergoing morphogenesis in w^{1118} and br^5 mutant animals. Pairs of or single leg imaginal discs were dissected from -18 hr and -4 hr larvae, and 0 hr (onset of metamorphosis), +2 hr and +4 hr prepupae from w^{1118} and br^5 animals. Note that the leg imaginal discs are a flat epithelium in mid third instar larva (-18 hr) in both w^{1118} and br^5. In wild type larvae, elongation begins about 4 hrs before the formation of puparium (0 hr). By 0 hr, the elongation and segmentation of the w^{1118} leg disc is obvious, and continues through the +4 hr time point. In br^5 mutant animals, elongation is noticeably arrested by +2 hr. There is little additional elongation that occurs in br^5 mutant leg disc, even through +24 hr (not shown).

Figure 3.2

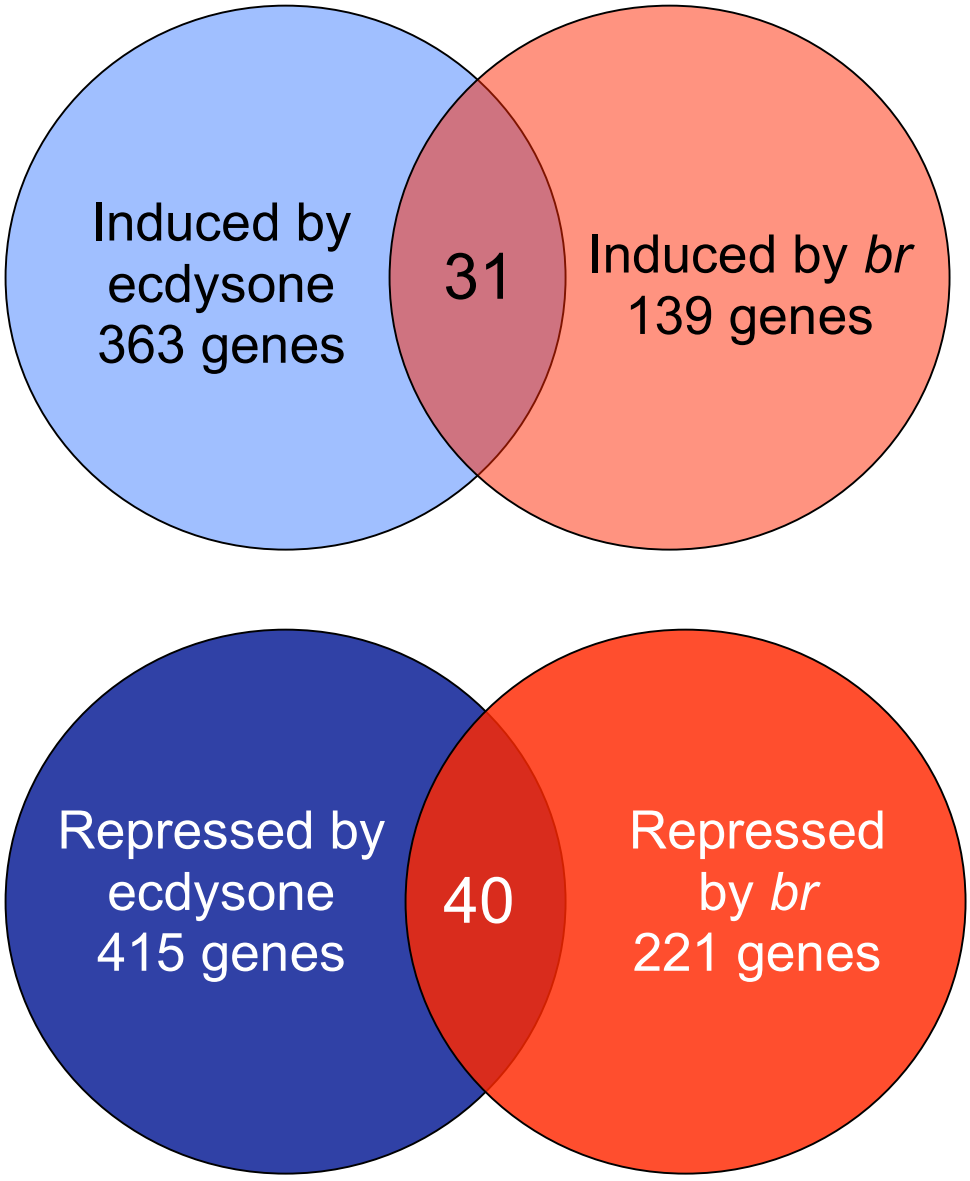

Fig. 3.2. Summary of the microarray results showing that only a small set of *br*-regulated genes are regulated by ecdysone at the onset of metamorphosis. 363 genes are induced by ecdysone (light blue) at the onset of metamorphosis, whereas 139 genes are induced by *br* (pink). Only 31 of these genes are in common. Similarly, of the 415 genes repressed by ecdysone (royal blue) and the 221 genes (deep red) repressed by *br*, only 40 are in common.

Figure 3.3

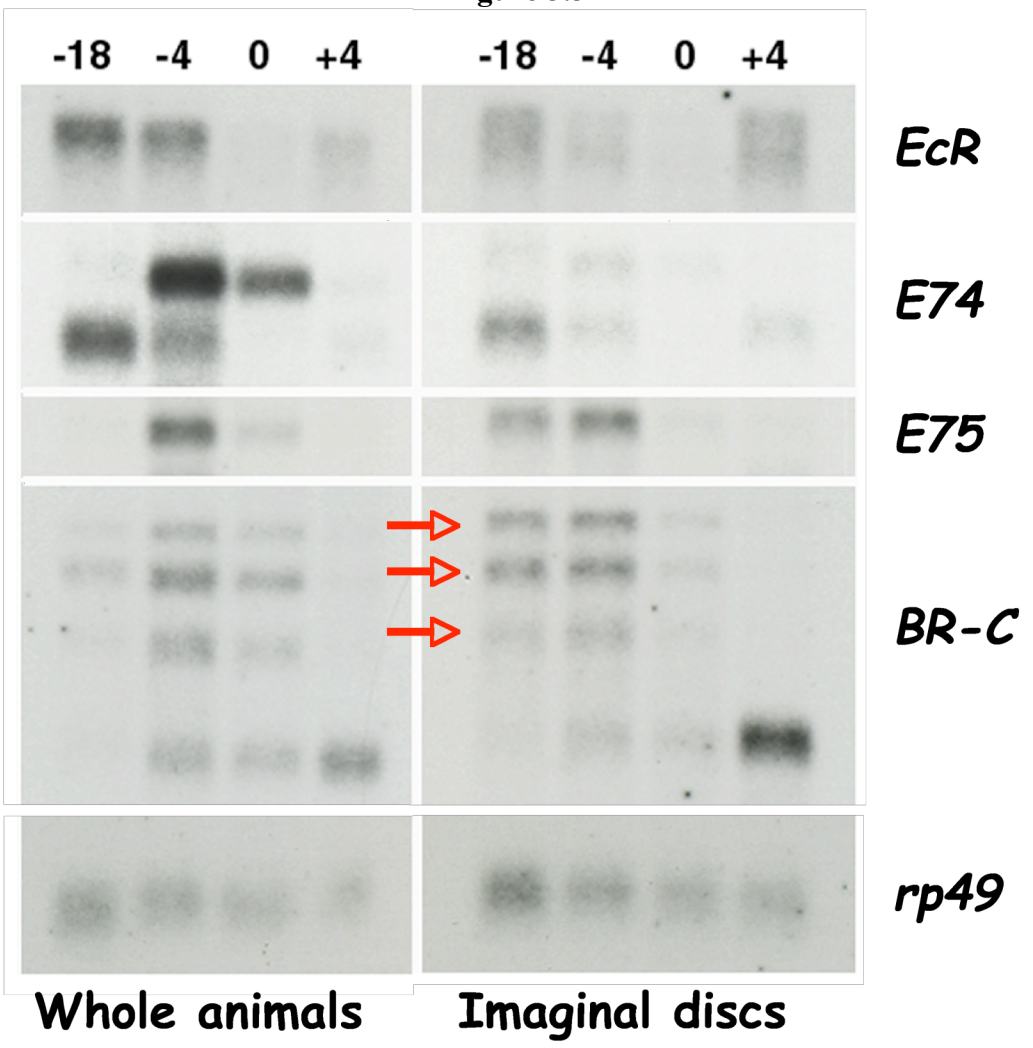

Fig. 3.3. Northern blot analysis of ecdysone signaling in whole animals and imaginal discs. Total RNA was isolated from w^{1118} (wild type) whole larvae (-18 hr and -4 hr relative to puparium formation) and pupae (0 hr and +4 hr) or from leg and wing imaginal discs. The RNAs were separated by electrophoresis, transferred to nylon membranes and probed against the ecysone signaling genes indicated. There are four transcripts encoded by *BR-C*, of which the lower band represents the *Z1* isoform and the upper 3 bands (red arrows) indicate *Z2* and/or *Z3* isoforms. Note that *Z2*/*Z3* isoforms are already expressed in mid third instar larval imaginal discs (-18 hr) before the late third instar larval ecdysone pulse (which peaks between -4 and 0 hr).

Figure 3.4

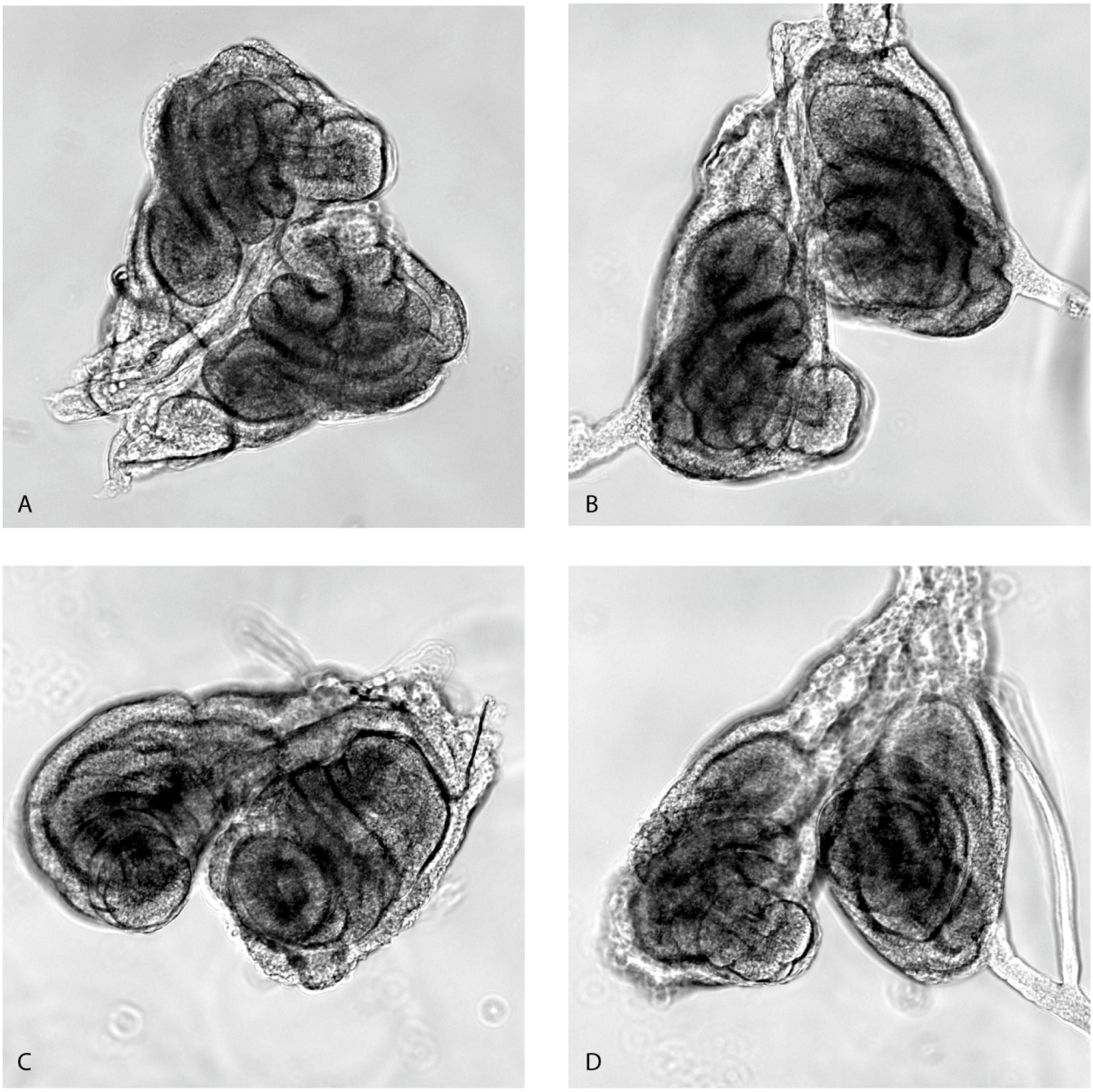

Fig. 3.4. Neither early induction of *br Z2* nor ecdysone feeding of mid third instar larvae leads to precocious elongation of leg imaginal discs. Brightfield photomicrographs of leg imaginal discs dissected from 0 hr w^{1118}*; hs-br-Z2; hs-br-Z2* prepupae that were kept at 21°C for its whole life (A), or that was heat shocked to induce *Z2* expression in mid third instar (B), or that was fed with ecdysone-mixed yeast paste beginning in early third instar and maintained at 21°C (C), or that was heat shocked to induce *Z2* expression in early third instar, and then was fed with ecdysone-mixed yeast paste (D). Note that the extent of leg elongation at 0 hr was similar under all of these conditions, and was consistent with wild type discs at the onset of metamorphosis (compare to Figure 3.1)

Figure 3.5

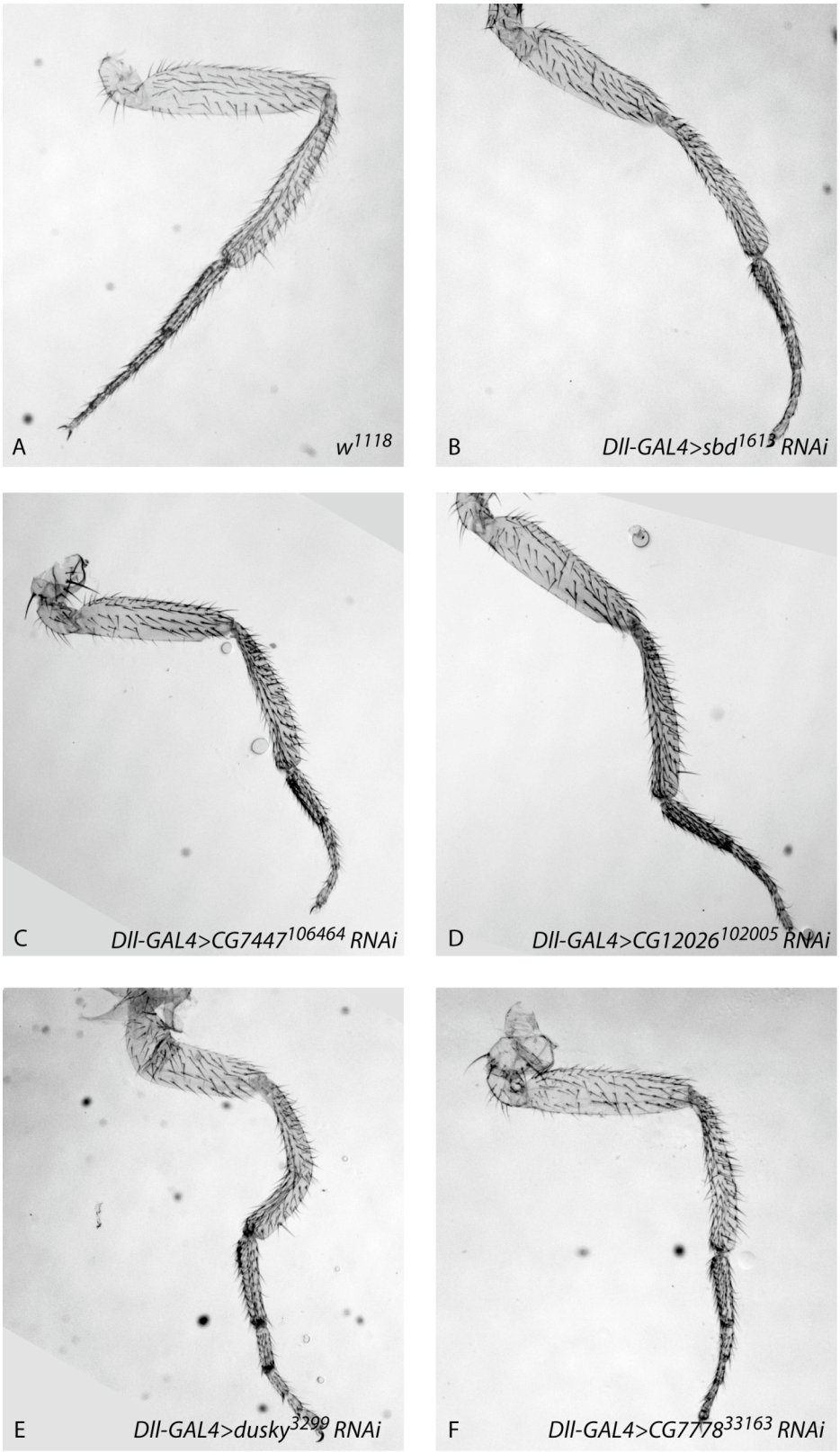
A
w^{1118}
B
Dll-GAL4>sbd^{1613} RNAi
C
Dll-GAL4>$CG7447^{106464}$ RNAi
D
Dll-GAL4>$CG12026^{102005}$ RNAi
E
Dll-GAL4>$dusky^{3299}$ RNAi
F
Dll-GAL4>$CG7778^{33163}$ RNAi

Fig. 3.5. Representative malformed legs generated by RNAi-induced attenuation of ecdysone- and *br*- induced genes in leg imaginal discs. Brightfield photomicrographs of adult legs from the third thoracic segment**.** (A) w^{1118} leg. (B) *Dll-Gal4/ UAS-sbdRNAi*. (C) *Dll-Gal4/ UAS-CG7447RNAi.* (D) *Dll-Gal4/ UAS-CG12026RNAi.* (E) *Dll-Gal4/ UAS-duskyRNAi.* (F) *Dll-Gal4/ UAS-CG7778RNAi.* Note that all of the malformations are characterized by short fat tarsal segments along with either shortening of the tibia (C, D, and F) or a sharp bend in the tibia corresponding to the boundary of Dll-Gal4 expression (E).

Supplemental Fig. 3.1

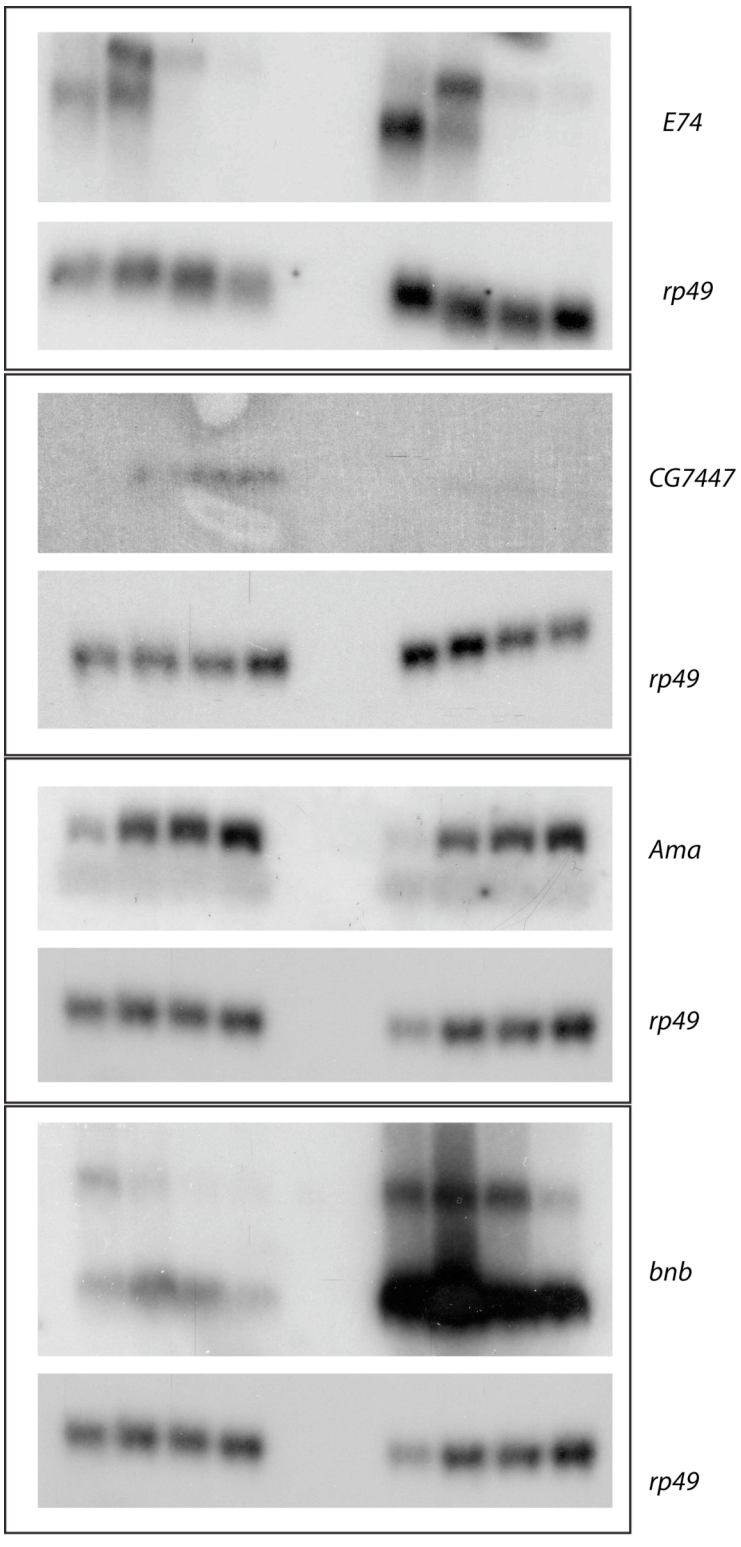

Supplemental Fig. 3.1. Validation of ecdysone- and *br*-regulated genes by Northern blot analysis. Anterior tissue sections (primarily consisting of all the imaginal discs, brain, salivary glands and epidermis) were dissected from -18, -4, 0 and +2 hr w^{1118} and br^{5} mutant animals. Total RNA extracted from these samples were separated by electrophoresis and transferred to nylon membranes and probed with the indicated genes. *E74* was used a control to monitor the late larval ecdysone pulse. The switch from *E74B* to *A* indicates that both the w^{1118} and br^{5} mutant animals experienced an ecdysone pulse from -4 to 0 hr (top panel). *rp49* is used as a control for loading and transfer in all these experiments. *CG7447* and *Ama* are two putative cell adhesion molecules that were determined by the microarray to be induced by ecdysone and *br* at the onset of metamorphosis. The northern blot confirms these observations. Similarly, *bnb* is a gene that was determined by microarray to be repressed by *br*, as was confirmed by the Northern blot shown in the bottom panels.

Table 3.1

br-induced genes expressed in leg discs that are also induced by ecdysone at the onset of metamorphosis

Gene name	Fold induction[a]	Function
CG15756	7.49	chitin binding
Enhancer of split	6.12	Notch signaling
E(spl) region transcript mα	5.47	Notch signaling
TweedleE	5.44	nutrient reservoir activity
dusky	4.72	structural constituent of chitin-based cuticle
CG7447	4.2	EGF-like calcium-binding
CG5639	3.88	serine-type endopeptidase inhibitor
CG3831	3.86	unknown
CG10625	3.78	structural constituent of cuticle
CG9312	3.49	unknown
Ecdysone-inducible gene E3	3.35	unknown, imaginal disc eversion
CG16733	2.78	aryl sulfotransferase activity; retinol dehydratase activity
CG1969	2.75	glucosamine 6-phosphate N-acetyltransferase activity
CG4914	2.69	serine-type endopeptidase activity
vermiform	2.59	chitin binding
knickkopf	2.45	dopamine beta-monooxygenase activity
CG9416	2.27	peptidase activity
dawdle	2.05	transforming growth factor beta receptor binding
CG7778	2.03	unknown
Heat shock gene 67Ba	1.98	Heat shock protein Hsp20
Amalgam	1.97	Immunoglobulin-like fold
CG12026	1.95	Claudin
CG33993	1.92	protein binding, SH2
pale	1.84	tyrosine 3-monooxygenase activity; iron ion binding
CG6776	1.65	glutathione transferase activity
serpentine	1.64	chitin binding
Stubble	1.64	serine-type endopeptidase activity
Unc-76	1.62	kinesin binding
CG3842	1.57	oxidoreductase activity, acting on CH-OH group of donors
methuselah-like 5	1.53	G-protein coupled receptor activity
CG6361	1.51	serine-type endopeptidase activity

[a]Fold induction by *br*: represents relative mean expression difference between w^{1118} and br^{5} in 0 hr leg discs.

Table 3.2

br-repressed genes in leg discs that are also repressed by ecdysone at the onset of metamorphosis

Gene name	Fold repression[a]	Function
CG17843	42.99	flavin-linked sulfhydryl oxidase activity
CG14984	15.37	unknown
CG9877	8.60	unknown
CG7465	8.15	unknown
Tie-like receptor tyrosine kinase	7.36	protein tyrosine kinase activity
CG4484	7.18	sucrose:hydrogen symporter activity
Cuticular protein 64Aa	6.67	structural constituent of chitin-based larval cuticle
Transferrin 1	6.46	ferric iron binding
Glutathione S transferase E6	5.95	glutathione transferase activity
Odorant-binding protein 99a	5.54	odorant binding
CG6643	5.03	unknown
MYPT-75D	5.01	myosin phosphatase regulator activity
CG6579	4.87	unknown
CG10527	4.87	farnesoic acid O-methyltransferase activity
CG1648	4.75	unknown
Aldehyde dehydrogenase	4.63	aldehyde dehydrogenase (NAD) activity
Cht7	4.29	chitinase activity
CG6045	4.22	xanthine dehydrogenase activity
CG3546	3.42	unknown
CG15282	3.18	unknown
CG12643	3.18	unknown
CG15093	2.83	3-hydroxyisobutyrate dehydrogenase activity
Tetraspanin 42El	2.61	unknown
Glutathione S transferase E1	2.53	glutathione transferase activity
easter	2.50	serine-type endopeptidase activity
outspread	2.31	unknown
CG17738	2.26	unknown
ken and barbie	2.11	transcription factor activity
CG7800	2.00	protein binding
CG30196	1.97	unknown
CG30217	1.97	unknown
CG34349	1.97	unknown
Lamin C	1.95	structural molecule activity
Chitinase-like	1.92	chitinase activity
methuselah-like 3	1.84	G-protein coupled receptor activity
CG9338	1.76	unknown
CG10237	1.75	retinal binding, vitamin E binding
Tequila	1.73	serine-type endopeptidase activity
CG33110	1.63	unknown
CG34388	1.55	unknown
cracked	1.55	chitin binding

[a]Fold repression by *br*: represents relative mean expression difference between br^{5} and w^{1118} in 0 hr leg discs.

Table 3.3

Control experiments for dominant malformed legs in VDRC RNAi and GAL4 lines

Drosophila stock[a]	% malformed (*n*)[b]
sbd^{1613}	0(91)
CG7447^{106464}	0(75)
CG7447^{30934}	0(99)
dy^{3299}	0(86)
dy^{102255}	0(57)
CG12026^{42480}	0(73)
CG12026^{43385}	0(55)
CG12026^{102005}	0(85)
UASDicer; Dll-GAL4	2(83)

[a]Male flies from the indicated stocks were crossed to w^{1118} virgin females at 25°C except for *UASDicer; Dll-GAL4, in which P{UAS-Dcr-2.D}1,* w^{1118}*; Dll-GAL4 /CyO, dfd-YFP* virgin female was crossed with w^{1118} male. Allele designations represent the VDRC stock numbers. [b]% malformed indicates the percentage of animals heterozygous for the indicated genotype showing a malformed leg phenotype in at least one leg. *n*, total number of flies of the indicated genotype that were scored.

Table 3.4

Malformed leg phenotypes produced by leg disc induced RNAi

			% malformed (*n*)[a]			
Gene Symbol	**Annotation Symbol**	**VDRC Line**	***Dll* (*Dicer*, 25°C)**	***Dll* (*Dicer*, 21°C)**	***Dll* (25°C)**	***esg* (*Dicer*, 25°C)**
CG1969	*CG1969*	103542	0(0)	0(0)	0(0)	0(0)
Ama	*CG2198*	22944	0(10)	2(45)	45(11)	1(148)
		22945	0(5)	1(69)	0(10)	1(161)
ImpE3	*CG2723*	16402	0(2)	0(58)	10(89)	1(124)
		16403	0(0)	0(0)	0(48)	1(171)
CG3831	*CG3831*	7405	8(13)	2(66)	3(104)	2(248)
		101921	0(0)	20(5)	10(138)	0(15)
CG3842	*CG3842*	7117	0(0)	31(13)	0(25)	0(41)
		107443	0(0)	25(4)	4(47)	0(4)
Hsp67Ba	*CG4167*	21806	0(0)	12(51)	0(2)	0(29)
		104341	0(0)	2(55)	6(53)	1(128)
sbd	*CG4316*	1613	100(4)	59(27)	78(32)	18(78)
CG5639	*CG5639*	1305	0(0)	0(0)	0(0)	3(76)
		1306	4(25)	4(78)	13(117)	1(182)
knk	*CG6217*	106302	0(0)	0(0)	0(0)	0(0)
CG6361	*CG6361*	28410	5(56)	0(106)	0(75)	0(116)
CG6776	*CG6776*	105274	0(0)	10(30)	10(99)	0(174)
CG6965	*CG6965*	101593	20(5)	0(50)	30(10)	0(65)
		3390	4(26)	1(125)	0(47)	0(44)
CG7447	*CG7447*	30934	40(55)	15(124)	30(30)	0(122)
		106464	76(54)	26(139)	23(73)	1(216)
CG7778	*CG7778*	33163	36(22)	4(69)	67(6)	0(114)
		102181	61(28)	30(89)	0(0)	1(168)
E(spl)mα	*CG8337*	35886	0(0)	0(0)	0(0)	0(0)
E(spl)	*CG8365*	37686	0(5)	2(91)	0(1)	0(117)
CG9312	*CG9312*	16646	22(9)	1(117)	10(10)	1(182)
dy	*CG9355*	3299	0(0)	100(33)	0(0)	1(118)
		102255	0(0)	91(79)	0(0)	2(124)
CG9416	*CG9416*	10064	25(12)	4(142)	4(23)	0(148)
		106330	0(1)	30(33)	83(35)	1(153)
CG10625	*CG10625*	26780	0(34)	2(109)	3(37)	0(62)
		102369	15(34)	0(126)	28(58)	1(180)
CG12026	*CG12026*	42480	8(25)	5(125)	23(66)	1(149)
		43385	40(10)	11(134)	0(2)	0(163)
		102005	59(51)	23(159)	39(51)	0(157)
TwdlE	*CG14534*	24867	15(47)	25(104)	0(1)	0(207)
		107483	0(4)	6(62)	0(0)	0(123)
CG15756	*CG15756*	30251	13(23)	15(131)	3(34)	0(214)
		105695	30(70)	38(69)	32(37)	1(142)
CG16733	*CG16733*	47019	3(33)	2(84)	0(0)	0(37)
		47020	12(25)	13(40)	4(23)	0(117)

daw	*CG16987*	13420	0(46)	2(61)	0(40)	1(113)
serp	*CG32209*	15466	25(4)	50(4)	0(0)	0(61)
CG33993	*CG33993*	40702	0(0)	0(0)	0(3)	0(19)
		102754	30(10)	21(67)	41(85)	0(8)

[a]% malformed indicates the percentage of animals heterozygous for the indicated specific RNAi line and heterozygous for the indicated *Gal4* driver showing the malformed leg phenotype in at least one leg. *n*, total number of flies of the indicated genotype that were scored.

Reference

Al-Shahrour, F., Minguez, P., Tarraga, J., Medina, I., Alloza, E., Montaner, D., and Dopazo, J. (2007). FatiGO +: a functional profiling tool for genomic data. Integration of functional annotation, regulatory motifs and interaction data with microarray experiments. Nucleic Acids Res 35, W91-6.

Al-Shahrour, F., Minguez, P., Tarraga, J., Montaner, D., Alloza, E., Vaquerizas, J. M., Conde, L., Blaschke, C., Vera, J., and Dopazo, J. (2006). BABELOMICS: a systems biology perspective in the functional annotation of genome-scale experiments. Nucleic Acids Res 34, W472-6.

Andres, A. J., Fletcher, J. C., Karim, F. D., and Thummel, C. S. (1993). Molecular analysis of the initiation of insect metamorphosis: a comparative study of Drosophila ecdysteroid-regulated transcription. Dev Biol 160, 388-404.

Andres, A. J., and Thummel, C. S. (1994). Methods for quantitative analysis of transcription in larvae and prepupae. Methods Cell Biol 44, 565-73.

Appel, L. F., Prout, M., Abu-Shumays, R., Hammonds, A., Garbe, J. C., Fristrom, D., and Fristrom, J. (1993). The Drosophila Stubble-stubbloid gene encodes an apparent transmembrane serine protease required for epithelial morphogenesis. Proc Natl Acad Sci U S A 90, 4937-41.

Bayer, C. A., Halsell, S. R., Fristrom, J. W., Kiehart, D. P., and von Kalm, L. (2003). Genetic interactions between the RhoA and Stubble-stubbloid loci suggest a role for a type II transmembrane serine protease in intracellular signaling during Drosophila imaginal disc morphogenesis. Genetics 165, 1417-32.

Bayer, C. A., von Kalm, L., and Fristrom, J. W. (1997). Relationships between protein isoforms and genetic functions demonstrate functional redundancy at the Broad-Complex during Drosophila metamorphosis. Dev Biol 187, 267-82.

Beaton, A. H., Kiss, I., Fristrom, D., and Fristrom, J. W. (1988). Interaction of the Stubble-stubbloid locus and the Broad-complex of Drosophila melanogaster. Genetics 120, 453-64.

D'Avino, P. P., Crispi, S., Polito, L. C., and Furia, M. (1995). The role of the BR-C locus on the expression of genes located at the ecdysone-regulated 3C puff of Drosophila melanogaster. Mech Dev 49, 161-71.

Davis, M. B., Carney, G. E., Robertson, A. E., and Bender, M. (2005). Phenotypic analysis of EcR-A mutants suggests that EcR isoforms have unique functions during Drosophila development. Dev Biol 282, 385-96.

DiBello, P. R., Withers, D. A., Bayer, C. A., Fristrom, J. W., and Guild, G. M. (1991). The Drosophila Broad-Complex encodes a family of related proteins containing zinc fingers. Genetics 129, 385-97.

Dietzl, G., Chen, D., Schnorrer, F., Su, K. C., Barinova, Y., Fellner, M., Gasser, B., Kinsey, K., Oppel, S., Scheiblauer, S., Couto, A., Marra, V., Keleman, K., and Dickson, B. J. (2007). A genome-wide transgenic RNAi library for conditional gene inactivation in Drosophila. Nature 448, 151-6.

Fristrom, D. (1976). The mechanism of evagination of imaginal discs of Drosophila melanogaster. III. Evidence for cell rearrangement. Dev Biol 54, 163-71.

Gates, J., Lam, G., Ortiz, J. A., Losson, R., and Thummel, C. S. (2004). rigor mortis encodes a novel nuclear receptor interacting protein required for ecdysone signaling during Drosophila larval development. Development 131, 25-36.

Gatti, M., and Baker, B. S. (1989). Genes controlling essential cell-cycle functions in Drosophila melanogaster. Genes Dev 3, 438-53.

Gotwals, P. J., and Fristrom, J. W. (1991). Three neighboring genes interact with the Broad-Complex and the Stubble-stubbloid locus to affect imaginal disc morphogenesis in Drosophila. Genetics 127, 747-59.

Halsell, S. R., and Kiehart, D. P. (1998). Second-site noncomplementation identifies genomic regions required for Drosophila nonmuscle myosin function during morphogenesis. Genetics 148, 1845-63.

Kiss, I., Beaton, A. H., Tardiff, J., Fristrom, D., and Fristrom, J. W. (1988). Interactions and developmental effects of mutations in the Broad-Complex of Drosophila melanogaster. Genetics 118, 247-59.

Lam, G., and Thummel, C. S. (2000). Inducible expression of double-stranded RNA directs specific genetic interference in Drosophila. Curr Biol 10, 957-63.

Le, T., Liang, Z., Patel, H., Yu, M. H., Sivasubramaniam, G., Slovitt, M., Tanentzapf, G., Mohanty, N., Paul, S. M., Wu, V. M., and Beitel, G. J. (2006). A new family of Drosophila balancer chromosomes with a w- dfd-GMR yellow fluorescent protein marker. Genetics 174, 2255-7.

Luschnig, S., Batz, T., Armbruster, K., and Krasnow, M. A. (2006). serpentine and vermiform encode matrix proteins with chitin binding and deacetylation domains that limit tracheal tube length in Drosophila. Curr Biol 16, 186-94.

McBrayer, Z., Ono, H., Shimell, M., Parvy, J. P., Beckstead, R. B., Warren, J. T., Thummel, C. S., Dauphin-Villemant, C., Gilbert, L. I., and O'Connor, M. B. (2007). Prothoracicotropic hormone regulates developmental timing and body size in Drosophila. Dev Cell 13, 857-71.

Milner, M. J. (1977). The eversion and differentiation of Drosophila melanogaster leg and wing imaginal discs cultured in vitro with an optimal concentration of beta-ecdysone. J Embryol Exp Morphol 37, 105-17.

Niederreither, K., Vermot, J., Messaddeq, N., Schuhbaur, B., Chambon, P., and Dolle, P. (2001). Embryonic retinoic acid synthesis is essential for heart morphogenesis in the mouse. Development 128, 1019-31.

Robertson, C. W. (1936). The metamorphosis of Drosophila melanogaster, including an accurately timed account of the principal morphological changes. . Journal of Morphology 59, 351-399.

Roch, F., Alonso, C. R., and Akam, M. (2003). Drosophila miniature and dusky encode ZP proteins required for cytoskeletal reorganisation during wing morphogenesis. J Cell Sci 116, 1199-207.

Taylor, J., and Adler, P. N. (2008). Cell rearrangement and cell division during the tissue level morphogenesis of evaginating Drosophila imaginal discs. Dev Biol 313, 739-51.

Thummel, C. S. (2001). Molecular mechanisms of developmental timing in C. elegans and Drosophila. Dev Cell 1, 453-65.

Vereshchagina, N., Bennett, D., Szoor, B., Kirchner, J., Gross, S., Vissi, E., White-Cooper, H., and Alphey, L. (2004). The essential role of PP1beta in Drosophila is to regulate nonmuscle myosin. Mol Biol Cell 15, 4395-405.

von Kalm, L., Fristrom, D., and Fristrom, J. (1995). The making of a fly leg: a model for epithelial morphogenesis. Bioessays 17, 693-702.

Ward, R. E., Evans, J., and Thummel, C. S. (2003). Genetic modifier screens in Drosophila demonstrate a role for Rho1 signaling in ecdysone-triggered imaginal disc morphogenesis. Genetics 165, 1397-415.

Ward, R. E., Reid, P., Bashirullah, A., D'Avino, P. P., and Thummel, C. S. (2003). GFP in living animals reveals dynamic developmental responses to ecdysone during Drosophila metamorphosis. Dev Biol 256, 389-402.

Chapter 4

Conclusions and future directions

When I began these studies, we knew that ecdysone and *br* regulated leg imaginal disc morphogenesis, and that the Rho1 signaling pathway played a central role in controlling the actin cytoskeleton during morphogenesis (Figure 4.1 A, C), but we were not sure how these components work together to control the cell shapes and cell rearrangement necessary for normal development. Previous dominant enhancer screens of *br* showed that in addition to Rho1 signaling, proteases and other proteins that can modify the extracellular matrix, such as Sb, are likely playing important roles in leg morphogenesis. I therefore used forward and reverse genetic approaches to identify other pathways important for leg morphogenesis. My characterization of *sec61*α has expanded our understanding of leg morphogenesis, and has specifically shown that secretion is likely essential during leg development (Figure 4.1 B). Interestingly, more than half of the 31 genes that are up-regulated by both ecdysone and *br* at the onset of metamorphosis are predicted to be secreted or transmembrane proteins. These 31 genes include a potential septate junction molecule (Figure 4.1 D), several extracellular matrix molecules (Figure 4.1 E), and several cuticle modification/binding molecules. Notably, RNAi induced knockdown of genes for all these categories of genes lead to malformed legs, suggesting that all these classes may contribute to morphogenesis. There are several genes whose functions are still unknown, and whose RNAi knockdown produce consistent and relatively frequent malformed legs. Future work in the lab should concentrate on studying how these genes may regulate cell shape changes and cell rearrangement necessary for proper morphogenesis.

We have begun characterization of some of the genes identified as *br*- and ecdysone-induced genes during the onset of metamorphosis. *CG12026* encodes a potential claudin, which is a structural component of the septate junctions. Septate junctions in *Drosophila* connect neighboring cells and provide a barrier to paracellular flow, a function corresponding to that of the tight junctions in vertebrates. Knockdown of *CG12026* driven by *breathless-GAL4* (expressed in the trachea) in embryos generated typical claudin mutants phenotypes (Wu, 2004), including convoluted trachea (length defects), and occasionally completely disrupted trachea that failed to fuse. This result suggests that like other claudins in Drosophila, *CG12026* may be required for septate junction organization and trachea tube expansion (Wu, 2004). We are currently trying to generate a loss of function mutation in *CG12026* by excision of a P-element in this gene. Other members of the Ward lab are characterizing *E(br)155*, now known to be a muation in *Mcr*, in which the septate junctions seem to be disrupted. Notably, *Mcr* mutants also have defects in both tracheal morphogenesis in the embryo and leg morphogenesis during metamorphosis. Taken together the results suggest that the septate junctions play an important role in leg morphogenesis. This is supported by former work by Fristrom (1982), who showed that septate junction structure is dramatically modified during leg morphogenesis. The characterization of these two novel genes and better descriptive work on septate junctions during development may therefore help us to understand how modification of septate junctions may function in this process.

Although ecdysone and *br* are both necessary for elongation (Fristrom and Fristrom, 1993; Bayer, 1997), the list of genes induced by ecdysone and *br* do not appreciably overlap,

suggesting that *br* does not function strictly downstream of ecdysone. Thus we wondered if either ecdysone signaling or *br* expression was sufficient for this developmental process. The methods and results were described in Ch.3, we did not observe any unusually elongated leg imaginal discs in 0 hr prepupae by activation of *br* or early supply of ecdysone alone, supporting our conclusion from Ch.3 that *br* and ecdysone might both be required to direct leg disc elongation.

Interestingly, an early supply of ecdysone and activation of *br* cannot induce precocious elongation of leg imaginal discs either. There are several possibilities to explain this result. First, there could be technical problems with the experiment. Larval feeding of ecdysone may not be sufficient to induce a high ecdysone signal in the imaginal discs. It will be important to conduct ecdysone titer experiments (or measurement of ecdysone signals through Northern blot analysis) to show that ecdysone signaling is occurring in these discs. Similarly, we need to confirm the heat-shock induction of *Z2* by Northern blot analysis. Alternatively, we may have to perform these experiments on cultured imaginal discs *in vitro* to address this question. Previous studies have shown that leg imaginal discs cultured in media with appropriate ecdysone concentrations can elongate in a similar manner as they do *in vivo* (Milner, 1977). Similarly, heat shock induction of *br-Z2* in the amorphic allele br^5 can rescue the mutant animals to the adult stage (Bayer, 1997). We will therefore next test if br^5 larval leg discs can precociously elongate by heat-shock inducing *br-Z2* and being cultured in media with ecdysone. To accomplish this we will first cross ybr^5*/binsn; +/+; +/+* female to w^{1118}*/Y; hs-br-Z2; hs-br-Z2* males to produce ybr^5*/Y; hs-br-Z2/+; hs-br-Z2/+* animals. We will then heat shock the early third instar larvae, and dissect a pair of leg imaginal discs from a number of animals. We will separate the pairs of discs and culture one set with ecdysone, and the other set without. We will also conduct similar

controls as we did in the previous experiment to test if ecdysone alone or *br* expression alone is capable of producing significant precocious elongation of leg discs. With this experiment, we will be able to test whether in cultured leg imaginal discs that lack *br* and ecdysone, providing *br* and ecdysone is sufficient to induce leg disc elongation. If we cannot produce premature elongation of the discs, it will raise the possibility that there is yet a third protein that is necessary, with ecdysone and *br*, to regulate morphogenesis. Perhaps the cloning of the other *E(br)* mutations will identify this additional competence factor.

In my graduate studies both forward and reverse genetic approaches were employed to identify genes that participate in ecdysone-regulated leg morphogenesis. *Sec61*α, one of the *E(br)* mutations identified from the forward genetic screen, was carefully characterized. Results from this characterization suggest that normal levels of one or more secreted protein are necessary for leg morphogenesis. Genes that were identified from forward and reverse genetic screens overlapped in the following classes, septate junction molecules, cell adhesion molecules and protease associated with the extracellular matrix. These findings suggest the important role of cell rearrangement in the hormone-regulated imaginal disc morphogenesis. Our lab will continue cloning and charactering the other *E(br)* mutations and genes identified from the microarray to better understand how ecdysone regulates leg disc morphogenesis. Detailed experiments to test whether ecdysone signaling and *br* expression are sufficient for leg imaginal disc elongation will be conducted as well. These studies will help us learn more about mechanisms by which morphogenesis is coordinated.

Figure 4.1

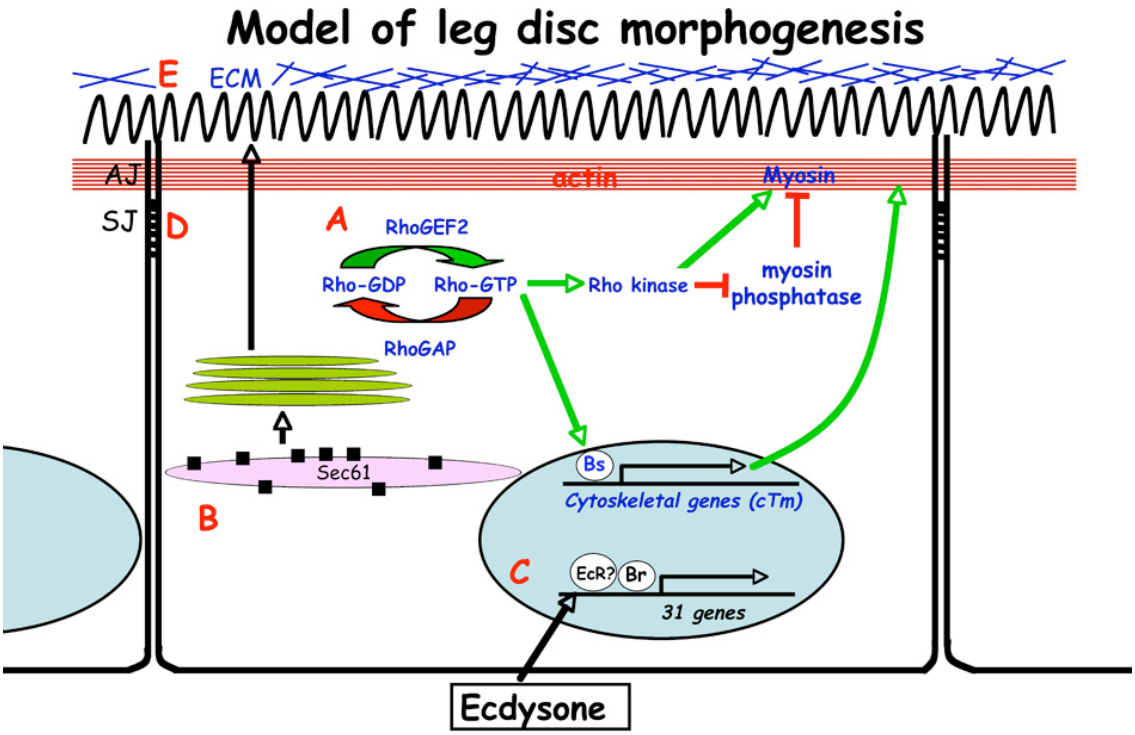

Fig. 4.1. The Model of leg imaginal disc morphogenesis. A. Rho signaling pathway. B. Secretion pathway. C. Ecdysone and *br* coordinate to activate 31 genes at the onset of metamorphosis. D. Cell adhesion structures. AJ: adhesion junction. SJ: septate junction. E. Extracellular matrix (ECM). Details of the Model are described in the text.

Reference

Bayer, C. A., L. von Kalm, et al. (1997). "Relationships between protein isoforms and genetic functions demonstrate functional redundancy at the Broad-Complex during Drosophila metamorphosis." Dev Biol 187(2): 267-82.

Fristrom, D. K. (1982). "Septate junctions in imaginal disks of Drosophila: a model for the redistribution of septa during cell rearrangement." J Cell Biol 94(1): 77-87.

Fristrom, D and Fristrom, J. (1993) The Development of Drosophila Melanogaster. 1993 Cold Spring Harbor Laboratory Press.

Milner, M. J. (1977). The eversion and differentiation of Drosophila melanogaster leg and wing imaginal discs cultured in vitro with an optimal concentration of beta-ecdysone. J Embryol Exp Morphol 37, 105-17.

Wu, V. M., J. Schulte, et al. (2004). "Sinuous is a Drosophila claudin required for septate junction organization and epithelial tube size control." J Cell Biol 164(2): 313-23.